Republic of Iraq
Ministry of Higher Education & Scientific Research
University of Kerbala
College of Engineering
Mechanical Engineering Department

Damping Behavior of a Porous Material Core Used in Sandwich Plate Structures

A Thesis
Submitted to the Council of the Faculty of the College of Engineering/University of Kerbala in Partial Fulfillment of the Requirements for the Master Degree in Mechanical Engineering

By:

Abbas Salah Hashem

Supervised by

Prof. Dr. Muhsin J. Jweeg

Asst. Prof. Dr. Ahmed K. Hassan

2025 A.D. **1447 A.H.**

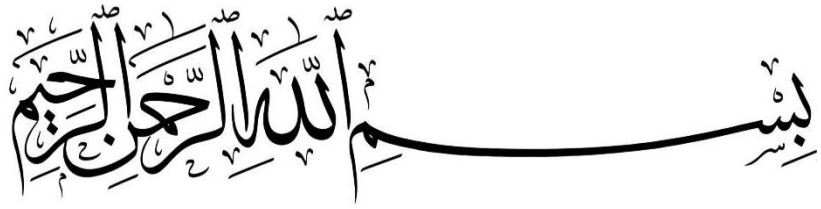

﴿وَحَمَلْنَاهُ على ذَاتِ أَلْوَاحٍ وَدُسُرٍ﴾

صَدَقَ اللهُ العَليّ العَظيمْ

[سورة القمر: أية (13)]

Examination committee certification

We certify that we have read the thesis entitled **"Damping Behavior of a Porous Material Core Used in Sandwich Plate Structures"** and as an examining committee, we examined the student **"Abbas Salah Hashem"** in its content and in what is connected with it and that, in our opinion, it is adequate as a thesis for the degree of Master of Science in Civil Engineering.

Supervisor

Signature:

Name : Prof. Dr. Muhsin J. Jweeg

Date: 15/9 / 2025

Supervisor

Signature:

Name : Asst. Prof. Dr. Ahmed K. Hassan

Date: 15/9/ 2025

Member

Signature:

Name : Prof. Dr. Emad Q. Hussein

Date: 15/9/ 2025

Member

Signature:

Name : : Dr. Mohammed S. Ali

Date: 15/9/ 2025

Chairman

Signature:

Name : Prof. Dr.Mohsin A. Al-Shammari

Date: 15/9/ 2025

Signature:

Name : Prof. Dr. Salah N. Abbood

Head of the Department of Engineering

Date: / 9/ 2025

Signature:

Name : Prof. Dr. Haider N. Azziz

Dean of the Engineering College

Date: / / 2025

Supervisor Certification

We certify that the thesis entitled " **Damping Behavior of a Porous Material Core Used in Sandwich Plate Structures**" was prepared by **Abbas Salah Hashem,** under our supervision at the Department of Mechanical Engineering, Faculty of Engineering, University of Kerbala as a partial of fulfilment of the requirements for the Degree of Master of Science in Mechanical Engineering.

Supervisor

Signature: M. J. Jweeg

Prof. Dr. Muhsin J. Jweeg

Date: 14/8/ 2025

Signature: K. H

Asst. Prof. Dr. Ahmed K. Hassan

Date: 14/ 8/ 2025

Linguistic Certification

This is to certify that I have reviewed linguistically the thesis entitled "**Damping Behavior of a Porous Material Core Used in Sandwich Plate Structures**",submitted by "**Abbas Salah Hashem**". Its language was amended to meet the style of the English language.

Signature:

Name: Dr. SAMIR ALI AMIN (Assistant Professor)

Linguistic Reviewer

samir.ali@uoalfarahidi.edu.iq

Date: / / 2025

Undertaking

I certify that research work titled "**Damping Behavior of a Porous Material Core Used in Sandwich Plate Structures**" is my own work. The work has not been presented elsewhere for assessment. Where material has been used from other sources, it has been properly acknowledged referred.

Signature:

Abbas Salah Hasham

Date: 12 / 8 / 2025

Dedication

To… Allah my Lord,

My homeland Iraq, the symbol of civilization and the country to which I proudly belong, despite the depth of its wounds.

To… My Family.

I dedicate this work...

Abbas salah hasham

Acknowledgment

First and foremost, I express my deepest gratitude to *"**Allah***", the Most Gracious and Most Merciful, and to His noble Prophet "***Mohammad***", (peace and blessings be upon him), as well as the Prophet's family, for granting me the strength and perseverance to complete this study. I am sincerely thankful to my supervisors, **Prof. Dr. Muhsin J. Jweeg** and **Assistant Prof. Dr. Ahmed K. Hassan**, for their invaluable guidance, continuous support, and encouragement throughout all stages of this thesis. Their expertise and constructive advice were instrumental in shaping the outcomes of this work. My appreciation is also extended to **Assistant Prof. Dr. Haider N. Azziz**, Dean of the College of Engineering at the University of Kerbala, for his support. I would also like to thank **Prof. Dr. Salah N. Abbood**, Head of the Department of Mechanical Engineering, **Prof. Dr. Mohammad Wahab**, and all members of the teaching staff in the department for their assistance and encouragement throughout my academic journey. Finally, I express my heartfelt thanks to my **Family**, **Friends**, and all those who supported me directly or indirectly during the course of this work. Their presence and encouragement have been a vital source of strength and motivation.

Abbas Salah Hashem

Abstract

Sandwich panels are commonly used in marine ships structures and aerospace applications due to their light weight and design flexibility In, like that is suitable for, automotive and civil engineering applications, as it offers reduced weight while maintaining mechanical strength, this study examines the effect of foam core density and thickness on the dynamic performance of sandwich panels, particularly focusing on natural frequencies and vibration behavior. Three foam densities (26, 34, and 40 kg/m^3) were studied, alongside two core thicknesses, (25 mm and 50 mm) were used to investigate their effects on the vibration characteristics of foam structure**s**.

The methodology combined Analytical calculations, experimental measurements, and numerical simulations. Analytical models were used to estimate the natural frequencies of sandwich panels based on material properties and geometry. Experimental, panels were fabricated with the selected foam cores and tested using three-point bending setups according to ASTM standards, along with impact tests simulating real-life conditions. Numerical simulations were carried out using ANSYS software to calculate the natural frequencies and validate the experimental data.

The results manifested that increasing the foam density generally led to a decrease in the fundamental natural frequency of the sandwich panels. This trend was observed for both thicknesses, though the decrease was more noticeable in thicker cores. The reduction in natural frequency with higher density is attributed to the added mass of the denser foam, which affects the panel's vibrational characteristics. Conversely, lower density foams resulted in higher natural frequencies in proportion 19%, which is advantageous in applications where the vibration control is critical, and The experimental damping coefficients were calculated at thicknesses of (25 and 50 mm) for three different foam densities (26, 34, 40 kg/m^3), with values ranging between (0.08253 - 0.15396).

List of Contents

List of Tables

List of Figures

List of Symbols

Abbreviation	Full Form
A	Density =26 kg/m3
B	Density =34 kg/m3
C	Density =40 kg/m3
$A1$	Density =26 kg/m3 At 50 mm Thickness
$B1$	Density =34 kg/m3 At 50 mm Thickness
$C1$	Density =40 kg/m3 At 50 mm Thickness
$A2$	Density =26 kg/m3 At 25 mm Thickness
$B2$	Density =34 kg/m3 At 25 mm Thickness
$C2$	Density =40 kg/m3 At 25 mm Thickness
$(AG)_{eq}$	equivalent shear rigidity
$(EI)_{eq}$	equivalent bending stiffness
A_c	Area of core section
E_c	Modulus of elasticity of core material
$E_{1,2}$	modulus of elasticity of Plate material
G_S	Shear modulus of core material
G_c	shear modulus of the core
t_s	Skin thickness
$\delta_{bending}$	sandwich deflection due to bending
δ_c	Core deflection
δ_{shear}	sandwich deflection due to shear
δ_{total}	total sandwich deflection under bending load
ρ_c	core density

CHAPTER ONE

Introduction

1.1 General

Composite materials are essential components in many modern applications, due to their advanced features, sophisticated manufacturing methods, and expanding range of uses. They have become a prominent field in modern engineering due to their ability to provide a high performance. Among these materials, sandwich structures are a special type of composite material, consisting of combining different materials together, exploiting the properties of each component to enhance the overall structural performance. These structures are widely used in mechanical structures that require a combination of stiffness, strength, and light weight.

Sandwich panels are a preferred choice for building lightweight, highly efficient structures, not only because of their structural performance and weight savings, but also because of their role in reducing costs. Therefore, interest continues in developing new materials and innovative core structures that combine high performance with low cost.

The wide variety of materials that can be combined to produce lightweight, high-performance sandwich structures allows for great flexibility in adapting designs to the requirements and challenges of different applications. As a result, these structures have seen widespread and increasing use in many sectors, such as marine (including military), aviation, railways, automotive, and wind turbine industries[1].

1.2 Sandwich Panel

A sandwich structure consists of a lightweight, thick core bonded between two thin, strong face sheets. This configuration offers a high resistance to bending due to the increased moment of inertia resulting from layer separation, while the low-density core adds minimal weight, as illustrated in Figure (1.1) [1]. Individually, the core is weak and flexible, and the face sheets lack sufficient strength. However, when combined, they form a stiff, structurally

efficient unit that can be shaped flat or curved. Sandwich panels do not possess physical and mechanical properties as homogeneous materials do; different manufacturing techniques can alter the performance dramatically [2]. Their properties can be suitably matched to functional requirements by means of an appropriate choice of materials, geometries and configurations [3].

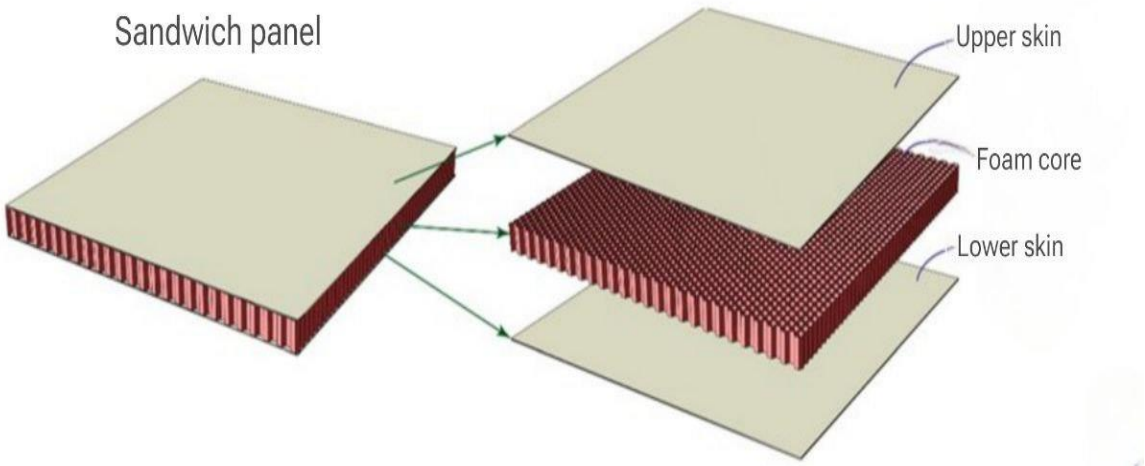

Figure 1.1: Sandwich Panels Construction [1]

In some designs, the central material of a sandwich like construction could be different from the face sheets and it can be placed strategically to form a complete support against such occurrences, like wrinkling / buckling, as compared to restricted to a narrow web system [4]. Consequently, it becomes critical to end up with a strong bond between the core and the face sheets. This is normally achieved by the use of high-strength adhesives, which though useful, have the potential of adding overall weight and providing limitations when it comes to design flexibility and implementation of the same [5]. The face sheets have the main role of countering the tensile and compressive loads that occur under flexural loading conditions. On the other hand, the core provides the support of shear stresses, the separation of face sheets is also constant, and there would not be any relative displacement between the face sheets, as shown in Figure (1.2). Despite its relatively low density, the core performs these structural functions efficiently, contributing to the sandwich

panel's characteristic light weight, while preserving its high stiffness-to-weight and strength-to-weight performance metrics [6].

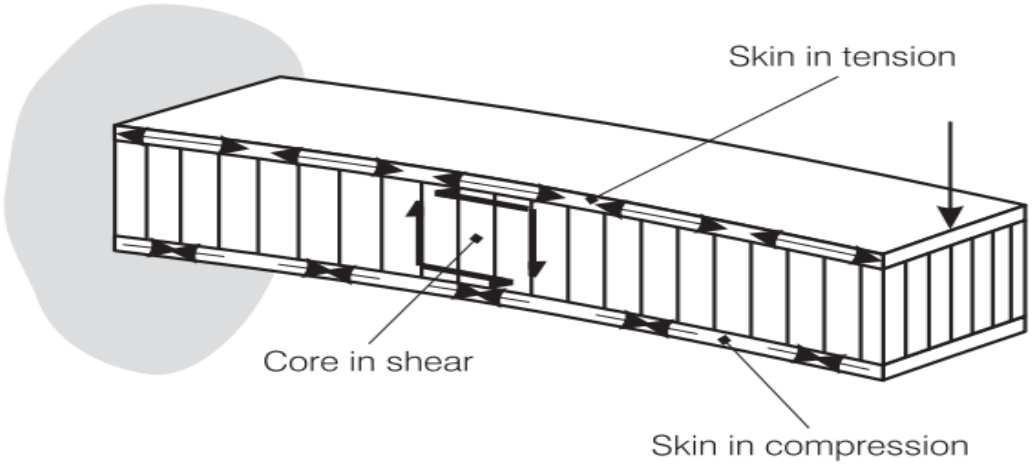

Figure 1.2: Sandwich Panel Stresses During Bending [6]

Besides strength and weight improvements, the potential economic benefits from low-cost core materials employment are significant, which makes sandwich construction an opportunity to be used in limited-budget applications [7]. Nonetheless, sandwich structures have complicated behavior and a variety of complex failure modes, see figure (1.3), making it difficult to predict how they will fail. Consequently, specifying materials for skins and core with proper configurations is challenging.

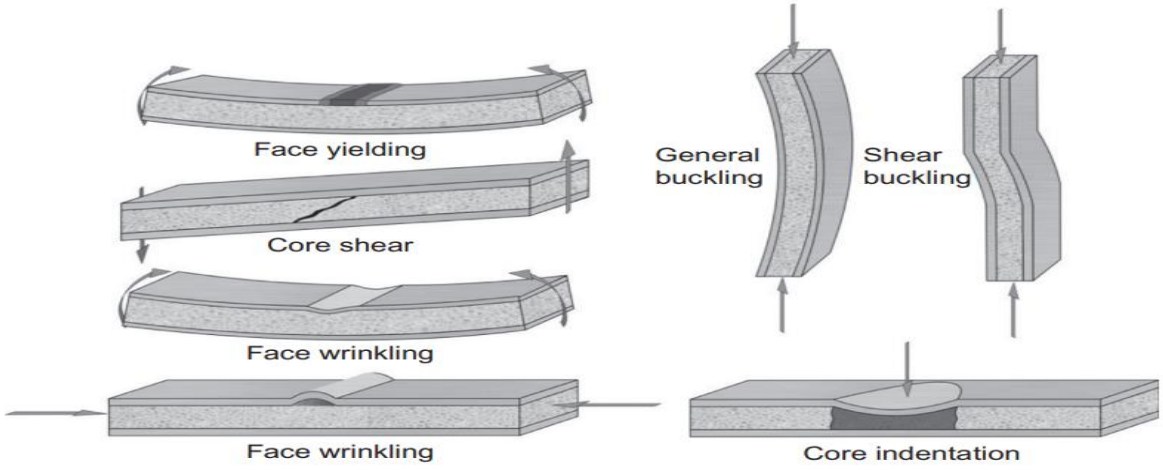

Figure 1.3: Failure modes of sandwich structures **[17]**

1.2.1 Skins

Almost any material that can be fabricated into thin sheets may serve as the facing component of a sandwich panel. These materials may be metallic, such as steel, titanium, or aluminum alloys or non-metallic, including commonly used reinforced plastics, plywood, or composites reinforced with glass, aramid, carbon, or Kevlar fibers. In many cases, these non-metallic materials offer superior strength-to-weight ratios compared to metals and can be formed more easily, even into double-curved shapes [8].

Regardless of the specific material chosen, the facing layers must possess sufficient stiffness to enhance the structural rigidity of the sandwich panel. Additionally, they should demonstrate high resistance to tensile, compressive, and impact forces. Furthermore, the appropriate surface finishing is essential to ensure the durability under various environmental conditions and to resist the wear over time [9].

Typically, both facing sheets are identical in terms of material and thickness, resulting in a symmetric sandwich configuration. However, in certain applications, asymmetry may be introduced by varying the material, thickness, or both between the faces. This design adaptation may be necessary when one face is subjected to different mechanical or thermal loads such as bearing the majority of the structural load, being exposed to extreme cold, or enduring high temperatures or corrosive environments [10].

1.2.2 Core

There are no restrictions on the types of materials that can be used in the fabrication of sandwich cores. Various materials, including polymers, metals, wood, paper, aramid fibers, and composites, can be utilized to manufacture different types of cores. The key is that the core must be produced with the lowest possible density. As a result, regardless of the required core thickness, this will enhance the stiffness of the sandwich structure while only slightly increasing its overall weight, as [11].

For a sandwich structure to perform effectively, the core must fulfill several essential mechanical requirements. Primarily, it must possess sufficient stiffness in the direction normal to the face sheets to preserve the spacing between them during the loading. Additionally, the core must exhibit adequate shear rigidity to prevent the face sheets from sliding relative to each other. If these conditions are not met, the face sheets would act independently as separate beams, thereby eliminating the structural advantages offered by the sandwich design.

Moreover, the core should contribute meaningfully to the overall bending stiffness of the structure by providing adequate flexural rigidity [12]. A variety of core configurations can be used in sandwich constructions, including naturally derived materials, like balsa wood and synthetic cores, such as foams and honeycombs, all of which feature the cellular architectures. Other engineered core types include corrugated cores, waffle-type cores, cross-banded designs, webs, and truss cores, with Figure (1.4) presenting several examples [13].

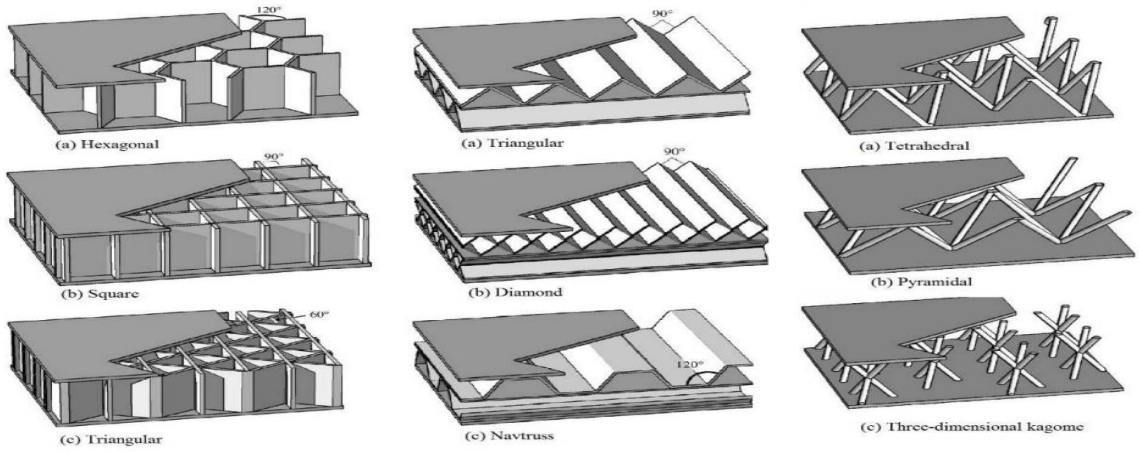

Figure 1.4: Different types of sandwich structures[13]

1.3 Cellular Materials

Cellular materials, whether naturally occurring or synthetically engineered, onsist of interconnected solid struts or plates arranged in two or three dimensions, forming either open or closed cells in periodic or random configurations. These structures are common in nature and can be observed in materials, such as wood, bone, cork, and sponges, as illustrated in Figure (1.5) [14]. They are inherently efficient, offering both structural integrity and functional performance while using minimal material volume.

This natural efficiency has inspired the development of engineered cellular solids, including foams and honeycombs, which exhibit enhanced physical and mechanical characteristics and are widely applied in various industries. A critical parameter in evaluating these materials is their relative density; the ratio of the cellular material's density to that of the solid material it is derived from. Also, the overall density of a cellular substance depends on the size and shapes of its cells, the thickness of the cell wall, the density of the underlying substance and the pattern, symmetry, and interconnectivity of the cell units [15].

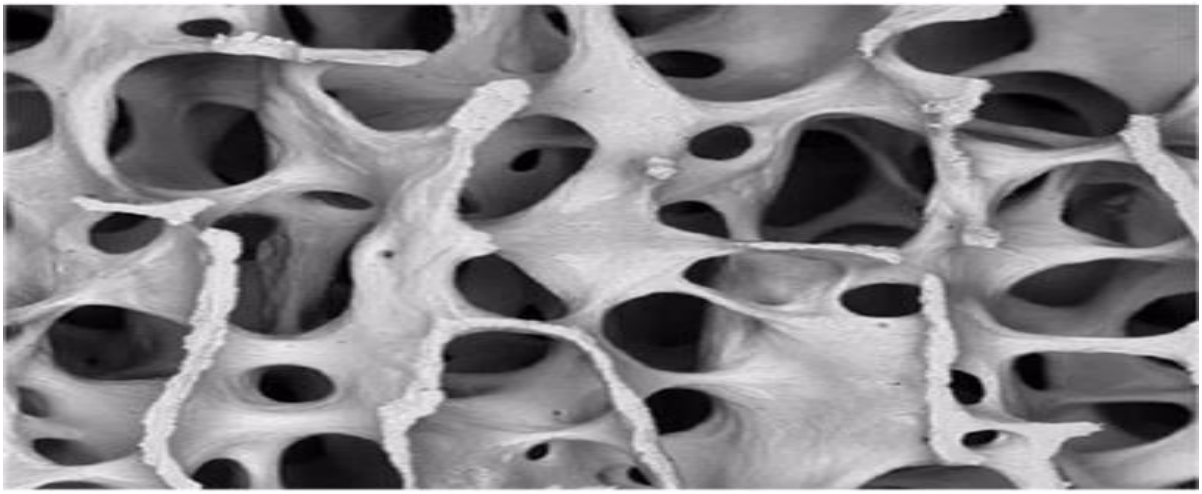

Figure 1.5: Natural cellular structures[14]

1.4 Sandwich Structure

The main idea of structural optimization lies in in accomplishing the maximum performance by the less amount of material possible [16]. When it comes to sandwich structures, this raises the rigidity to the maximum and weight reduction to the bare minimum. In this, high-strength materials of the face sheets-metals or fiber-reinforced composites with multiple design variables are very essential because of their outstanding performance in mechanism properties [17].

On the same note, cellular cores of different types have been designed and improved to aim at creation of lightweight designs that will also be structurally efficient. Achieving this requires a deep understanding of the core's mechanical behavior and the influence of its geometry and properties on the overall performance of the sandwich structure. Modifications in core type or geometrical dimensions can significantly affect the behavior of both the core and the entire sandwich structure [19].

1.5 Aims and Objectives of the Present Work

The main objective of the current work is to investigate the damping effects of a core material used in sandwich panel through the studying of the natural frequencies for such types of structures.To achieve this Aim, the following steps are followed:

1. **To perform Analytical calculations** for estimating the natural frequencies based on classical vibration theory, considering various densities and thicknesses.
2. **To conduct experimental tests including**:
    A. **Compression tests** for determining the elastic modulus and material strength.
    B. **Bending tests** to evaluate the flexural behavior.
    C. **Vibration tests** to measure the natural frequency and damping ratio.
3. **To develop numerical models using ANSYS** for simulating the dynamic response of the structure under different foam configurations.
4. To validate and compare the results obtained from Analytical, numerical, and experimental methods, and analyze the discrepancies among them.

CHAPTER TWO

Literature Review

2.1 General

Core composite structures present a practical engineering solution for lightweight systems that demand efficient vibration damping, making them highly applicable in fields, such as aerospace, marine, and automotive engineering. In recent years, substantial attention has been directed toward understanding their performance, with a particular focus on how the distribution of porosity and the inherent properties of core materials influence the dynamic responses.

Typically, these structures are composed of two stiff outer layers inside a lightweight core. Incorporating such core materials has proven to be a viable strategy for enhancing damping capabilities while keeping the overall weight to a minimum. Research findings suggest that the manner in which porosity is distributed within the core plays a crucial role in the vibrational characteristics of the structure; in particular, the graded porosity has been shown to enhance both damping performance and structural stiffness.

More recent advances in the design of sandwich plates have included ever more frequent usage of porous core structures as one way of enhancing damping response[17].

E.A. Flores-Johnson and Q.M. Li (2011) [20] conducted experimental studies to analyze the quasi static indentation response of the sandwich panels made up of a polymer foam core bonded together between sheets of aluminum. They discovered that the density of the core factor is substantial on how much resistance that the panel gives to indentation with the resistant cores of a larger density having superior load-bearing capacities and more supportive to local deformation. This emphasizes the need for choosing ideal core densities, in order to achieve the maximum mechanical response of sandwich structures under the indentation loading.

Afshin et al. (2011) [21] carried out a detailed analysis of the vibration and damping behavior of cylindrical sandwich panels featuring viscoelastic flexible cores. Theis study proved that the addition of porous core materials into them results in a great increase in damping capacity that ultimately enhances the global dynamic performance and structural stability of the panels. To a great extent, this enhancement is owing to the capacity of the viscoelastic porous cores to connote the productive stream of the energized vibrations, diminish the amplitude of the vibrations, and alleviate any risks of harm transpiring due to the dynamic loading. This work indicates that when choosing core materials, their choice should aim to optimize the tradeoff among stiffness, weight, and damping efficiency in sandwich composite structure.

Boukharouba et al. (2014) [22] created a numerical model to analyze the fatigue composition of sandwich composite panel in three-point bend. The findings indicated that the degree of stiffness degradation under loading was evident and underwent three identifiable stages of damage, although the emphasis in the study is on fatigue, the findings furnish some relevant information on how the stiffness changes with repeated loading, that is, of relevance to the current research as it concerns the effect of core density and configuration on the stiffness and dynamic response.

Parikh and Mahamuni (2015) [23] used a combination of experimental arrangement along with the finite element analysis to study the modal properties of hexagonal honeycomb sandwich plates. The dynamic behavior of the honeycomb core structure was assessed by carrying out free vibration tests. A range of core and face sheet materials was tried out which comprised epoxy carbon, titanium, and aluminum, to determine the effect on the natural frequency. This paper established that the epoxy carbon composition has the highest natural frequency of all the compositions that were tested.

Sunith Babu Loganathan, et al. (2015) [24] studied the issue of how the differences in core thickness and density influence the specification of energy absorption of sandwich structures during the drop-weight impactation tests. Findings revealed that the core thickness greatly increased the energy-absorbing capabilities of the core, and the reduced core-density also produced a beneficial effect in the panel dissipation of impact energy, as the indentation prior to densification was increased.

These researchers decreed that the ideal mix of core density and increased thickness may be utilized to enhance an impact resistance with no structural trade off. These results appeaared the importance of core configuration in sandwich panel design in terms of energy absorption.

G. Sakar (2015) [25] conducted analytical and experimental study to investingate the free vibration of aluminum honeycomb sandwich beams. The analysis or examination of the natural frequencies and mode shapes were compared with changing structural parameters. It was discovered that the root natural frequency dropped as the cell width was increased but was very much enhanced as the foil thickness and core height were brought up. A significant effect on the natural frequency on the beam was established to be the core height, compared to all the other parameters considered.

Muhsin J. Jweeg (2016) [26] proposed an analytical solution to analyze the natural frequency of sandwich composite plates (honeycomb structured) based on several parameters of design. the differential equation of motion that governs the vibration analysis was solved in order to determine the impact of various geometric parameters. The influential parameters, like core height, cell angle, and cell size were studied after their effect on the most basic natural frequency. The findings depicted that there was a direct proportionality between the natural frequency and the majority of the honeycomb parameters with the exception of the face sheet thickness that had an opposite influence on the same.

Huang et al. (2016) [27] studied the vibration and damping behavior of viscoelastic core sandwich plates through analytical models together with finite element modelling. this research involved the investigation of the effects of fundamental material attributes (i.e. viscoelastic modulus, loss factor) and core thickness on the damping performance over varying frequency regimes. The findings indicated that the larger the core thickness, the better the damping that relates to the increase of the ability to dissipate energy. Moreover, the fundamental properties of materials, in particular, the loss factor played a very major role in lowering the levels of vibration, especially at mid to high frequencies. The authors found out that in order to design sandwich structures with better vibrational behavior, the selection of material and core geometry is critical.

Huang et al. (2016) [28] investigated analytically and numerically the vibration and damping of sandwich plates of viscoelastic porous core. This research was concerned with the impact of the introduction of porosity to the viscoelastic core materials on the performance in damping of a series of frequencies. The findings indicated that the porous viscoelastic cores contributed to an overall damping efficiency at medium and high frequencies as the internal friction and energy dissipation increase. The authors reached the conclusion that the core porosity, as well as material properties, is a key factor to enhance the dynamic performance of sandwich

Soraia Pimenta, Cihan Kaboglu, et al. (2017) [29] improved the comprehension of the effectual behavior of sandwich designs that employed varying core materials. It was discovered that the density of core material is a key that helps in defining the structural response to the load of impact. The core strength and density augmentation was found to greatly enhance the sandwich structure impact resistance.

Yu and Lesieutre (2017) [30] explored the synthesis of three-dimensionally-manufactured multimode metamaterial cores into sandwich panels to regulate vibrational behaviour. The analysis was carried out through the use of finite element modelling and experimental verification of the dynamic behaviour of such structures.the authors showed that simply optimising the core design as a metamaterial, so that it contains periodic features within its internal structure, and then analysing its dynamic response using finite element analysis, it was possible to create multiple vibration stop bands which are effective in attenuating undesired dynamic responses across particular frequency bands. These stop bands are due to local resonance processes and Bragg scattering, and such cores are especially valuable in vibration isolation or noise reduction in state of the art structures.

Rajesh Kumar and Shivdayal (2019) [31] took a look at the structural behavior of sandwich panels that had square and octagonal honeycomb cores under blast. Despite its impact-oriented conditions, the research revealed that the octagonal cores achieved the lowest degree of deformations and the best energy absorption than square cores. This tempers the view though that the core geometry, as with octagonal geometry, can result in improved mechanical performance, factors that are pertinent in the current study that focuses on core geometry and its effect on the stiffness and dynamic behavior, like the vibration response.

Mingze Ma et al. (2020) [32] used a three-point bending test fixture in carrying out bending fatigue tests on honeycomb sandwich panels. The results evinced that the core shear failure is the most common type of failure in these kinds of structures. It was shown that the fatigue life of the panels may be conveniently estimated on the basis of core shear stress. More so, the longitudinal or the transverse direction of the core was a major determinant of the fatigue failure characteristic. It was determined that the estimating fatigue life based on core

stress is a reliable and an efficient method which makes the overall process of predicting fatigue life simple.

Singh and Harsha (2021) [33] examined the influence of the porosity distribution of the free vibration and buckling of sandwich plates under the sigmoid function as a representation of the material that is functionally graded material (FGMS). They demonstrated the use of finite element analysis by depicting that it is possible to enhance the damping performance by using non-uniform profiles of porosity that concentrate another in the limits of the structure, but ensuring that the structural stability is not affected. this work, in which the tuning of the time-varying response of sandwich structures is important with regard to matters of core design, the significance of controlling the dynamic behavior with the material gradation and porosity is noted in this study.

Alejandra et al. (2021) [34] explored the effect of low-temperature conditions on the impact response of sandwich composites, using a drop tower impact system to simulate real-world low-velocity impact scenarios. The study found that while the bending stiffness increased as the temperature dropped, the extent of damage from impact also became more severe. Although the focus was on thermal effects, the study reinforces the idea that the external conditions and material state, such as temperature, core density, and structure can significantly influence the mechanical performance of sandwich panels. This aligns with the present work's interest in understanding how the core configuration parameters affect the stiffness and dynamic response.

Zaitoun et al. (2021) [35] created a computational model to investigate the vibrational behavior of the functionally graded sandwich plates upon the exposure to the hygrothermal environments. It was revealed that the porous cores were found to enhance the damping behavior, even in varied moisture and temperature regimes, and although the data are not comparable to that which

was investigated in the current study, the results demonstrated the overall importance of core porosity and material gradation in augmenting the dynamic performance. This concurs with the focus of this work as to how the core structure and density affect the properties of vibration, irrespective of the exterior environment.

Garg et al. (2022) [36] researched the vibration and buckling characteristics of sandwich plates functional graded metal foam core, and the producers concentrate on the role of graded porosity. The findings indicated that when the porous contents had a gradual increase to the center of the core, they had an increased damping effect and greater buckling resistance. The latter was explained by better distribution of stress and dissipation of the energy. The fact that the core structure and gradient of material on it are the most important factors which influence the dynamic behavior of sandwich panels that may be considered as the support of this idea, and this fact is also related to the set topic of the current work.

Li et al. (2022) [37] achieved the study of the free vibration and sound resistance of porous cores, functionally graded honeycomb sandwich plates. It was also concluded that the graded porosity enhanced the acoustic insulation through the limited wave propagation, which is a result of decreased amplitude of vibration, thus enhancing the damping. The results supported the contribution of the core structure and porosity in enhancing the dynamic performances of sandwich panels which are pertinent to the present research study based on core density and vibration response.

Ngo Dinh et al. (2022) [38] mentioned that in addition to a new three-point bending test fixture, the bending fatigue tests of honeycomb sandwich panels were explored, using a new improved three-point bending test fixture, and the outcomes indicated that the shear failure of the core is the most common mode of failure in honeycomb sandwich panels. The core shear stress is able to predict the fatigue life of the sandwich panel. The core direction (L or W) plays a major

role in the geometry of fatigue failure. The life of sandwich panels may be estimated by the stress in the core, and the process may well become simplified.

Al-Itbi and Noori (2022) [39] examined the free vibration response of a FGNSBs by analytical approach. They have observed that by enhancing the porosity of the material of core, the natural frequency goes down, and this helps the damping type behavior as there is more energy dissipation. This paper indicates that the way the porosity is distributed is crucial in setting the dynamic behaviour of sandwich structures a factor which is directly concerned with the current investigation.

Wattan Asakulpong and Eiadtrong (2022) [40**]** researched about the dynamic response of sandwich plates with functional-graded porous core plates with time-variant loading. The results revealed that an increase in porosity level in the core results to an improvement of flexural stiffness and deflection of the plates decreased. It shows vehemently the importance of core porosity design on the mechanical performance of sandwich composite structures in dynamic loads, to provide informative areas to consider in lightweight structures with optimized mechanical properties.

Taşkin and Demir (2023) [41] explored the impact of porosity distribution on the vibration and damping of inhomogeneous curved sandwich beams that have fractional derivative viscoelastic cores. They found out that the variations on the porosity gradients greatly affect the modal characteristics of these beams resulting in significant changes in natural frequencies and vibration modes. All this implies that introducing a controlled porosity distribution in the core can be used as an effective tool to tailor and optimize the dynamic behavior of sandwich structures, especially in situations where the viscoelastic cores with novel material properties can be explored. The relevance of the study is that it shows how the porosity distribution can be used to reduce the vibrations and damping which in turn improves the overall life of the structure, and allows it to better withstand the incident vibrations. Also, the results of these studies lead to

new ways of creating a lightweight and composite structure with enhanced mechanical and engineering features that can be used in the highest applications, like aerospace works, marine engineering, and building construction.

Yuan et al. (2024) [42] performed a nonlinear vibration study of blast loaded plates to determine the vibration performance of functionally graded sandwich plates. They found that the porous cores play a great role in increasing the energy absorptions and damping effects of the plates against the high pressures applied. This observation shows the significance of core design to enhance the resilience and dynamic behaviour of sandwich structures against the high-intensity impacts.

Li et al. (2024) [43] studied the vibration and stability of plates made of progressive porous sandwich structures and moved by moving loads, i.e. vehicles or equipment. The broad study showed that one can control and modulate the dynamic responses of the structure effectively with its porosity distribution varied in the core effectively. Moreover, such customized porosity gradients also have a major contribution in improving the structural stability in general, since the chances of dynamic instabilities or collapses due to complex load conditions causing the movement of masses are minimized due to these structured porosity gradients. This paper points to the significance of assuring to attain maximum performance, durability of sand wich composite structures through designing graded porosity profiles in realistic dynamic conditions.

2.2 Concluding Remarks

As previously discussed, sandwich panels are not characterized by fixed properties; instead, they can be tailored to meet specific application requirements. These requirements are influenced by factors such as the choice of materials, manufacturing techniques, and the designer's ability to define suitable geometric parameters to achieve the desired structural performance. Accordingly, much of the existing research has focused on improving the stiffness and strength of sandwich panels by employing high performance composite materials or by optimizing geometric configurations. In many cases, studies combine multiple variables to achieve the targeted performance. In the present study, however, only the core density and thickness are considered as the primary factors influencing the mechanical behavior of the panels. Furthermore, analyzing different types of cores allows for a clearer assessment of the impact of geometric parameters.

CHAPTER THREE

Analytical and Numerical Analysis

3.1 General

Vibrations are complicated dynamic phenomena that have a significant influence on how well the engineering structures work, especially when there are several material layers involved. The mathematical model for vibrations in a system consisting of two plate layers separated by a foam substance is presented in this chapter. The system is fixed as simply supported. In order to examine this system's behavior, the Rayleigh method is used, a powerful vibration analysis tool. This methodology employs spectral analysis and energy principles to identify the system's inherent frequencies and vibrational modes. The system's reaction to dynamic loading circumstances may be accurately estimated by using the Rayleigh approach.

Also, the hamilton's concept is applied, which offers a thorough mathematical foundation for studying dynamics. The study of intricate dynamic systems is made easier by this approach, which enables to convert the equations of motion into a versatile and effective form. this provides a comprehensive model that allows for an accurate comprehension of vibrational activity in the system under study by combining the Rayleigh approach with Hamilton's principle. The foam component is essential to this model because it enhances the dampening and acoustic insulation, which lessens the negative impacts of vibrations. This study will help better understand how to create structures that are more effective and can handle vibration-related problems[23].

By offering a comprehensive scientific understanding of the vibrational behavior of composite systems, it contributes to the creation of creative engineering solutions that improve the structural performance in a range of applications.

3.2 Mathematical Modelling

A Sandwich plate, is shown in Figure (3.1).

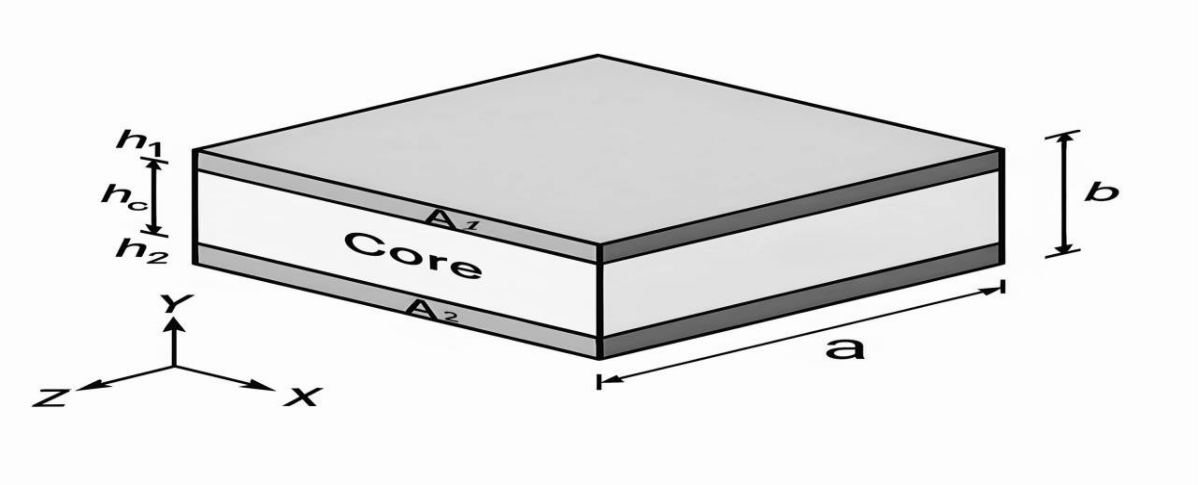

Figure 3.1 : Sandwich plate

Using plate theory,the displacement model is given by [23]:

$$\boldsymbol{u(x,y,z,t) = u_0(x,y,z) - z\frac{\partial w}{\partial x}} \qquad \textit{(3.1)}$$

$$\boldsymbol{v(x,y,z,t) = v_0(x,y,z) - z\frac{\partial w}{\partial y}} \qquad \textit{(3.2)}$$

$$\boldsymbol{w(x,y,z) = w_0(x,y,z)} \qquad \textit{(3.3)}$$

Where: $\boldsymbol{u}$ is the displacement in x-direction.

$\boldsymbol{v}$ is the displacement in y-direction.

$\boldsymbol{w}$ is the displacement in z-direction.

Using energy principle, the strain energy model is given by[24]:

$$\boldsymbol{U = strain\ energy = U_{bending} + U_{shear}} \qquad \textit{(3.4)}$$

$$\boldsymbol{U_b = \frac{1}{2}\int_V D(k_x^2 + 2(1-\vartheta)k_x k_y + k_y^2)dV} \qquad \textit{(3.5)}$$

$$\boldsymbol{U_s = \frac{1}{2}\int_V C_c(\gamma_x^2 + \gamma_y^2)dV} \qquad \textit{(3.6)}$$

$$T = \frac{1}{2}\int_V \rho . W^2 \, dV \qquad (3.7)$$

Where: D is the bending modulus.

k_x and k_y are the longitudinal strain in x-direction and y-direction, respectively.

ϑ is the Poisson's ratio.

V is the volume.

C_c is the shear modulus.

γ_x and γ_y are the shear strain in x-direction and y-direction,respectively.

T **is the kinetic energy.**

ρ **is the density.**

Applying Rayliegh Ritz method gives

$$w(x, y, t) = w(x, y)e^{i\omega t} \qquad (3.8)$$

Using Hamilton's principles,

$$\delta = \int_0^T (T - U)\, dt = 0 \qquad (3.9)$$

The plate stiffness model is given by [25].

$$D = \frac{E_1 h_1^3}{12(1-\vartheta^2)} + \frac{E_2 h_2^3}{12(1-\vartheta^2)} + E_c h_c\left(\frac{hc^2}{4} - \frac{h_c^2}{12}\right) \qquad (3.10)$$

Where: E_1 and E_2 are the Young's modulus for upper plate and lower plate, respectively.

h_1 and h_2 are the thickness for upper plate and lower plate,

respectively.

h_c is the thickness of foam.

$$k_x = \frac{\partial^2 w}{\partial x^2}\ , k_y = \frac{\partial^2 w}{\partial y^2} \qquad (3.11)$$

$$U_b = \frac{1}{2} D \int_0^a \int_0^b \left(\left(\frac{\partial^2 w}{\partial x^2}\right)^2 + 2(1-\vartheta)\frac{\partial^2 w}{\partial x^2}\frac{\partial^2 w}{\partial y^2} + \left(\frac{\partial^2 w}{\partial y^2}\right)\right) dx\, dy \qquad (3.12)$$

$$\gamma_x = \frac{\partial w}{\partial x}\ ,\ \gamma_y = \frac{\partial w}{\partial y} \qquad (3.13)$$

$$U_s = \frac{1}{2} C_c A_C \int_0^a \int_0^b (\gamma)^2\, dx\, dy \qquad (3.14)$$

$$U_s = \frac{1}{2} C_c A_C \int_0^a \int_0^b \left(\left(\frac{\partial w}{\partial x}\right) + \left(\frac{\partial w}{\partial y}\right)\right)^2 dx\, dy \qquad (3.15)$$

Where: A_C *is the cross sectional area of the foam.*

$$A_c = b h_c \qquad (3.16)$$

$$T = \frac{1}{2} \int_V \rho . (w)^2\, dV \qquad (3.17)$$

For a sandwiched plate,

$$T = \frac{1}{2}(\rho_1 h_1 + \rho_c h_c + \rho_2 h_2) \int_0^a \int_0^b (w^2)\, dx\, dy \qquad (3.18)$$

$$Let\ \bar{\rho} = \rho_1 h_1 + \rho_c h_c + \rho_2 h_2 \qquad (3.19)$$

$$T = \frac{1}{2} \bar{\rho} \int_0^a \int_0^b w^2\, dx\, dy \qquad (3.20)$$

Where: ρ_1 and ρ_2 are the densities for upper and lower plates, respectively.

ρ_c is the density of the foam.

Assume that the deflected shape is given by [26]:

$$w(x, y, t) = w_0 \sin\left(\frac{m\pi x}{a}\right) \sin\left(\frac{n\pi y}{b}\right) e^{i\omega t} \qquad (3.21)$$

Where, ω is the frequency.

w_0 is the maximum of amplitude.

$$U = \frac{1}{4} D \left(\frac{m^2\pi^2}{a^2} + \frac{n^2\pi^2}{b^2}\right) w_o a\, b + \frac{1}{4} C_c A_c \left(\frac{m^2\pi^2}{a^2} + \frac{n^2\pi^2}{b^2}\right) w_0^2 a\, b \qquad (3.22)$$

$$T = \frac{1}{4} \bar{\rho} w^2 w_0^2 a\, b \qquad (3.23)$$

Where: $\boldsymbol{m}$ and $\boldsymbol{n}$ are integer values that denote the horizontal and vertical modes of vibration, respectively.

$\boldsymbol{a}$ and $\boldsymbol{b}$ are the length and width of specimen, respectively.

$\boldsymbol{\omega}$ is the natural frequency.

Applying Hamilton's principles,

$$\boldsymbol{\delta = \int_0^T (T - U)\, dt = 0} \qquad \textit{(3.24)}$$

This gives

$$\boldsymbol{\left(D\left(\frac{m^2\pi^2}{a^2} + \frac{n^2\pi^2}{b^2}\right) + C_c A_c \left(\frac{m^2\pi^2}{a^2} + \frac{n^2\pi^2}{b^2}\right) - \bar{\rho}\omega^2 . w_0\right) = 0} \qquad \textit{(3.25)}$$

Since $w_0 \neq 0$

$$\boldsymbol{\omega^2 = \frac{D\left(\frac{m^2\pi^2}{a^2}+\frac{n^2\pi^2}{b^2}\right)+C_c A_c\left(\frac{m^2\pi^2}{a^2}+\frac{n^2\pi^2}{b^2}\right)}{\bar{\rho}}} \qquad \textit{(3.26)}$$

$$\boldsymbol{\omega = \frac{1}{2}\sqrt{\frac{D\left(\frac{m^2\pi^2}{a^2}+\frac{n^2\pi^2}{b^2}\right)+C_c A_c\left(\frac{m^2\pi^2}{a^2}+\frac{n^2\pi^2}{b^2}\right)}{\bar{\rho}}}} \qquad \textit{(3.27)}$$

$$\boldsymbol{D_{eq}\nabla^4 w + \rho h \ddot{w} = 0} \qquad \textit{(3.28)}$$

Where: $\dot{w} = \frac{\partial w}{\partial t}$; $\ddot{w} = \frac{\partial^2 w}{\partial t^2}$; ρh is the mass per unit area of the sandwich plate.

$$\boldsymbol{\nabla^4 = \frac{\partial^4}{\partial x^4} + 2\frac{\partial^4}{\partial x^2 \partial y^2} + \frac{\partial^4}{\partial y^4}} \qquad \textit{(3.29)}$$

$w(x, y, t)$ is the transverse displacement as a function of time.

$$\boldsymbol{D_{eq} = \frac{E_f h_f^3}{12(1-t_f^2)} + \frac{E_{Al} h_{Al}^3}{12(1-t_{Al}^2)}} \qquad \textit{(3.30)}$$

Assume a separable solution for $w(x, y, t)$,

$$\boldsymbol{w(x, y, t) = X(x)Y(y)T(t)}$$

By putting this into the Eq (3.28),

$$\boldsymbol{D_{eq}\left(\frac{\partial^4(XYT)}{\partial x^4}+2\frac{\partial^4(XYT)}{\partial x^2\partial y^2}+\frac{\partial^4(XYT)}{\partial y^4}\right)=\rho h\frac{\partial^2(XYT)}{\partial t^2}} \quad \textbf{(3.31)}$$

Dividing by XYT gives

$$\boldsymbol{D_{eq}\left(\frac{1}{X}\frac{\partial^4 X}{\partial x^4}+2\frac{1}{XY}\frac{\partial^4 XY}{\partial x^2\partial y^2}+\frac{1}{Y}\frac{\partial^4 Y}{\partial y^4}\right)=\rho h\frac{1}{T}\frac{\partial^2 T}{\partial t^2}} \quad \textbf{(3.32)}$$

L.H.S Eq(3.32) is a function of x and y.

R.H.S(3.32) is a function of t.

Therefore:

$$\boldsymbol{D_{eq}\left(\frac{1}{X}\frac{\partial^4 X}{\partial x^4}+2\frac{1}{XY}\frac{\partial^4 XY}{\partial x^2\partial y^2}+\frac{1}{Y}\frac{\partial^4 Y}{\partial y^4}\right)=\lambda} \quad \textbf{(3.33)}$$

Where:

$$\boldsymbol{\lambda=\rho h\frac{1}{T}\frac{\partial^2 T}{\partial t^2}} \quad \textbf{(3.34)}$$

Time solution is:

$$\boldsymbol{\frac{d^2T}{dt^2}=+\frac{\lambda}{\rho h}T=0} \quad \textbf{(3.35)}$$

$$\boldsymbol{T(t)=T_0.e^{i\omega t}} \quad \textbf{(3.36)}$$

$$\boldsymbol{\omega^2=\frac{\lambda}{\rho h}} \quad \textbf{(3.37)}$$

The frequency depends on λ.

Spatial solution is:

$$\boldsymbol{\frac{\partial^4 X}{\partial x^4}+2\frac{\partial^4 XY}{\partial x^2\partial y^2}+\frac{\partial^4 Y}{\partial y^4}=\frac{1}{D_{eq}}XY} \quad \textbf{(3.38)}$$

Using the separation of variables,

$$\boldsymbol{\frac{1}{X}\frac{\partial^4 X}{\partial x^4}+2\frac{1}{XY}\frac{\partial^4 XY}{\partial x^2\partial y^2}+\frac{1}{Y}\frac{\partial^4 Y}{\partial y^4}=\frac{\lambda}{D_{eq}}} \quad \textbf{(3.39)}$$

The L.H.S depends on x.

$$Let\ \frac{1}{X}\frac{\partial^4 X}{\partial x^4} = \mu \qquad (3.40)$$

$$\frac{1}{Y}\frac{\partial^4 Y}{\partial y^4} = \frac{\lambda}{D_{eq}} - \mu \qquad (3.41)$$

These can be solved independently.

For S.S. plate along $x = 0, a\ ;\ y = 0, b$

$w = 0$ (zero displacement)

$\frac{\partial^2 w}{\partial x^2} = 0$ (zero bending moment)

The solution is:

$X(x) = \sin\frac{m\pi x}{a}\ ;\ Y(y) = \sin\frac{n\pi y}{b}$

m and n are the mode numbers.

From the plate equation,

$$\lambda = D_{eq}[\left(\frac{m\pi}{a}\right)^2 + \left(\frac{n\pi}{b}\right)^2]^2 \qquad (3.42)$$

Using $\omega = \frac{\lambda}{\rho h}$

$$\omega_{mn} = \pi^2\sqrt{\frac{D_{eq}}{\rho h}(\frac{m^2}{a^2} + \frac{n^2}{b^2})} \qquad (3.43)$$

3.3 Mode Shape

An important topic in the study of how the materials behave under external forces is the modal shapes of plates in the setting of vibrations. The mathematical model has been derived to represent the types of modal shapes for plates and how the various shapes that metal plates might acquire during vibration impact their stability and performance, in order to comprehend how plates interact with the ambient motions and forces. Examining the modal forms of plates can help build better structures plates, lower the vibrations, and increase the efficiency of industrial operations, especially in sandwich.

For the S.S. plate,

$$\boldsymbol{w_{m,n}(x,y,t) = w_0\, sin(\frac{m\pi x}{a})\, sin(\frac{n\pi y}{b}) e^{i\omega t}} \qquad \textbf{(3.44)}$$

Where: $\boldsymbol{w_0}$ is the amplitude of the mode.

$$\boldsymbol{w_{m,n} = sin(\frac{m\pi x}{a})\, sin(\frac{n\pi y}{b})} \qquad \textbf{(3.45)}$$

$w_{m,n}$ is the spatial part of the mode shape.

Note: Each mode shape $w_{m,n}(x,y)$ represents a standing wave.

The nodes lines occur where:

$$\boldsymbol{sin(\frac{m\pi x}{a}) = 0 \;\; or \; sin(\frac{n\pi y}{b}) = 0}$$

Which gives

$$\boldsymbol{x = \frac{ka}{m}} \;,\; \boldsymbol{y = \frac{lb}{n}}$$

$k = 0,1,2, \ldots\ldots,$; $l = 0,1,2, \ldots\ldots,$

- Lowest mode $m = 1$, $n = l$ (the entire plate vibrates without internal nodes).
- Higher modes include more nodes lines.

Frequency is:

$$\boldsymbol{\omega_{mn} = \pi^2 \sqrt{\frac{D_{eq}}{\rho h}\left(\frac{m^2}{a^2} + \frac{n^2}{b^2}\right)}} \qquad \textbf{(3.46)}$$

Mode shapes are:

$$\boldsymbol{w_{m,n}(x, y, t) = w_0 \, sin\left(\frac{m\pi x}{a}\right) sin\left(\frac{n\pi y}{b}\right) e^{i\omega t}} \qquad \textbf{(3.47)}$$

3.4 Finite Element Modelling

The quality of the mesh has a significant impact on the accuracy and stability of numerical calculations. Key indicators, such as node distribution, element smoothness, and skewness are essential for evaluating the mesh quality. Regardless of the mesh type used in the computational domain, verifying the mesh quality is a crucial step. The evaluation criteria vary depending on the element types employed. For this finite element analysis (FEA), the Hex 20 element was selected. It is a three-dimensional solid element consisting of 20 higher-order nodes with quadratic displacement behavior, offering a high accuracy and solution stability. The structure of the Hex 20 element is illustrated in Figure (3.2). Each node in this element possesses three degrees of freedom, translations in the x, y, and z directions, making it well-suited for modeling complex behaviors, such as plasticity, hyper elasticity, creep, strain stiffening, large deflections, high compressive capacities, and vibration analysis in ANSYS 2018 R2 that provides a variety of element types available for meshing, as shown in Figure (3.3). The modeled plate has dimensions of (300 mm) in length, (300 mm) in width, and (1 mm) in thickness, with varying core densities. The total number of elements and nodes used in the simulation is presented in Table (3.1), and the mesh configuration is depicted in Figure (3.4). This meshing procedure was first applied to Model (A), and the same approach was extended to the remaining models due to the similarity in their geometry and structural features.

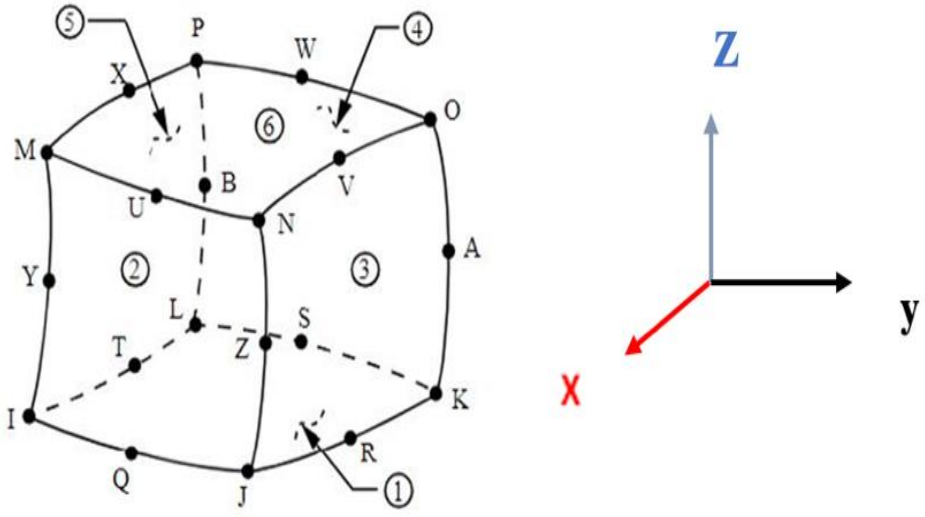

Figure 3.2 : Element type

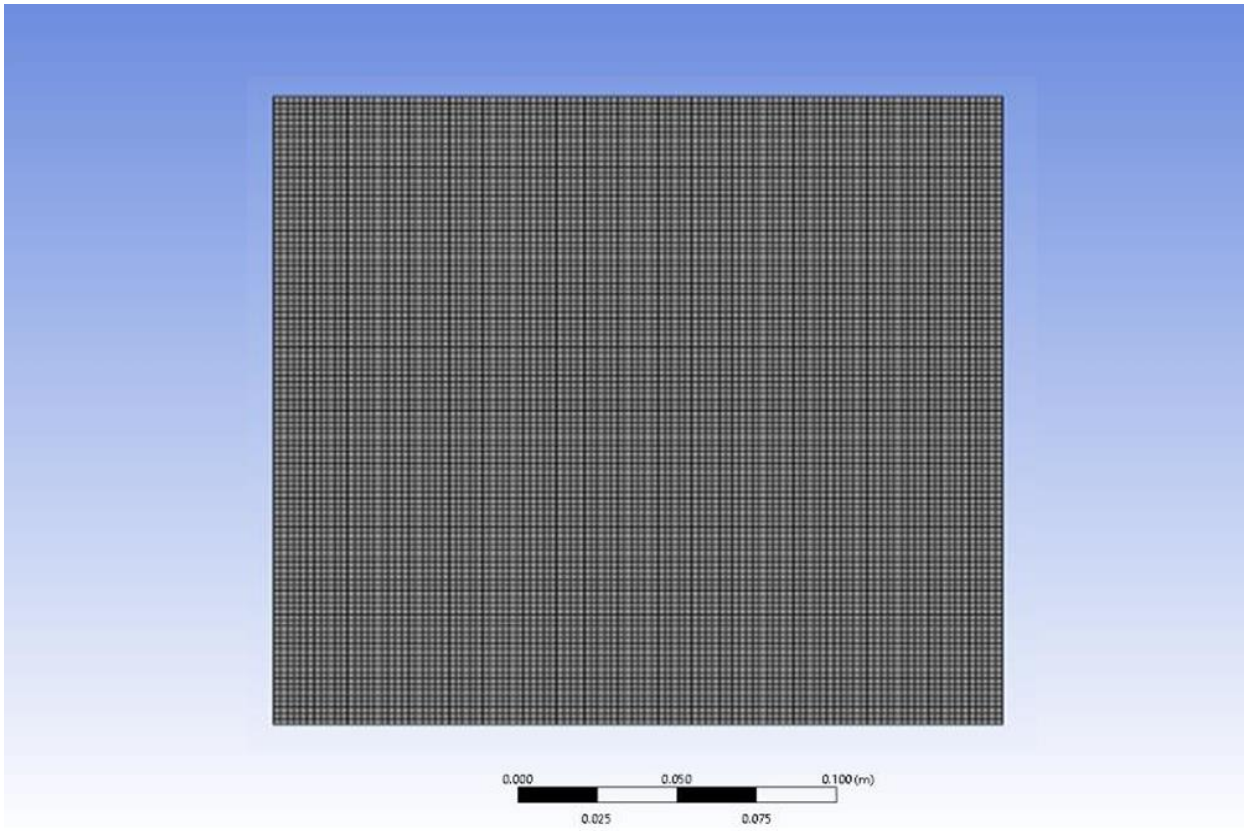

Figure 3.3: Mesh generation model

Table 3.1: Finite Element Models Properties

Parameters	ModelA	ModelA	ModelA	ModelA	ModelA	ModelA
Foam Thickness	25 mm	30 mm	35 mm	40 mm	45 mm	50 mm
Number of elements	24265	26541	28644	35955	37000	37000
Number of nodes	52800	54700	56000	56800	58000	60000

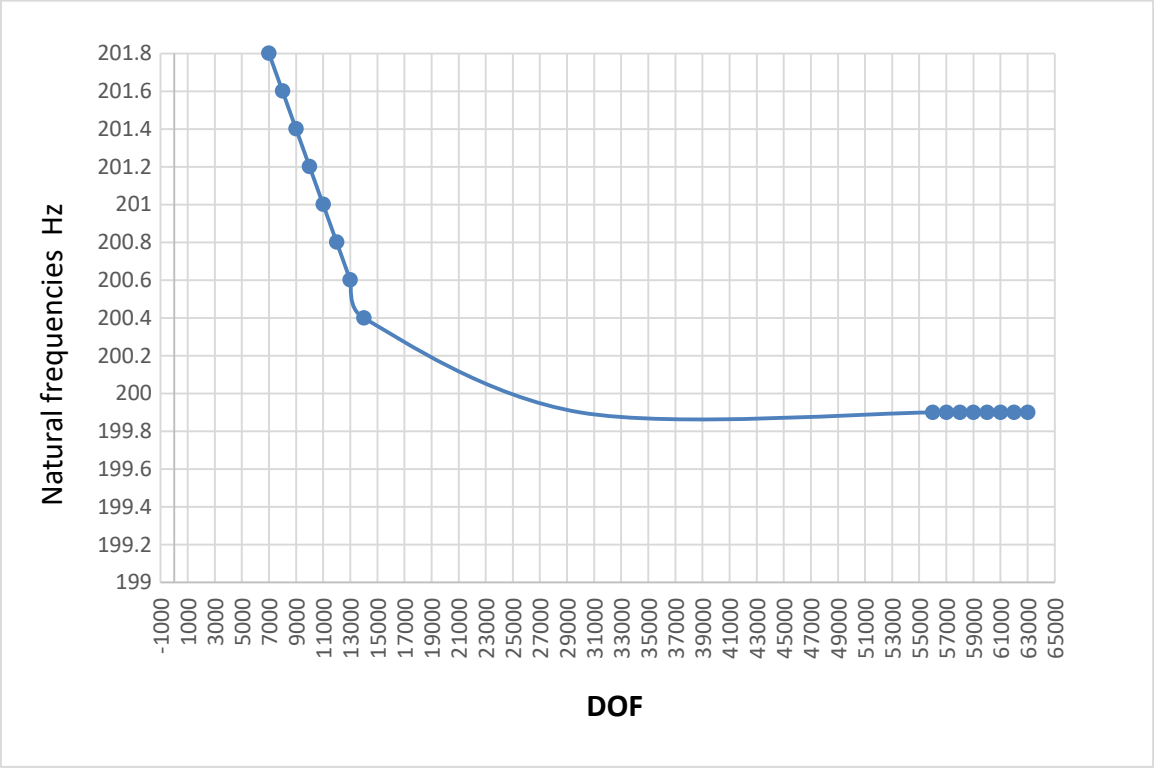

Figure 3.4: Convergence test

Figure 3.4 shows the convergence test of natural frequencies with respect to DOF. The results indicate that the frequencies stabilize after about 50,000 DOF, confirming sufficient mesh refinement.

CHAPTER FOUR

Experimental Work

4.1 General

To study the effect of a specific material property, it is necessary to identify the parameters that govern it. This allows for preparing and testing samples with different values of that property, thereby revealing its impact on the material behavior. In this case, the property is the foam core density, governed by cell size, cell wall thickness, and the density of the solid material making up the core. To investigate the effect of core density, sandwich panel samples with various core configurations were prepared. Each configuration includes three different cell sizes, resulting in three distinct core densities. By varying the cell size while keeping other parameters constant, the density is effectively controlled. Subjecting these samples to standardized tests provides a comprehensive understanding of how the core density influences the behavior of sandwich panels.

4.2 Experimental Work

The experimental program is shown in Figure (4.1) .

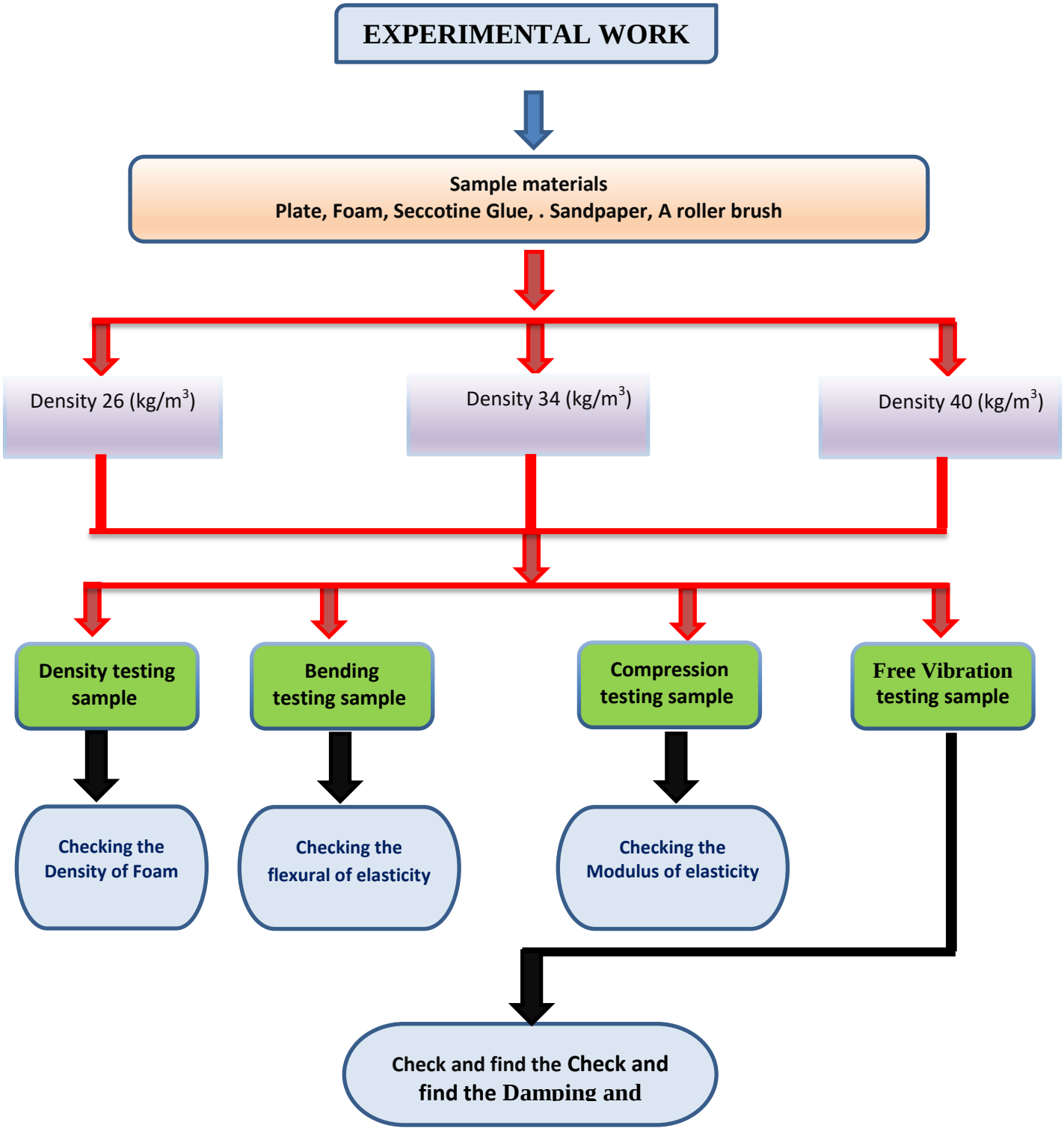

Figure 4.1: Schematic of experimental work.

4.3 Manufacture of Samples for Tests

This paragraph includes the manufacture of samples and is explained in detailed Section as follows:

4.3.1 Preparation of the materials

Sandwich panels were prepared using polymer foam cores of three densities (26, 34, 40 kg/m³) and two thicknesses (25 mm, 50 mm), bonded between composite face sheets. All materials were inspected for uniformity, and panels were cured under controlled conditions before testing.

4.3.1.1 Reinforcing materials

1. Foam

Foam is a colloidal system consisting of gas bubbles surrounded by a liquid or solid substance. The gas bubbles are trapped within the liquid or solid. Foam is used in a variety of applications, including firefighting, insulation, and packaging, due to its unique properties, such as light weight and shock absorption. Foam material was purchased from local companies in various densities, and the density was calculated Analytical using a balance and sample dimensions.

2. Plate

Aluminum sheet is a flat, even sheet made of aluminum metal. It is used in a wide range of industrial and commercial applications due to its distinctive properties. Standard specifications such as ASTM B209 specify the requirements for aluminum sheets, strips, and alloys, including chemical composition and mechanical properties.

3. Seccotine glue

Secotene is a high-strength, water resistant adhesive suitable for bonding various materials.

4. Sandpaper

It is an abrasive material used to roughen, smoothen, and shape various surfaces, such as wood and metal.

5. Roller brushes

The roller is a key tool for quickly and efficiently applying paint to large surfaces, consisting of an absorbent cylinder and a handle.

4.3.1.2 Sandwich panel frame production

1. Roughening the slab surface.
2. Coating the slab and foam surfaces.
3. The slab and foam were bonded together and left for 12 hours to achieve proper adhesion, as shown in Figure (4.2).

Figure 4.2: Hands-On Preparation and Analysis of a Sandwich Sample

4.4 Three-point Bending Test

Three Point Bending test is a standard method used to measure the flexural behavior of materials. A load is applied at the center of a simply supported specimen, allowing the evaluation of bending stiffness and core shear strength, A universal testing machine (Model WDW-100F) was employed to conduct three-point bending tests. A perpendicular force was applied at the center of each specimen, generating force-displacement curves. Specimens of three different densities were tested, and the average values were reported. This test provided the measurements of the flexural modulus of elasticity and bending strength for each specimen. Specimen preparation followed the ASTM standard C393. Tests were performed at the room temperature (±25°C) with a loading speed of 100 mm/min, as shown in figure (4.3), All experimental tests were carried out in the Materials Engineering Laboratories at the University of Kufa.

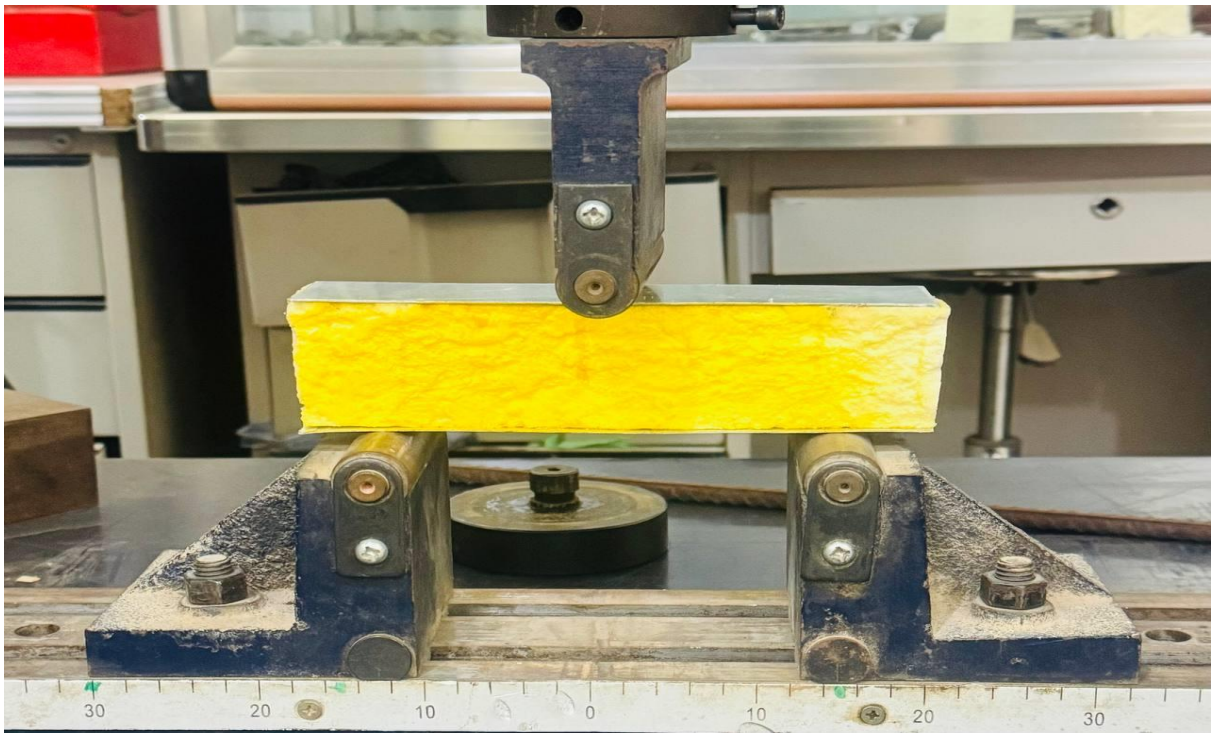

Figure 4.3: Three-point bending test .

Samples geometry refers to the physical dimensions and internal structure of the tested sandwich panels. In this study, specimens were designed with consistent face sheet dimensions, while the core geometry varied based on foam thickness (50 mm) and density, using an interlocking octagonal cell configuration.

The cross section of test specimen is shown in figure (4.4).

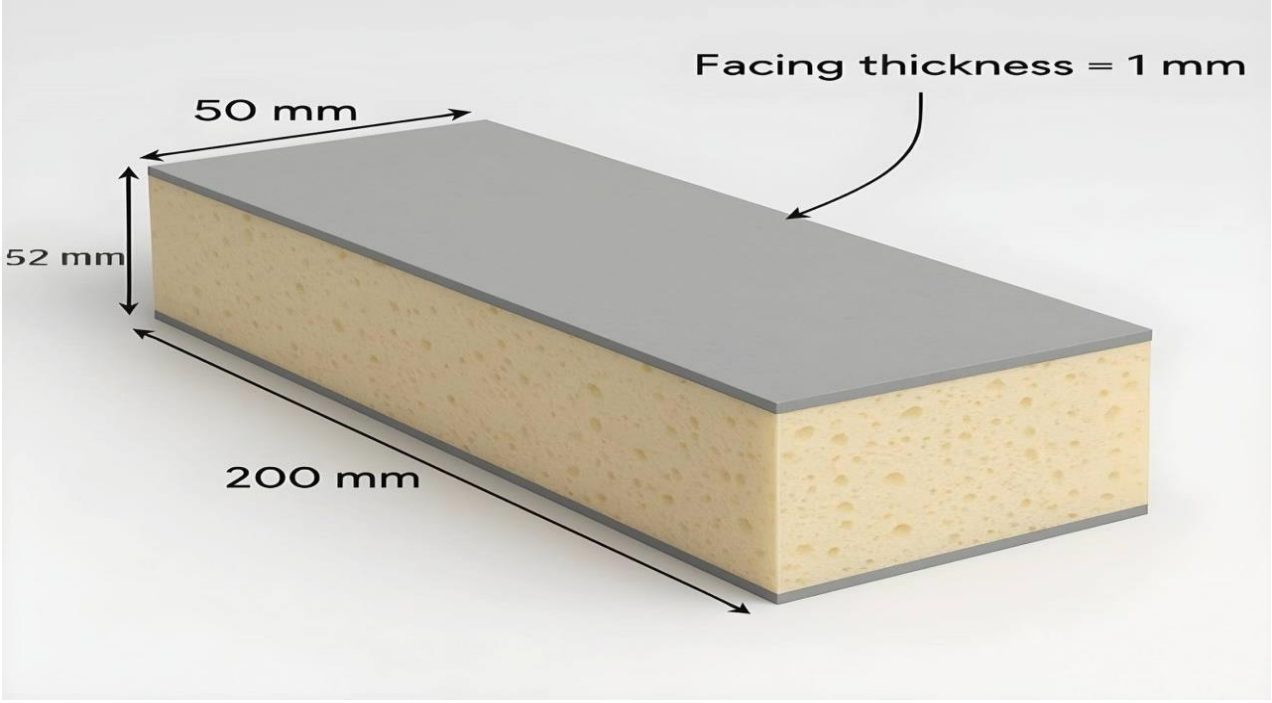

Figure 4.4: Sample geometry with selected dimensions.

- Where:
- Specimen length = 200 mm
- Specimen width = 50 mm
- Specimen thickness =52 mm
- Upper and lower facing thickness = 1 mm

4.5 Compression Testing

A universal testing machine was used to conduct the compression test. Then, curves representing the relationship between strength and deformation were drawn for each specimen, followed by curves representing the relationship between stress and strain for each specimen. Three specimens were tested for each laminated composite material, and the average value was determined. The strain resistance was determined, and ASTM standard C 365 was used to prepare compression-coated composite material specimens [95]. The test was conducted at the room temperature (±25°C) at a test speed (strain rate) of 100 mm/min, as shown in figure (4.5), The experimental work was conducted in the laboratories of the Department of Materials Engineering at the University of Kufa.

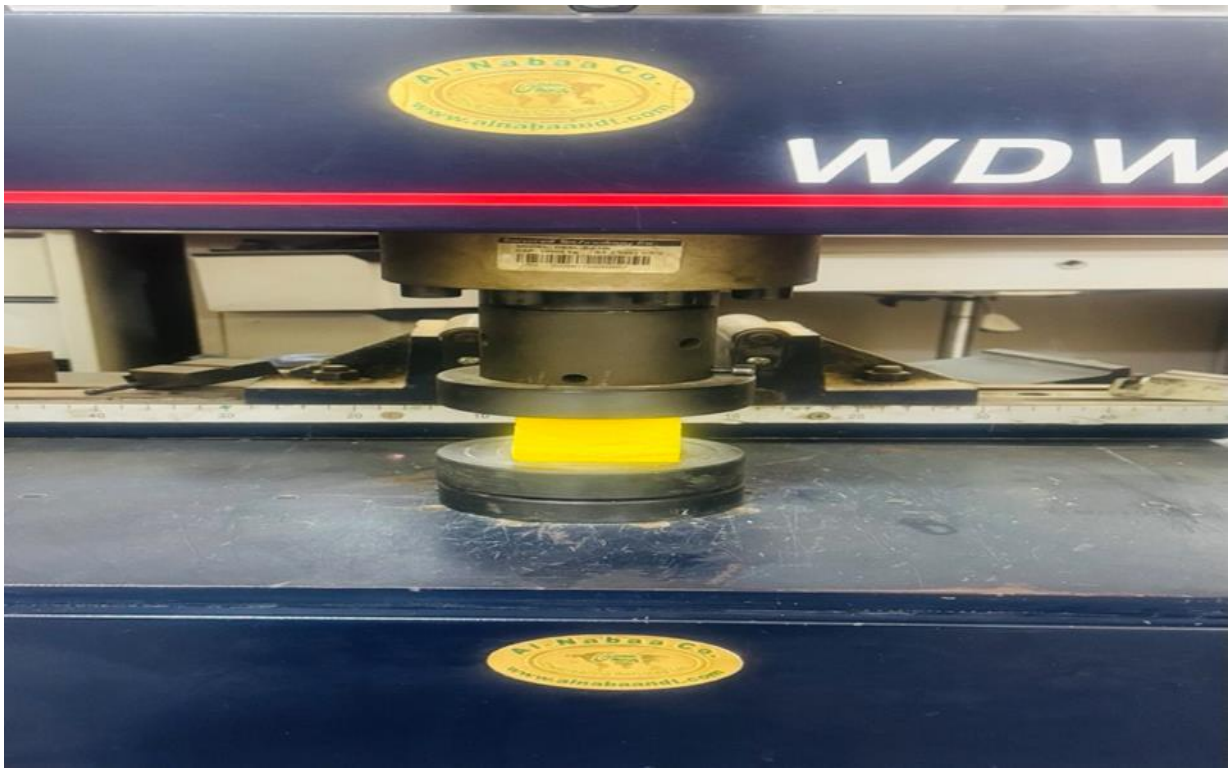

Figure 4.5: Compression test

Samples Geometry

The cross section of test specimen is shown in figure (4.6).

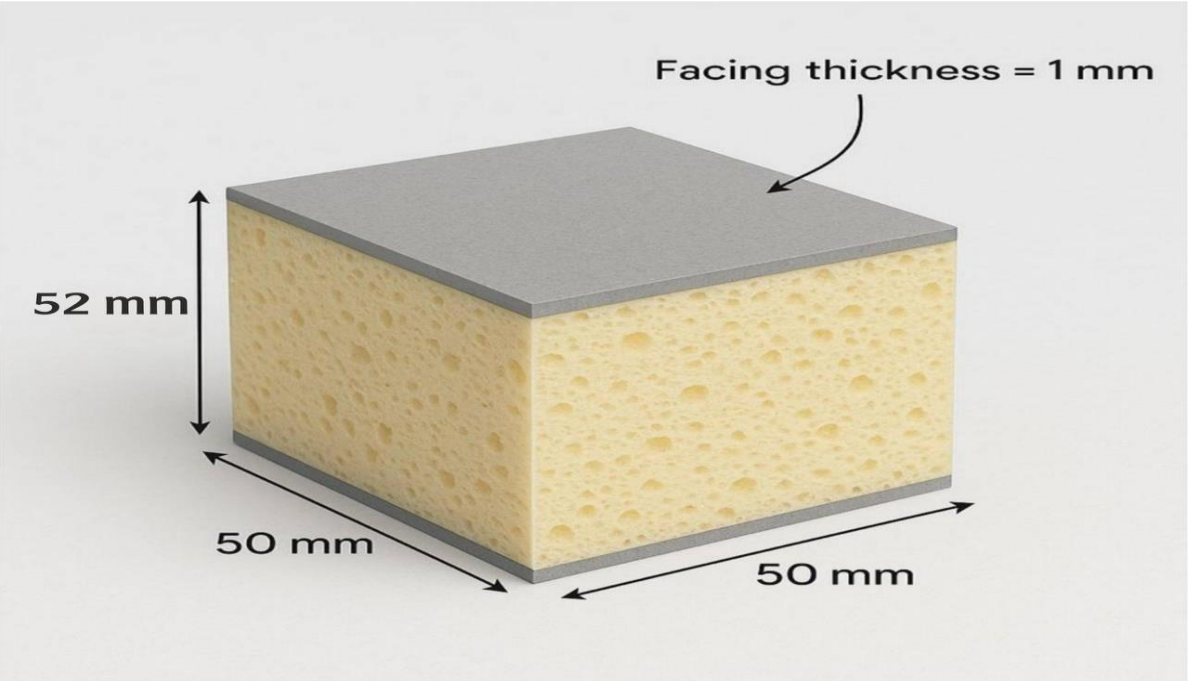

Figure 4.6: Sample geometry with selected dimensions.

Where:

- Specimen length = 50 mm
- Specimen width = 50 mm
- Specimen thickness = 52 mm
- Upper and lower Facing thickness = 1 mm

4.6 Free Vibration Test

Free vibration testing is used in engineering, including mechanical engineering, to reveal the hidden dynamics of structures. It is used to study the natural frequencies and corresponding mode shapes of the structure. By understanding the natural frequencies of a structure, one can determine how it will respond to different loads and disturbances. This is an important aspect of mechanical engineering, because it allows to design the structures that are safe, functional, and cost-effective

Samples geometry

The cross section of test specimen is shown in figure (4.7).

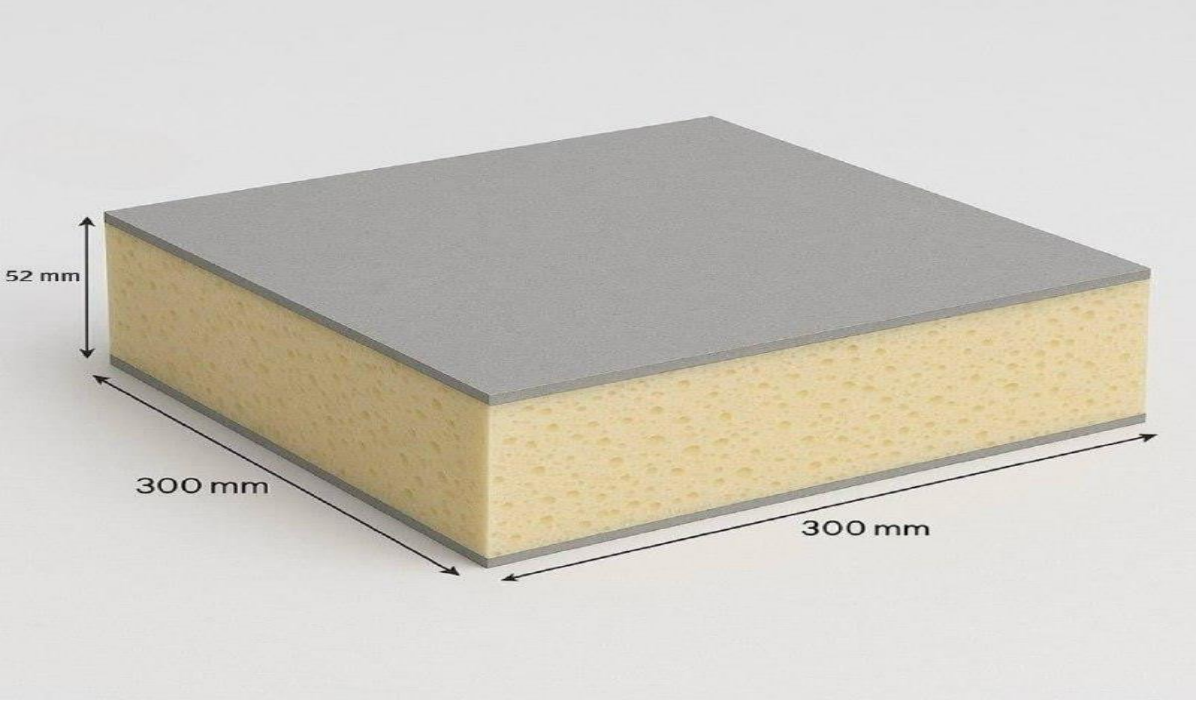

Figure 4.7: Sample geometry with selected dimensions.

Where:

- Specimen length = 300 mm
- Specimen width = 300 mm
- Specimen thickness =52 mm
- Upper and lower Facing thickness = 1 mm

4.6.1 Boundary plate condition

The top and bottom plates are simply supported on one side of the foam core, which acts as a Winkler foundation composed of independent linear springs. Due to its brittle nature, the foam significantly contributes to vibration absorption and damping, as shown in figure (4.8). The system was modeled based on the stiffness of brittle elastic foundations with simply supported boundary conditions, This model was used to evaluate the natural frequencies of composite slabs with varying thicknesses and dimensions, for both defect-free and defective cases

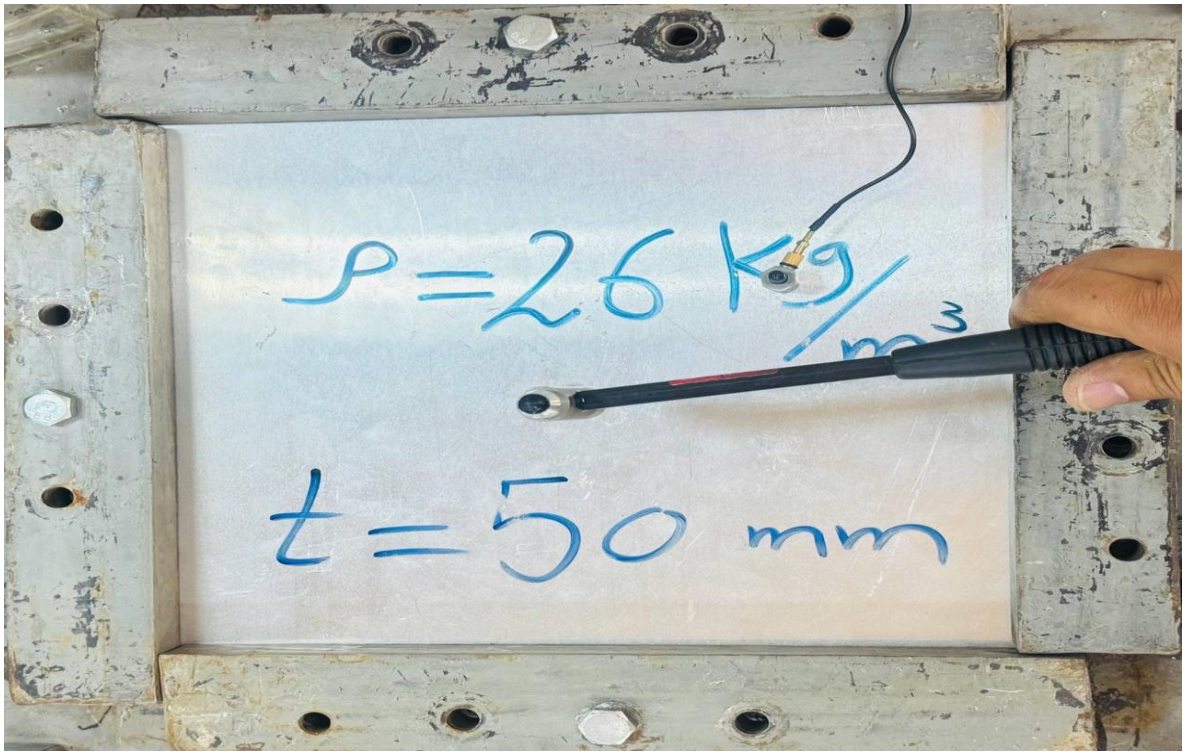

Figure 4.8: Boundary Condition of the Sandwich Plate

4.6.2 Impact hammer

The hammer consists of an integrated ICP quartz force sensor mounted on the striking end of the hammer head. This sensor transmits the impact force into an electrical signal from the plate to the sensor for displaying and analysis. Tips with different stiffness allow varying the pulse width and force frequency content. The striking end of the hammer has a threaded hole for mounting a variety of impact ends. These tips transfer the impact force to the sensor and protect the sensor face from damage. See figure (4.9). The focus was on performing dynamic analysis on the polymer matrix composites using rubber of different types and thicknesses, empioying both FEM and experimental investigations.

Figure 4.9:Impact Hammer

4.6.3 Accelerometer

It is a motion sensor device commonly used in release measuring devices for structures, buildings, and mechanical parts that are exposed to vibration or vibrations that occur in various mechanical works. The accelerometer was attached to the model to be examined using a transparent adhesive, See figure (4.10).

Figure 4.10: Accelerometer

4.6.4 Conditioning amplifier

The type 2626 amplifier (figure 4.11) is a compact signal amplifier designed for use with vibration sensors. It features a frequency range of 0.1 Hz to 30 kHz and gain of 0 to 60 dB. The internal resistance is 100 kΩ, and the output is 50 Ω, with a constant current of 6 mA. The compact, vibration- and shock-resistant design makes it suitable for use in measuring .

Figure 4.11: Amplifier

4.6.5 Digital Oscilloscope

It is a device specialized in analyzing the dynamic vibration and oscillation signals. Here are the main specifications of this model:

1. Frequency range: 0 Hz to 100 kHz, Number of input channels: 2 independent channels, Sampling rate: Up to 1 giga sample per second.
2. Analogue-digital conversion resolution: 12 bits.
3. Frame memory size: 4 MB sample per channel.
4. Display options: Frequency spectrum, vector wave and histogram .
5. Analysis functions: Spectrum analysis (including FFT), statistical measurements, and random spectroscopy.
6. Computer connection: USB interface for remote control and analysis .
7. Dimensions: 320 x 159 x 130 mm, containing a RAM port .

This analyzer (figure 4.12) provides the ability to capture and analyze the vibration signals with a high accuracy and reliable performance and is commonly used in the vibration measurement applications for machinery, vehicles and infrastructure.

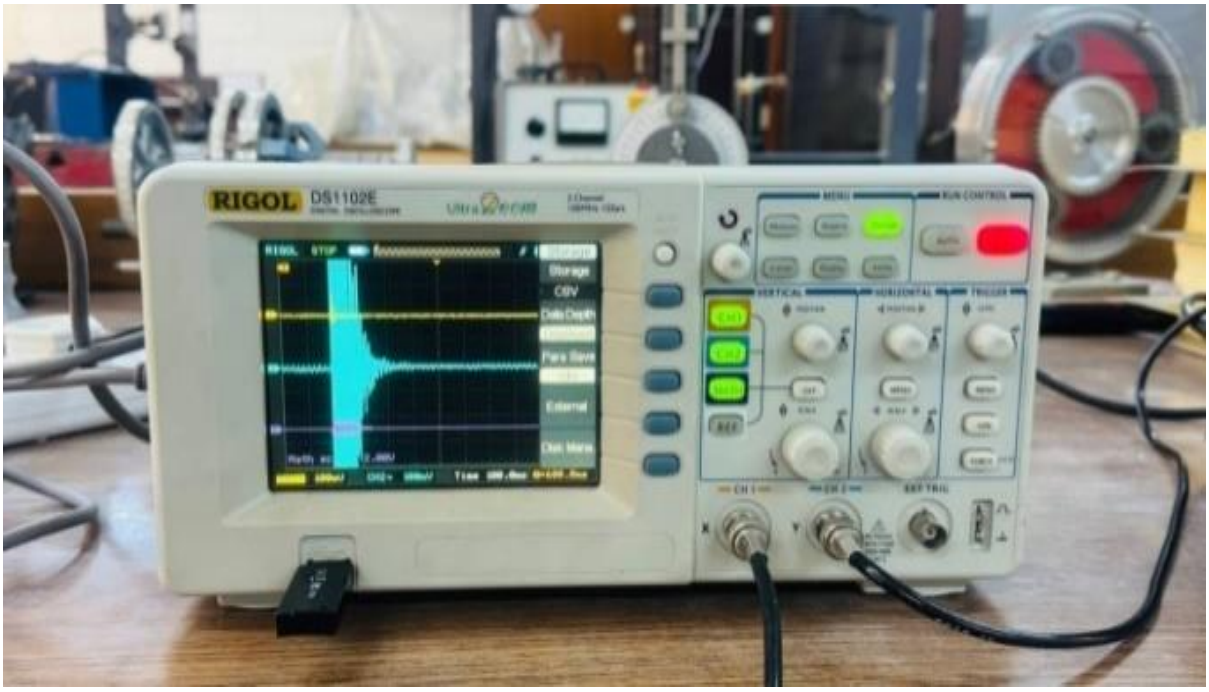

Figure 4.12: Oscilloscope

4.7 Steps for Vibration Examination of Plate Samples

The following procedure will be conducted to get free vibration frequency, Figure (4.13):

1. Mounting the plate sample on the vibration test device.
2. Placing the accelerometer onto the board.
3. Connecting the accelerometer sensor to the amplifier.
4. Connecting the amplifier to a digital storage oscilloscope.
5. Connecting the flash memory to the digital storage card.
6. Loading the input pulse using the hammer tool.
7. Capturing the plate reaction using an accelerometer.
8. Recording the load and response signals to flash memory.
9. Transferring the load and response signals to the computer with digital storage via flash memory.
10. Using the waveform analysis software such as Sig View to process the signals.
11. Evaluating the fundamental natural frequency using Fast Fourier transform function (FFT) of the response signal (figure 4.14).

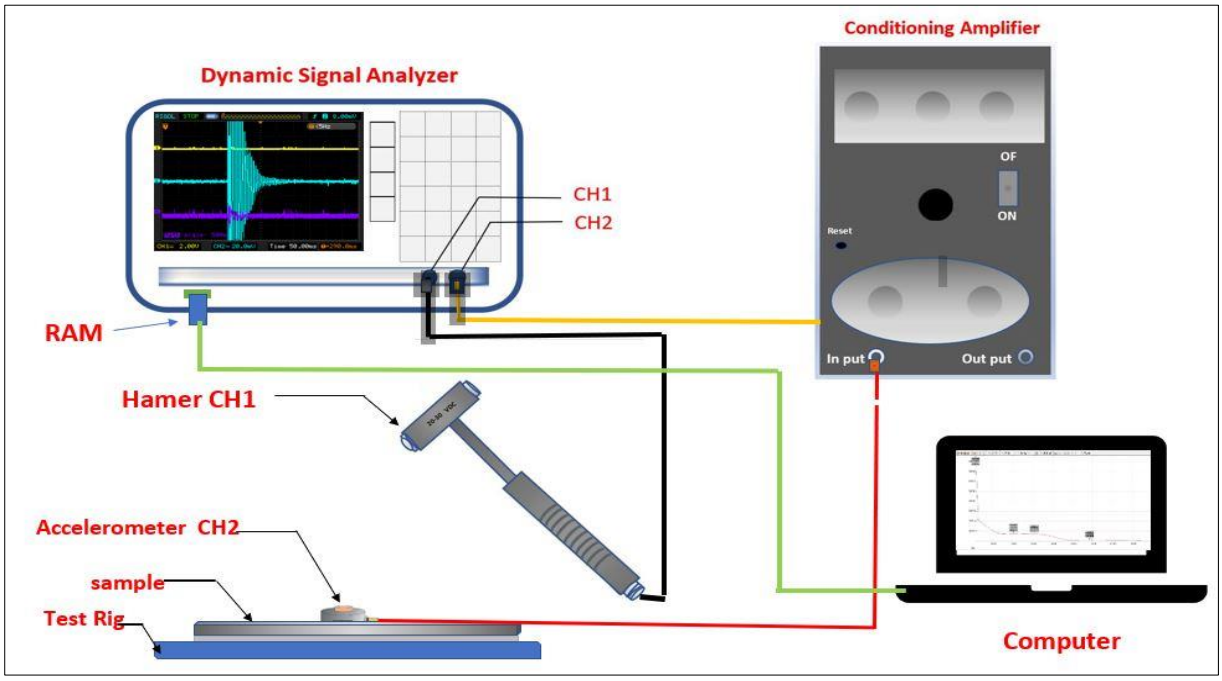

Figure 4.13: Free Vibration test

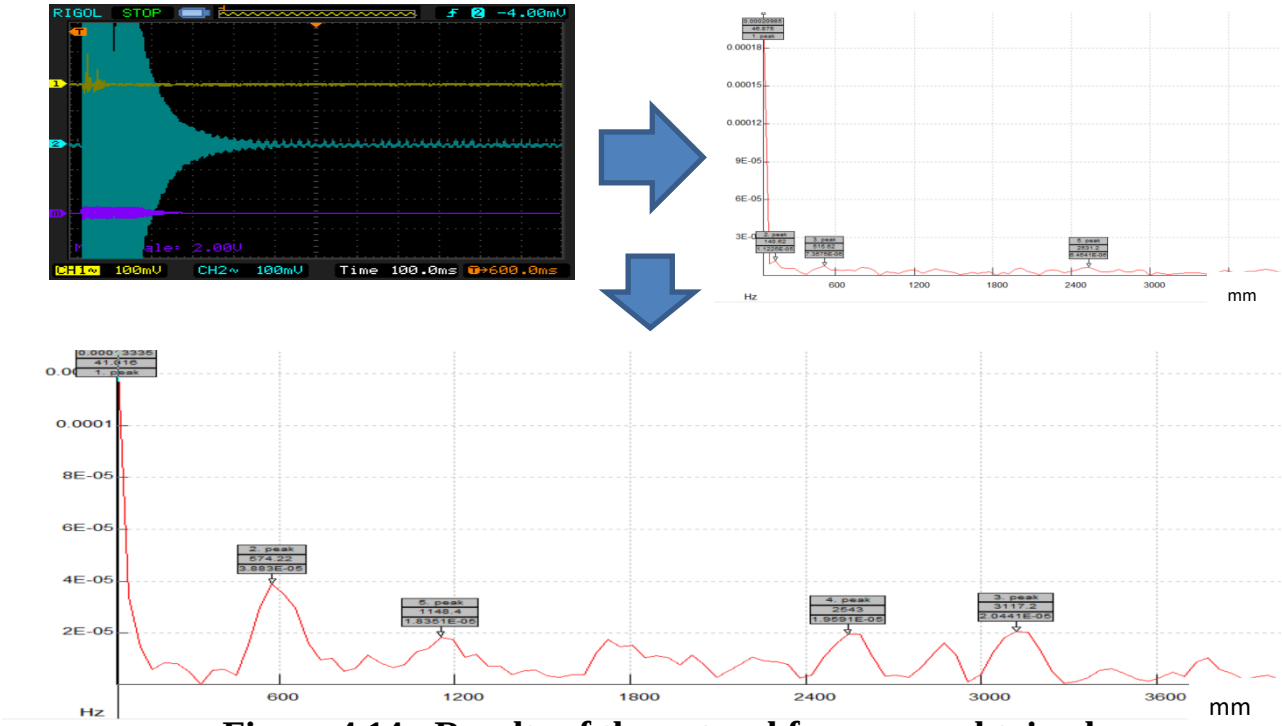

Figure 4.14: Results of the natural frequency obtained

CHAPTER FIVE

Results and Discussion

5.1 General

This chapter provides a comprehensive presentation and analysis of the Analytical, numerical, and experimental results. Initially, the Three Point Bending test data for polylactic acid (PLA) were examined to establish its mechanical properties for integration into simulation models. Subsequently, all available Analytical solutions were reviewed to identify the key influencing parameters, followed by a comparative assessment of the experimental, Analytical, and numerical findings to evaluate their consistency.

5.2 Experimental Results

5.2.1 Density determination results

To calculate the density in a simple way, the mass of each specimen was first measured using a precise scale. Then, the volume was calculated by multiplying the specimen's dimensions (length × width × thickness), using the basic formula:- Density = Mass ÷ Volume

These calculations allowed to classify the foam samples into different density groups (26, 34, and 40 kg/m³), which were used in the mechanical analysis and testing, see in (Table 5.1)

Table 5.1: Density test results for foam

Model	Mass in Air (gram)	Volume (cm^3)	Density (g/cm^3)	Computed Results	Density (kg/m^3)
1	13	5*5*20	0.026		26
2	17	5*5*20	0.034		34
3	20	5*5*20	0.040		40

It is important to note that the computed density value is reasonably similar to the numbers provided by the manufacturers [56] .

5.2.2 Three Point Bending test results

The bending test was conducted to evaluate the flexural strength and deformation behavior of the sandwich panel specimens. Samples with foam core thicknesses of (25 mm and 50) mm were subjected to a gradually increasing load until failure, as shown in Figure (5.1),According to the experimental data presented in Table (5.2),(5.3) and (5.4), the (25 mm and 50) thick samples demonstrated resistance to bending loads, making it more suitable for applications requiring higher bending capacity. These findings are consistent with the results reported in Reference [27]. Furthermore, the calculated bending stiffness coefficients were incorporated into the ANSYS simulation as input parameters to validate and compare the numerical results with the experimental observations [25].

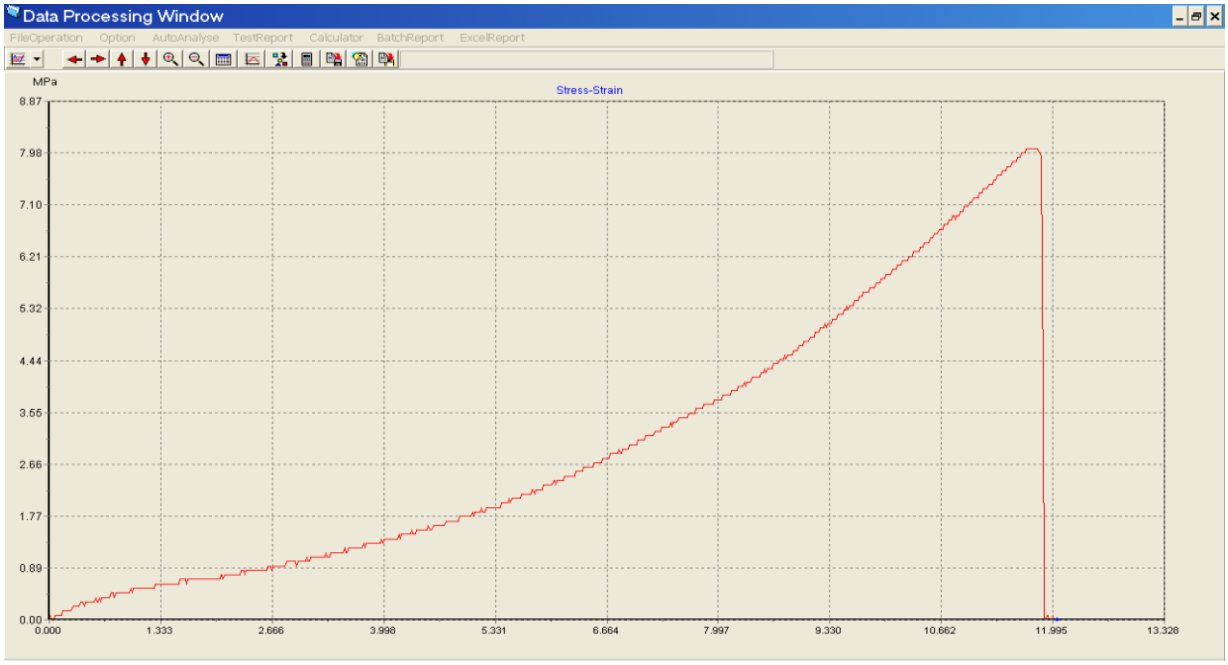

Figure 5.1: Test model stress – strain to sandwich plate

Table 5.2 Results of foam three-point bending test for type (A)

T1			T2			T3		
Strain%	Stress (Mpa)	Flexural modulus (Mpa)	Strain%	Stress (Mpa)	Flexural modulus (Mpa)	Strain%	Stress (Mpa)	Flexural modulus (Mpa)
10.98	7.98	82.3	11.98	7.98	72.3	12.87	8.93	70.1
$E = \delta\ \sigma Ave/\ \delta\ \epsilon Ave$					72.3 Mpa			

Table 5.3 Results of foam three-point bending test for type (B)

T1			T2			T3		
Strain%	Stress (Mpa)	Flexural modulus (Mpa)	Strain%	Stress (Mpa)	Flexural modulus (Mpa)	Strain%	Stress (Mpa)	Flexural modulus (Mpa)
13.73	9.77	92.3	10.90	10.99	100.6	14.11	11.87	119.8
$E = \delta\ \sigma Ave/\ \delta\ \epsilon Ave$					100.6 Mpa			

Table 5.4 Results of foam three-point bending test for type (C)

T1			T2			T3		
Strain%	Stress (Mpa)	Flexural modulus (Mpa)	Strain%	Stress (Mpa)	Flexural modulus (Mpa)	Strain%	Stress (Mpa)	Flexural modulus (Mpa)
14.91	10.2	119.3	10.16	12.76	123.3	15.11	13.80	149.9
$E = \delta\ \sigma Ave/\ \delta\ \epsilon Ave$					123.3 Mpa			

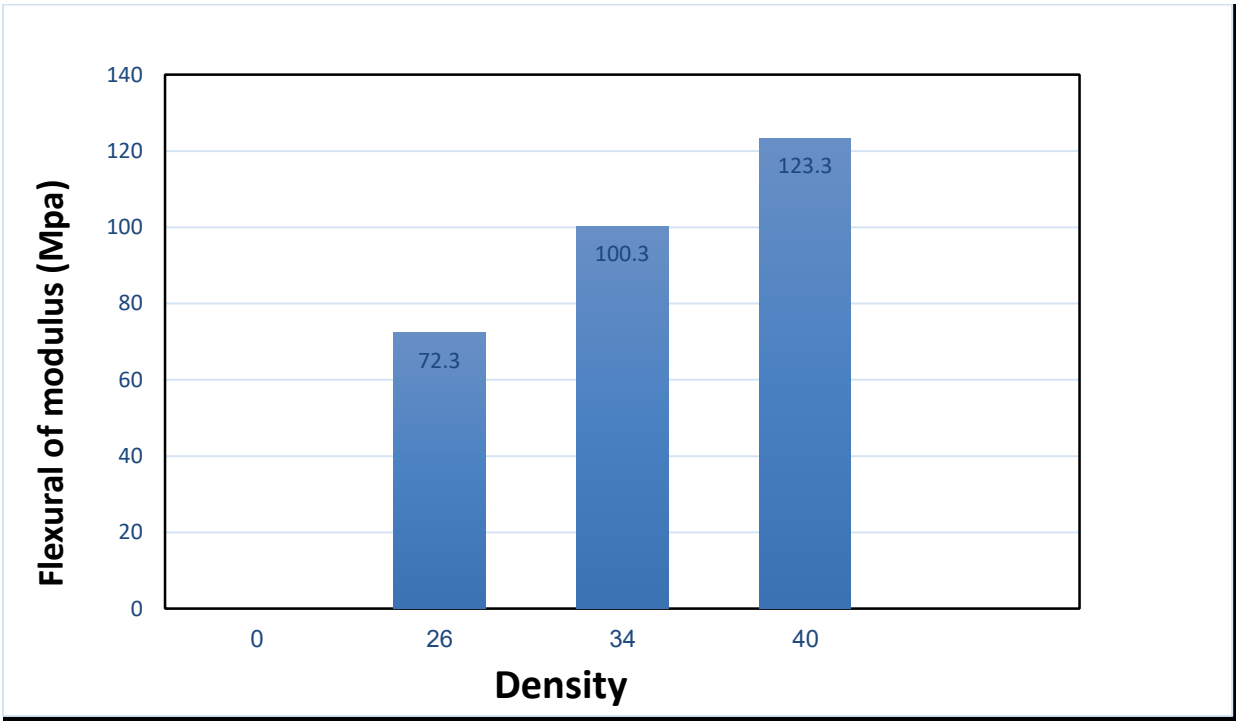

Figure 5.2 : The flexural of elasticity of the all types of foam materials (A, B and C)

5.2.3 Compression test results

When manufacturing the samples, the selected materials must be able to withstand environmental conditions and applied loads. This necessitates sufficient compressive strength, as the primary load is transferred through the core**.** As illustrated in Figure (5.3) and presented in Tables (5.5)**,** (5.6), and (5.7), the compressive strength of the foam increases with the density. This behavior is attributed to the enhanced internal cell structure of higher-density foams, which improves their load-bearing capacity. In addition, the results show that compressive strength also increases for higher-density foams, reflecting their greater mechanical resistance under the axial compression.

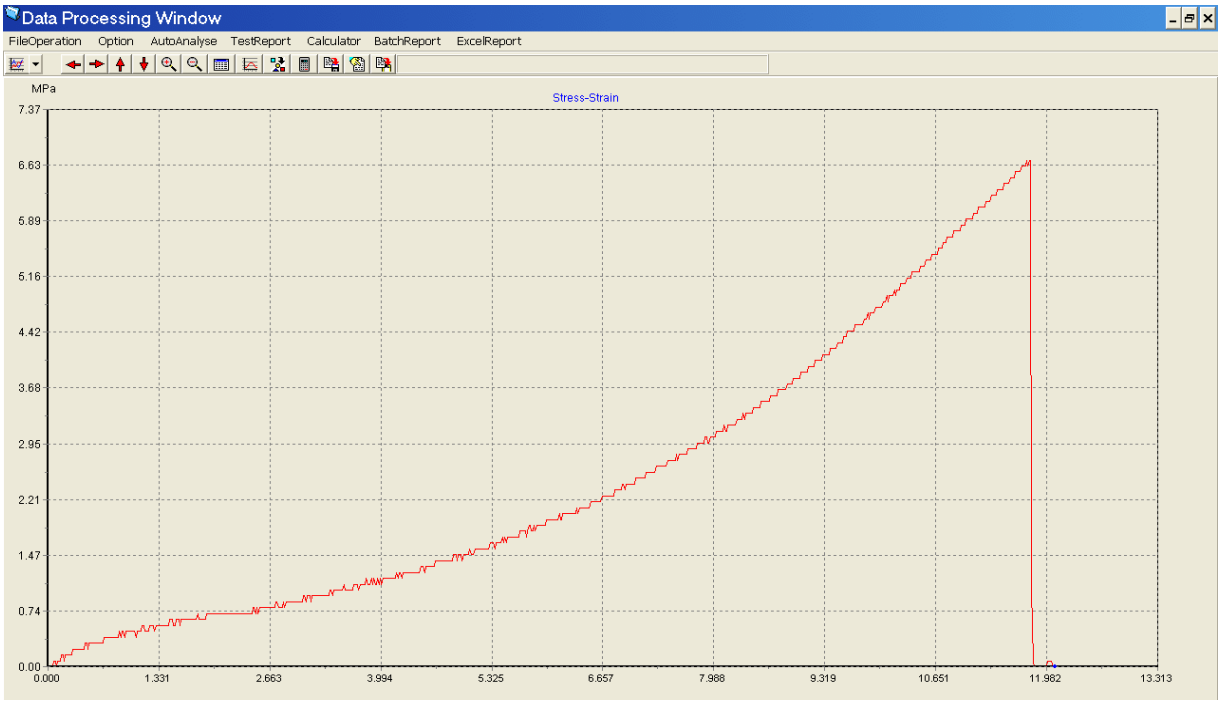

Figure 5.3: Test model stress – strain to sandwich plate

Table 5.5: Results of foam compression test for type (A)

T1			T2			T3		
Strain%	Stress (Mpa)	Young's modulus (Mpa)	Strain%	Stress (Mpa)	Young's modulus (Mpa)	Strain%	Stress (Mpa)	Young's modulus (Mpa)
10.98	5.98	54.12	11.27	6.63	58.82	12.05	7.28	60.66
$E = \delta\ \sigma Ave/\ \delta\ \epsilon Ave$					58.82 MPa			

Table 5.6: Results of foam compression test for type (B)

T1			T2			T3		
Strain%	Stress (Mpa)	Young's modulus (Mpa)	Strain%	Stress (Mpa)	Young's modulus (Mpa)	Strain%	Stress (Mpa)	Young's modulus (Mpa)
12.01	7.80	9.23	12.90	8.35	69.58	13.06	9.91	76.34
$E = \delta\ \sigma Ave/\ \delta\ \epsilon Ave$					69.58Mpa			

Table 5.7: Results of foam compression test for type (C)

T1			T2			T3		
Strain%	Stress (Mpa)	Young's modulus (Mpa)	Strain%	Stress (Mpa)	Young's modulus (Mpa)	Strain%	Stress (Mpa)	Young's modulus (Mpa)
12.91	9.20	71.31	13.16	9.87	75.92	13.98	10.83	77.69
$E = \delta\ \sigma Ave/\ \delta\ \epsilon Ave$					75.92 Mpa			

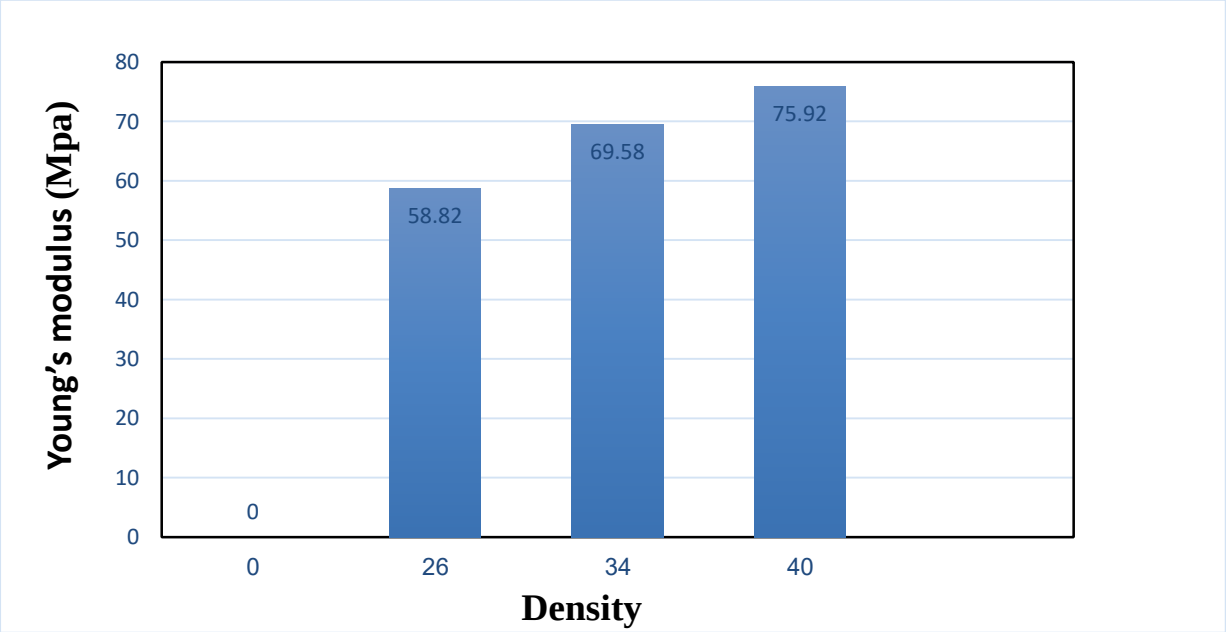

Figure 5.4: The modulus of elasticity of the all types of foam materials (A, B and C)

5.2.4 Free Vibration Test

5.2.4.1 Damping Caculations

In this section, the damping coefficients were experimentally determined for foam samples with two thicknesses (25 mm and 50 mm) and three different densities (26, 34, and 40 kg/m³). The aim is to evaluate the influence of both thickness and density on the damping behavior of the foam materials.

Table 5.8: The experimental findings of the damping coefficient

No	Density (kg/m³)	Thickness (mm)	Peak.1 (mv)	Peak.2 (mv)	$\delta = ln\frac{pea1}{peak2}$	$\xi = \frac{\delta}{\sqrt{4\pi^2+\delta^2}}$
1	26	50	0.00021	0.00012	0.53831	0.08769
2	26	25	0.00017	0.00002	0.98205	0.15396
3	34	50	0.00013	0.00012	0.69642	0.08594
4	34	25	0.00016	0.00008	0.92710	0.14387
5	40	50	0.00027	0.00016	0.53871	0.08253
6	40	25	0.00013	0.00003	0.83690	0.13734

5.2.4.2 Natural Frequency Caculations

In this section, the natural frequencies of the foam specimens were experimentally evaluated at two thicknesses (25 mm and 50 mm) and three different densities (26, 34, and 40 kg/m³). The purpose of these calculations is to investigate the effect of foam thickness and density on the dynamic stiffness and vibrational response of the material.

1. Foam model (density = 26 kg/m³)

A. Foam Core Sample with 50 mm thickness

Figure (5.5) evinces the response image in the oscillations of a model (A1) which was obtained in the laboratory and was analyzed and converted into a Fast Fourier waveform for the response of the SIGVIEW program. After finding the natural frequency values through it for three strokes, in each stroke, the accelerating sensor differs to show whether there is a difference in the natural frequency values, as shown in the Figures (5.6), The detailed test results are presented in Table (5.9).

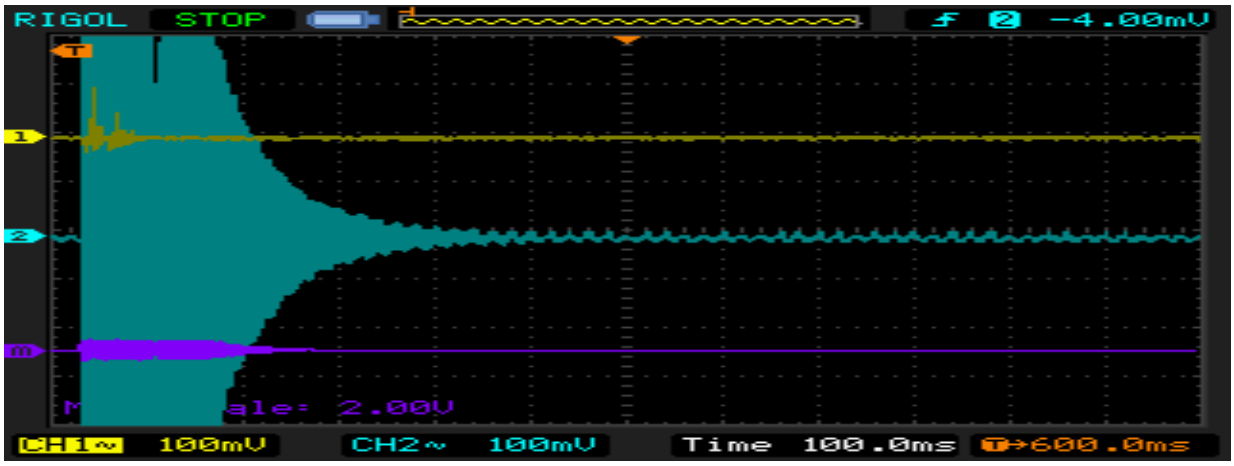

Figure 5.5: Image of response in the oscilloscope for model A1

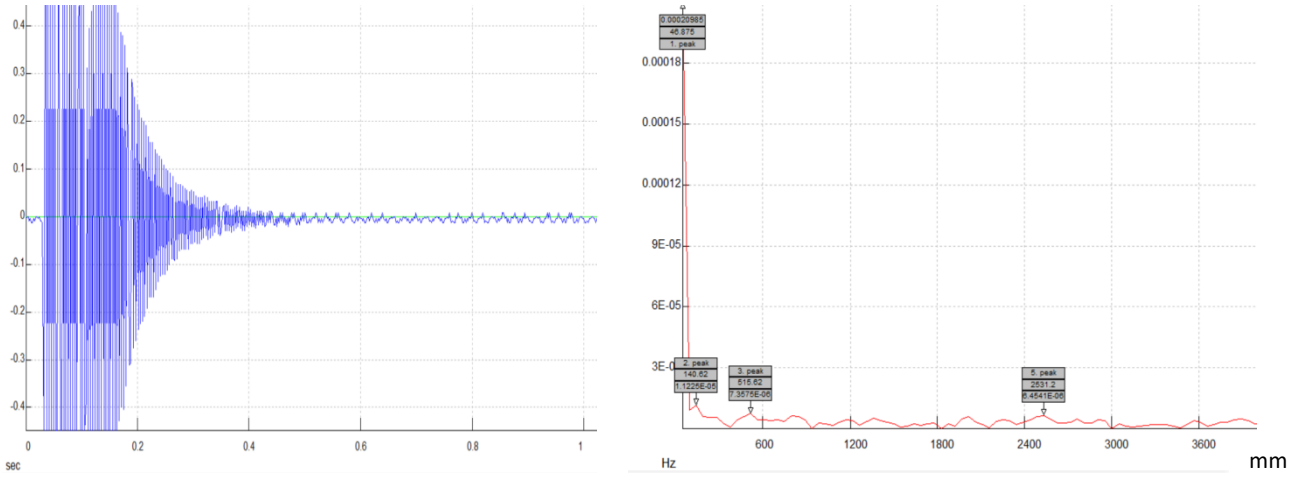

Figure 5.6: First stroke FRF analysis of the response waveform (SIGVIEW program) for model A1

Table 5.9: The experimental findings of the damping frequency A1.

No	Natural frequency (HZ)	$w_n = 2\pi f$ (r.p.m)	$w_d = w_n\sqrt{1-\xi^2}$ (r.p.m)
1	46.87	296.6	293,87

B. Foam Core Sample with 25 mm thickness

Figure (5.7) manifests the response image in the oscillations of the model (A2) which was obtained in the laboratory and was analyzed and converted into a Fast Fourier waveform for the response of the SIGVIEW program, after finding the natural frequency values figure (5.8), The detailed test results are given in Table (5.10).

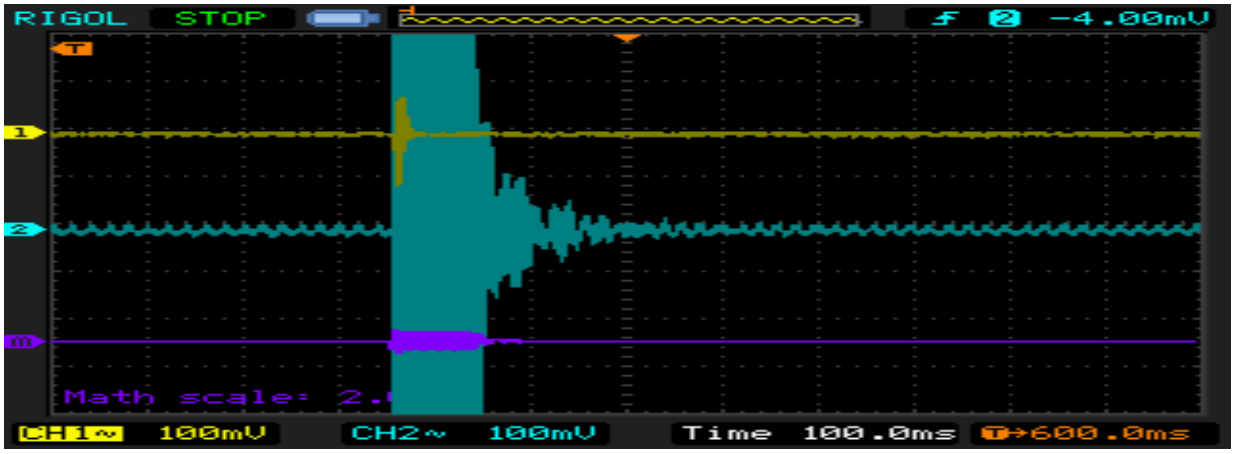

Figure 5.7: Image of response in the oscilloscope for model A2.

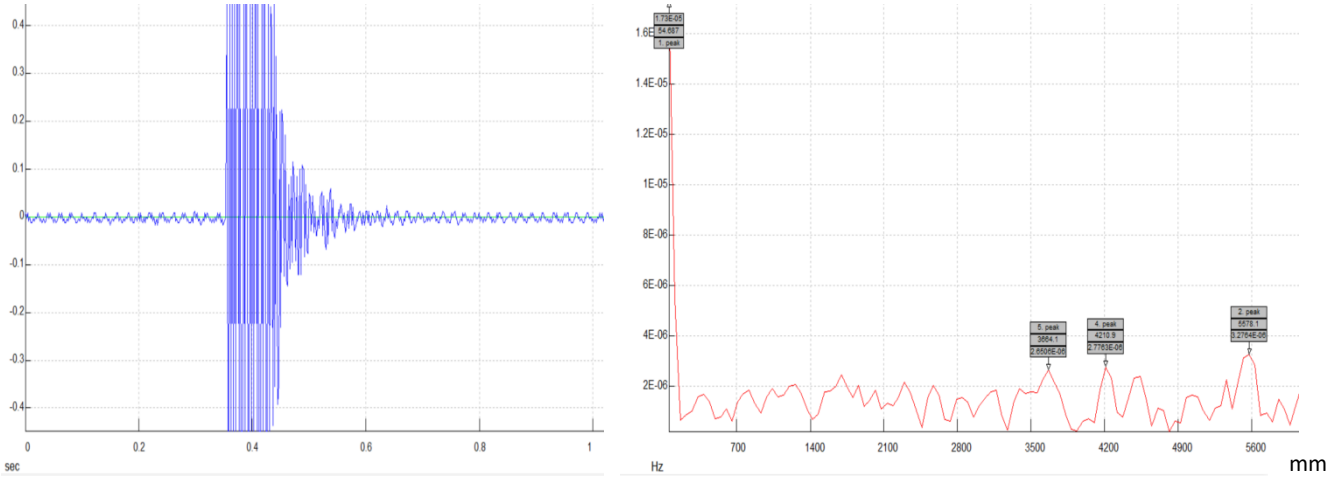

Figure 5.8: The FRF analyses of the response wave (SIGVIEW program) for model A2

Table 5.10: The experimental findings the damping frequency A2

Force No.	Natural frequency (HZ)	$w_n = 2\pi f$ (r.p.m)	$w_d = w_n\sqrt{1-\xi^2}$ (r.p.m)
1	54.68	350.79	344.91

2. Foam model (density = 34 kg/m³)

A. Foam Core Sample with 50 mm thickness

Figure (5.9) elucidates the response image in the oscillations of the model (B1) which was obtained in the laboratory and was analyzed and converted into a Fast Fourier waveform for the response of the SIGVIEW program, after finding the natural frequency values (figure 5.10), The detailed test results are depicted in Table (5.11).

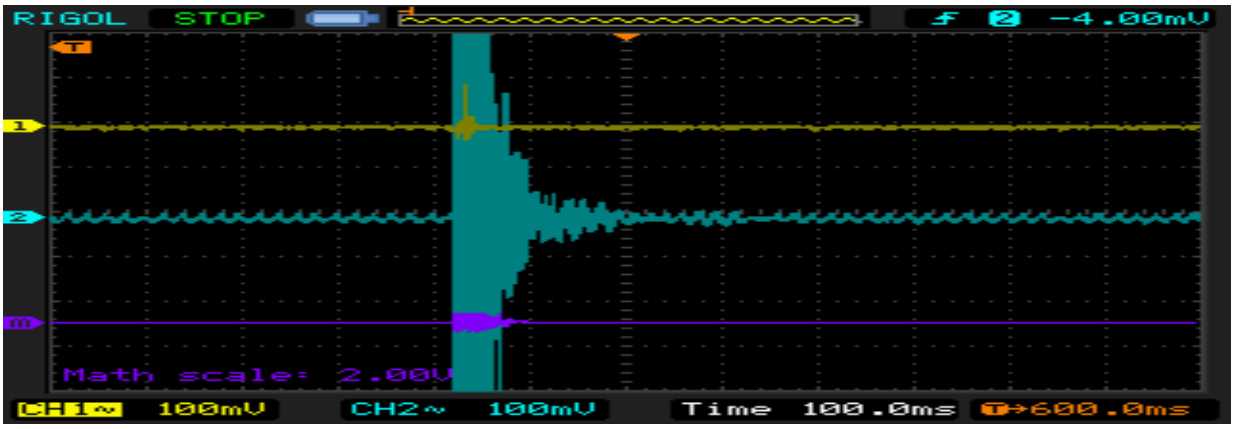

Figure 5.9: Image of response in the oscilloscope for model B1

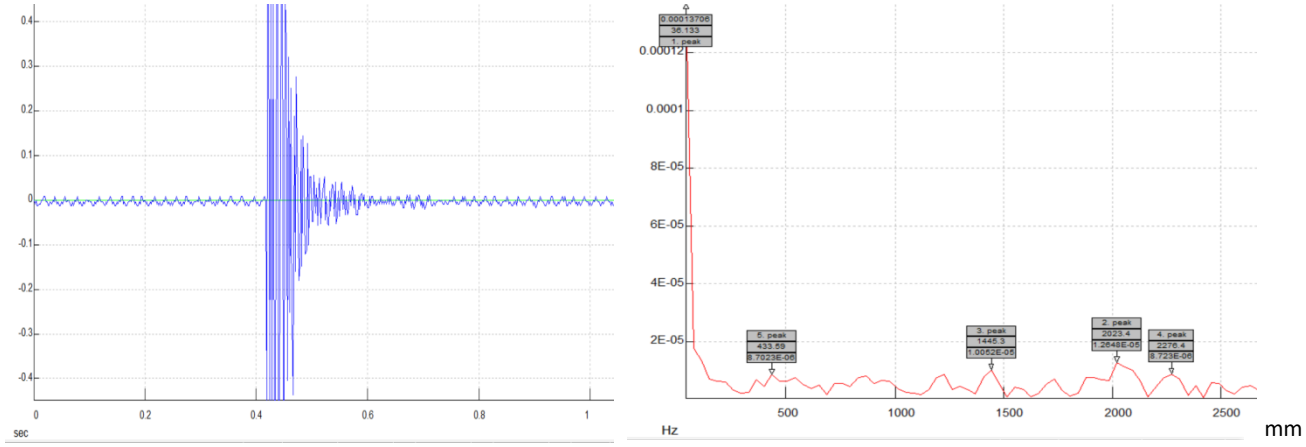

Figure 5.10: The FRF analyses of the response wave (SIGVIEW program) for model B1

Table 5.11: The experimental of findings the damping frequency B1

Force No.	Natural frequency (HZ)	$w_n = 2\pi f$ (r.p.m)	$w_d = w_n\sqrt{1-\xi^2}$ (r.p.m)
1	36.13	228.1	226.8

B. Foam Core Sample with 25 mm thickness

Figure (5.11) portrays the response image in the oscillations of the model (B2) which was obtained in the laboratory and was analyzed and converted into a fast Fourier waveform for the response of the SIGVIEW program, after finding the natural frequency values figure (5.12). The results are revealad in Table (5.12).

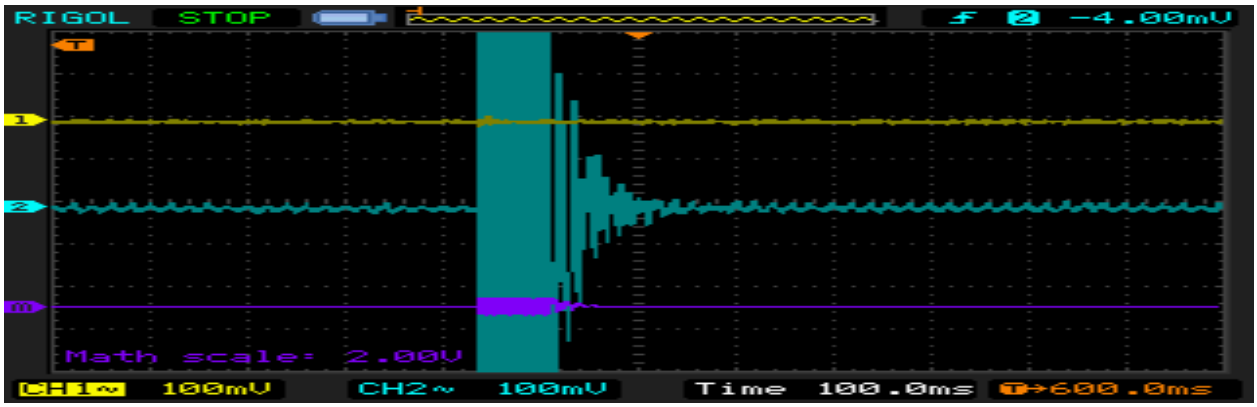

Figure 5.11: Image of response in the oscilloscope for model B2

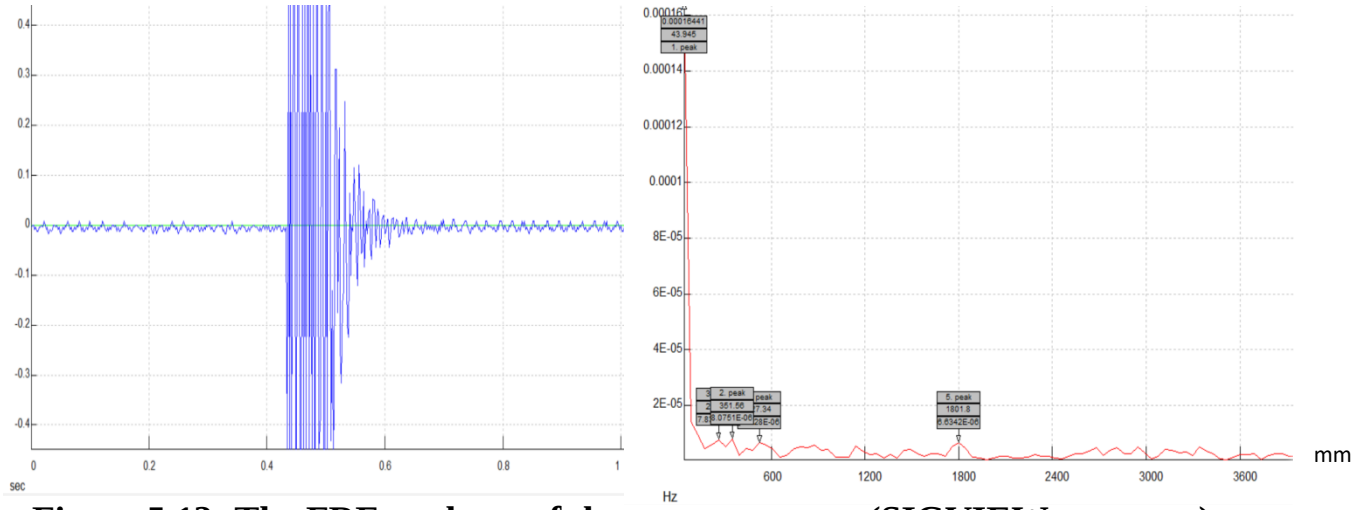

Figure 5.12: The FRF analyses of the response wave (SIGVIEW program) for model B2.

Table 5.12: The experimental of findings the damping frequency B2

Force No.	Natural frequency (HZ)	$w_n = 2\pi f$ (r.p.m)	$w_d = w_n\sqrt{1-\xi^2}$ (r.p.m)
1	43.94	278.2	276.03

3. Foam model (density = 40 kg/m³)

A. Foam Core Sample with 50 mm thickness

Figure (5.13) displays the response image in the oscillations of the model (C1) which was obtained in the laboratory and was analyzed and converted into a Fast Fourier waveform for the response of the SIGVIEW program, after finding the natural frequency values figure (5.14). The results are shown in Table (5.13).

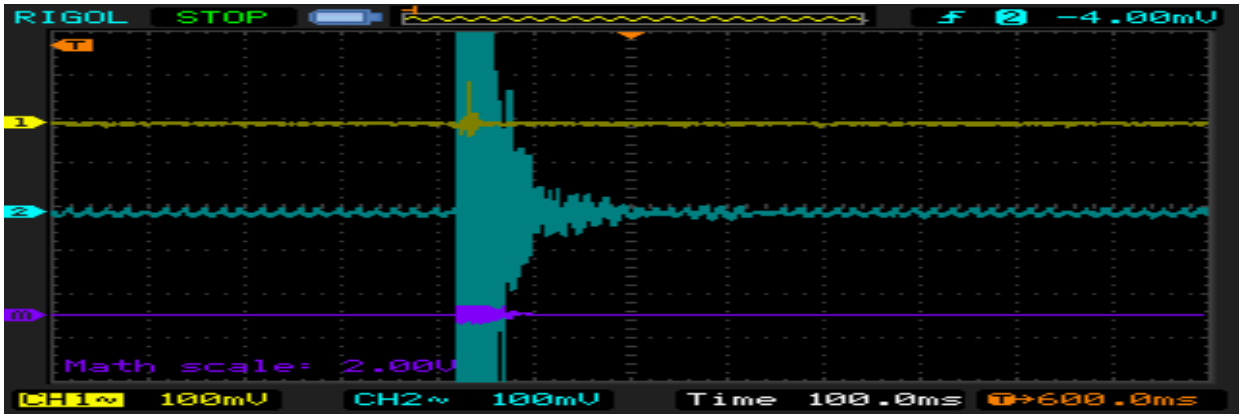

Figure 5.13: Image of response in the oscilloscope for model C1

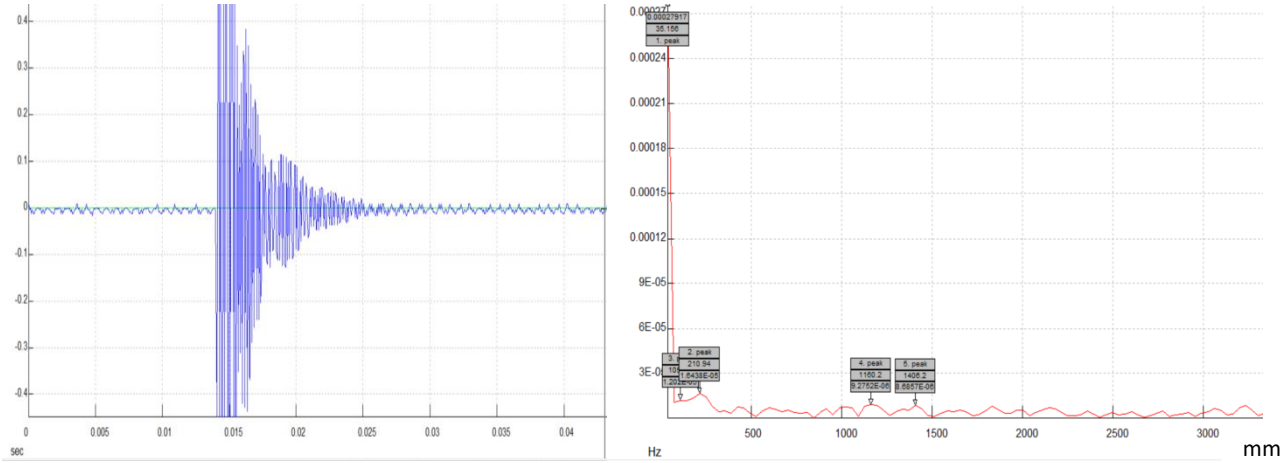

Figure 5.14: The FRF analyses of the response wave (SIGVIEW program) for model C1

Table 5.13: The experimental finding of the damping frequency C1

Force No.	Natural frequency (HZ)	$w_n = 2\pi f$ (r.p.m)	$w_d = w_n\sqrt{1-\xi^2}$ (r.p.m)
1	35.15	220.3	219.1

B. Foam Core Sample with 25 mm Thickness

Figure (5.15) demonstrates the response image in the oscillations of the model (C2) which was obtained in the laboratory and was analyzed and converted into a fast Fourier waveform for the response of the SIGVIEW program, after finding the natural frequency values figure (5.16), The detailed test results are presented in Table (5.14).

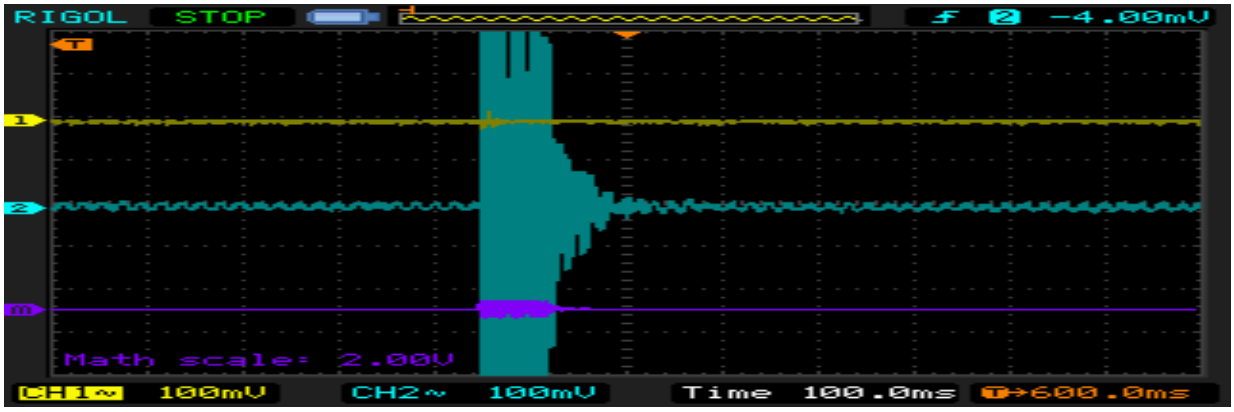

Figure 5.15: Image of response in Oscilloscope for model C2

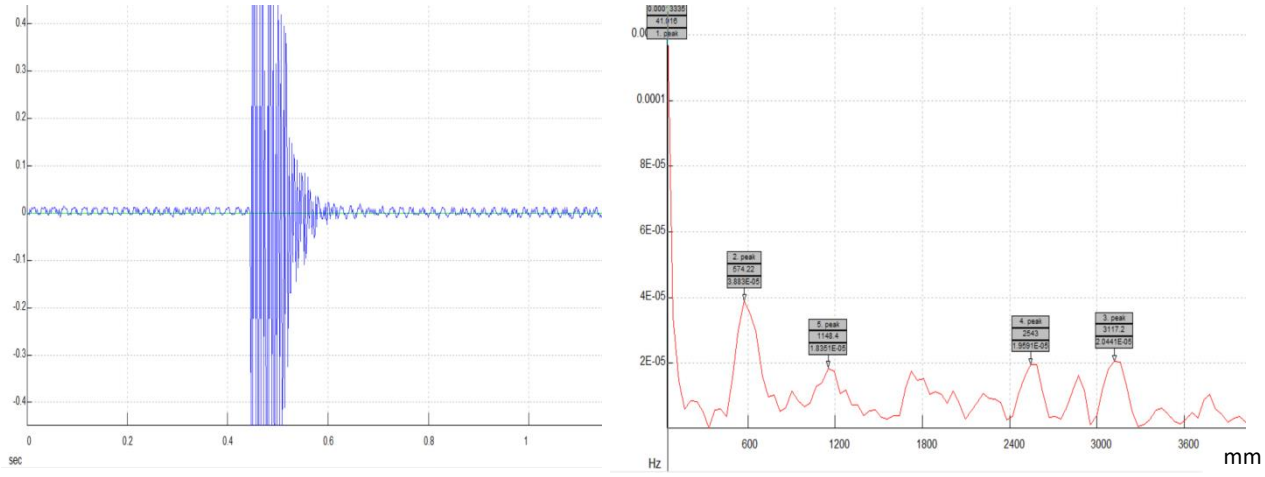

Figure 5.16: The FRF analyses of the response wave (SIGVIEW program) for model C2

Table 5.14: The experimental findings of the damping frequency C2

Force No.	Natural frequency (HZ)	$w_n = 2\pi f$ (r.p.m)	$w_d = w_n\sqrt{1-\xi^2}$ (r.p.m)
1	41.91	266.5	264.7

5.3 Analytical Results

The natural frequencies of sandwich specimens with the foam cores of varying densities (26, 34, and 40 kg/m³) were analytically calculated across a thickness range of 25 mm to 50 mm. These calculations were carried out using Equations (3.30) and (3.43), under the same boundary conditions applied during the experimental procedures to ensure the consistency. This methodology allowed for a direct and meaningful comparison between Analytical predictions and experimental results. The calculated values are graphically presented in Figure (5.17) and summarized in Table (5.15).

It was noted that the foam with a density of 26 kg/m³ consistently exhibited higher natural frequencies across all thicknesses compared to the higher density counterparts. This behavior is primarily due to its lower mass and relatively higher stiffness to weight ratio. Nonetheless, the minor variations in the recorded values may have resulted from the environmental conditions during the testing, such as fluctuations in temperature, humidity, or ambient laboratory vibrations. These factors tend to have a more pronounced effect on the low density materials, potentially influencing their dynamic response and leading to slight deviations in the measured outcomes.

Table 5.15: Effect of density of (26, 34, and 40 Kg/ m^3) density specimens *Analytical*

Thickness (mm)	Natural frequency (rad/s)		
	26 Kg/m^3	**34 Kg/m^3**	**40 Kg/m^3**
50	273.2	226.9	221.9
45	279.4	230.1	223.7
40	283.4	234.7	229.8
35	294.7	239.2	232.1
30	299.8	246.9	237.4
25	312.5	251.3	244.3

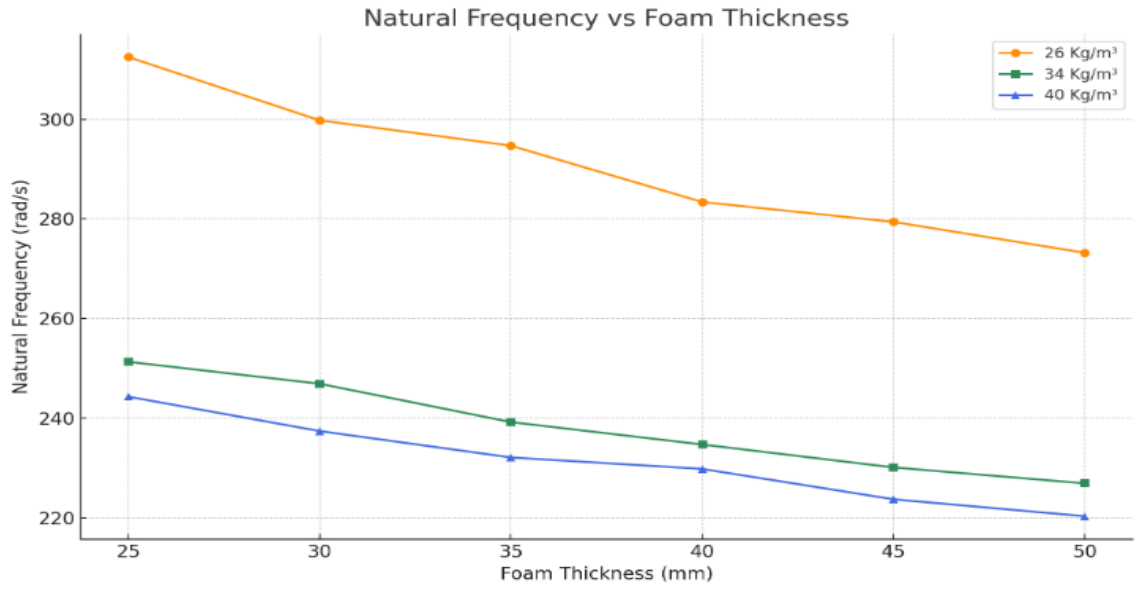

Figure 5.17: Variation of natural frequency with different foam thicknesses

5.4 Determination of the Numerical Analysis Results of Natural Frequencies

The first section includes a presentation of the mathematical results of calculating the natural frequencies in the ANSYS 2018 R1 program, taking into account their effect on the properties of different materials as well as the thickness and width of the Foam. A research study was conducted to match these different properties, where the equations and mathematical models were used to synthesize these results, providing a basis for an analysis to deal with the system. The plate properties for all models A , B and C are included in Tables (5.16) and (5.17) used as input data in the numerical models.

Table 5.16: Geometry and Meterial Properties for the Sandwich Plate

Property	Symbol	*Units*	Geometry Value	Type A	Type B	Type C
Length	a	***MM***	300	-	-	-
Width	b	***MM***	300	-	-	-
Thickness	h	***MM***	52	-	-	-
Flexural Modulus	E	***MPa***	-	72.30	100.60	123.30
Density	ρ	***kg/m³***	-	26	34	40
Poisson's Ratio	ν	-	-	0.31	0.33	0.35

Table 5.17: Mechanical properties of the Plate Meterial

Rectangular Sandwich Plate (mm)	Young's Modulus (Mpa)	Poisson's Ratio	Bulk Modulus (Mpa)	Shear Modulus (Mpa)
300*300*1	71000	0.33	69608	26692

Using ANSYS 2018 R1, the natural frequencies of each sample were calculated. The samples were modeled with simply supported boundary conditions, meaning the plates were supported along their edges. This type of support reflects realistic constraints commonly used in the vibration analysis of plates and provides an appropriate condition for calculating the natural frequencies. The Analytical natural frequencies of a plate with a square cross-section matched the expected values, measured in Hz, based on the acoustic condition of the plate, its thickness and density type, as shown in TableS (5.18), (5.19), and (5.20).

Table 5.18: Natural frequency Foam Type (A) for Sandwich Plate

Foam thickness mm	Mode				
	(1.1)	(1.2)	(1.3)	(1.4)	
50	290.4	469.2	605.5	684.9	Natural frequency Hz
45	306.5	491.3	632.2	712.7	
40	319.4	508.1	652.9	733.3	
35	329.7	519.7	668.7	741.5	
30	337.8	525.1	680.4	694.9	
25	344.2	525.1	659.8	686.2	

Table 5.19: Natural frequency Foam Type (B) for Sandwich Plate

Foam thickness mm	Mode				
	(1.1)	(1.2)	(1.3)	(1.4)	
50	230.3	364.4	503.5	583.9	Natural frequency Hz
45	234.9	396.4	541.6	610.3	
40	243.1	421.8	570.6	635.7	
35	259.2	441.6	592.1	638.1	
30	271.6	454.3	603.1	606.8	
25	282.5	464.3	581.5	613.1	

Table 5.20: Natural frequency Foam Type (C) for Sandwich Plate

Foam thickness mm	Mode				
	(1.1)	(1.2)	(1.3)	(1.4)	
50	218.7	338.1	441.2	455.1	Natural frequency Hz
45	221.8	357.1	459.1	519.1	
40	221.2	346.2	447.8	495.8	
35	223.1	352.3	453.5	508.4	
30	223.7	458.1	460.9	518.4	
25	223.8	356.3	457.8	514.1	

5.5 Mode Shape

In the analysis of free vibrations of square plates supported on a sandwich plate foundation, the mode shape is a critical factor defining the vibration response. The mode shape describes the spatial distribution of displacement amplitudes across the plate at its natural frequencies. These shapes are determined by the plate's geometric and material properties, such as thickness, elastic modulus, and Poisson's ratio, as well as by the boundary and foundation conditions.

For a square plate surrounded by foam, the mode shapes are influenced by the foam's mechanical properties, including its elastic modulus, Poisson's ratio, and the stiffness of the elastic foundation. The foam provides elastic support and damping, which affect both the natural frequencies and the resulting mode shapes of the plate.

5.5.1 The Mode Shape of Plate Foam

1. **Type (A1).**

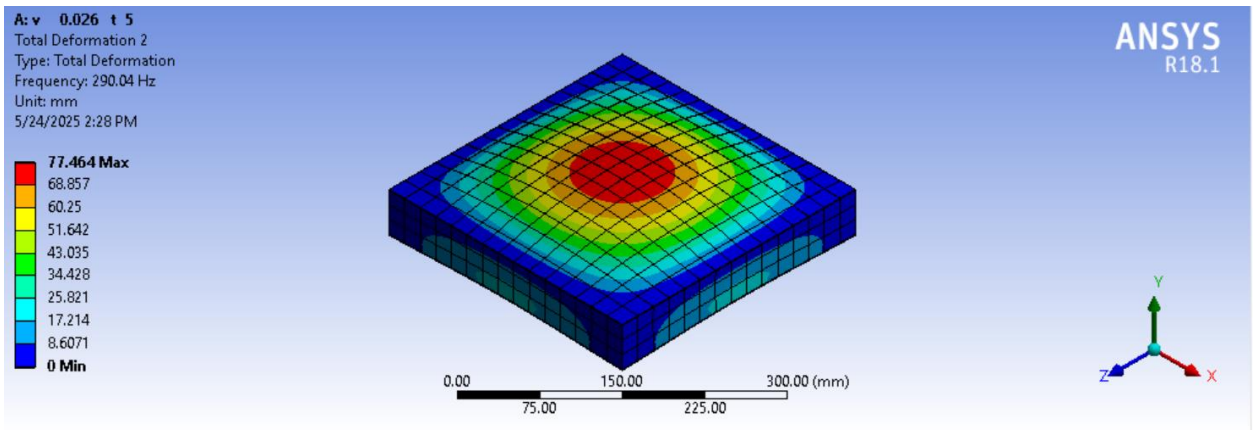

Figure 5.18: Mode Shape (1,1) of A1

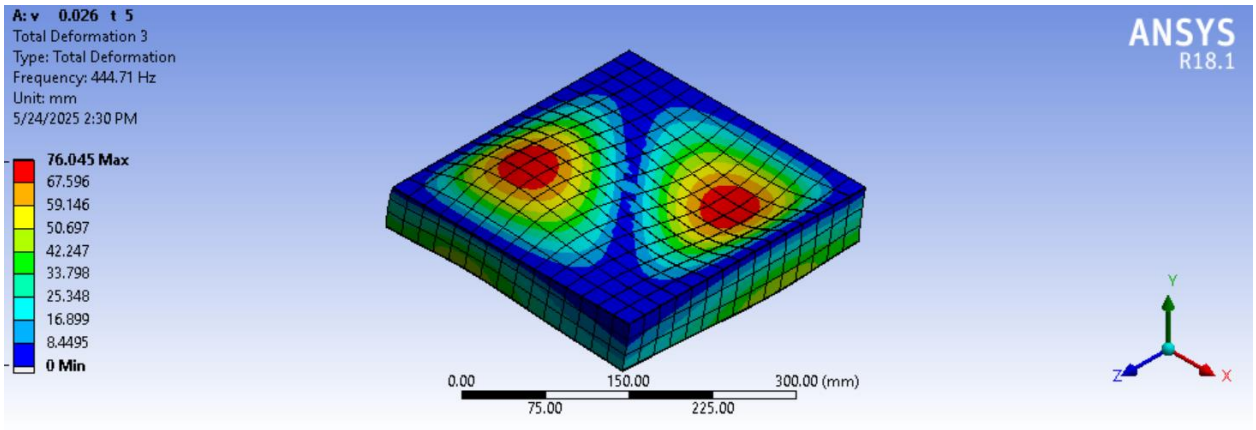

Figure 5.19: Mode Shape (1,2) of A1

Figure (5.18) Illustrates the mode shape of the foam core plate with a density of 26 kg/m³ and a thickness of 50 mm at a natural frequency of 290.04 Hz. The maximum deformation is concentrated at the center of the plate, while the edges remain nearly fixed.

Figure (5.19) Presents the second mode shape of the sandwich plate with a foam core density of 26 kg/m³ and thickness of 50 mm. The deformation pattern exhibits two symmetrical peaks, with a natural frequency of 444.71 Hz.

2. Type (A2).

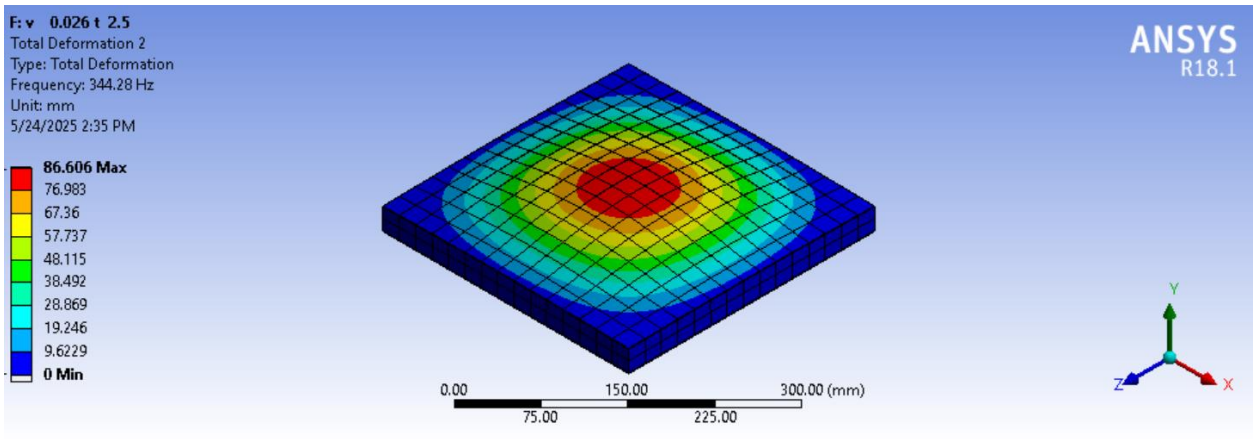

Figure 5.20: Mode Shape (1,1) of A2

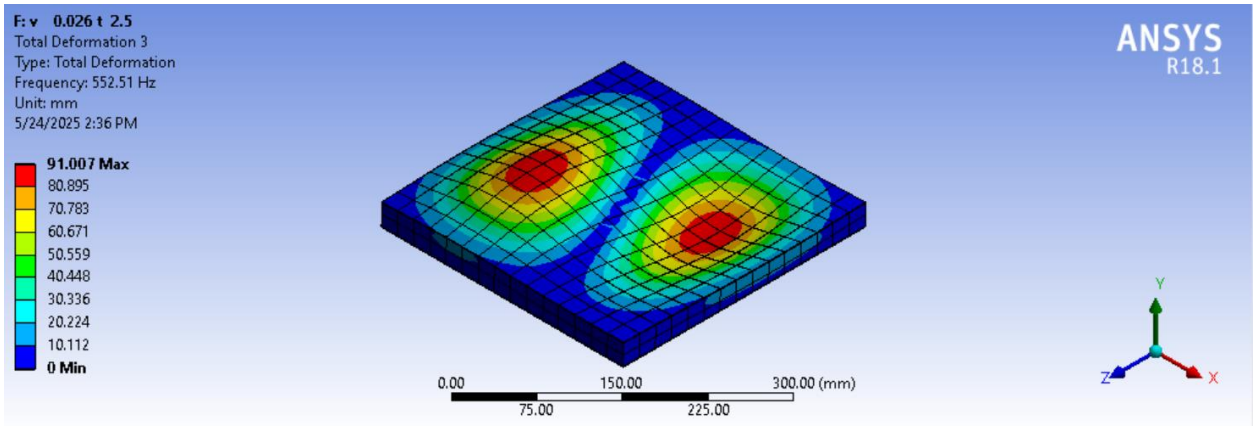

Figure 5.21: Mode Shape (1,2) of A2

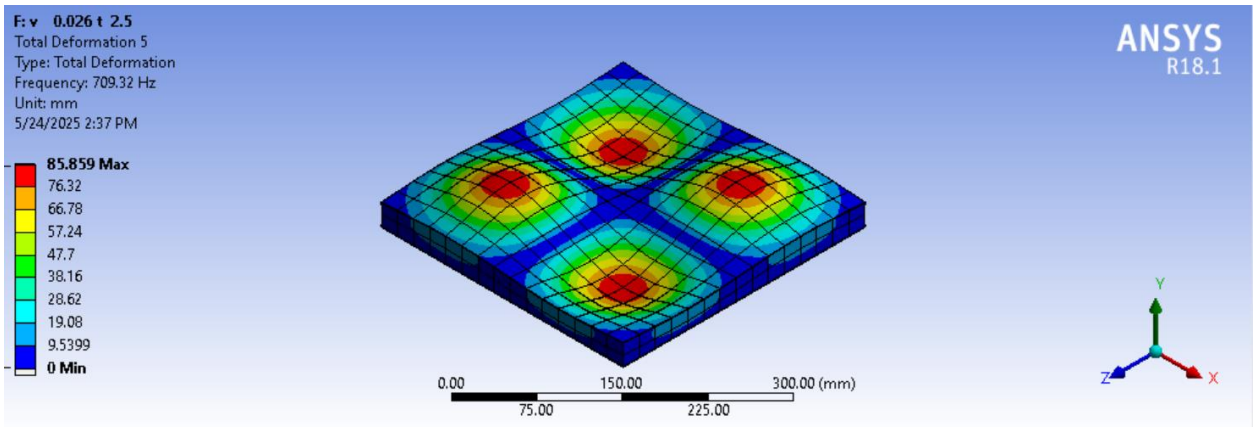

Figure 5.22: Mode Shape (2,2) of A2

3. Type (B1).

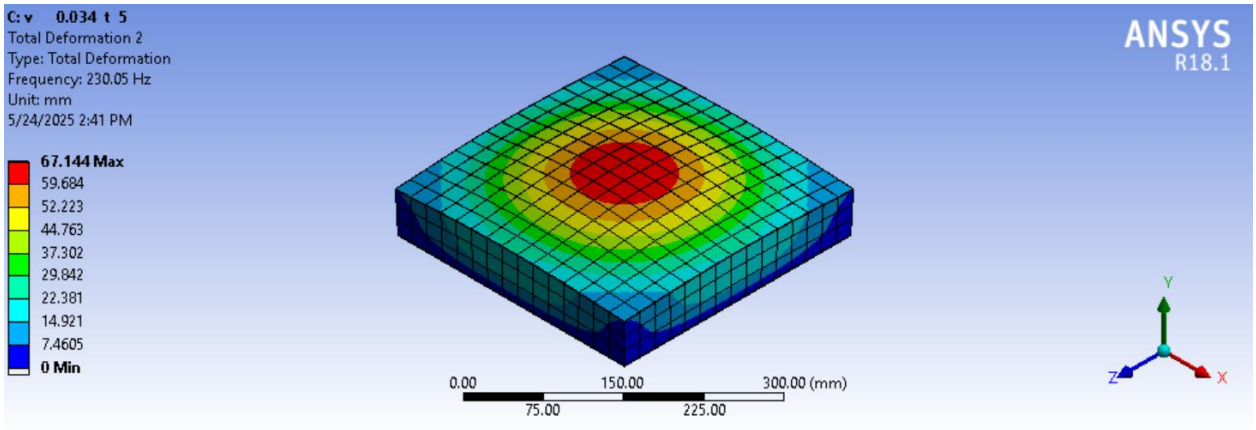

Figure 5.23: Mode Shape (1,1) of B1

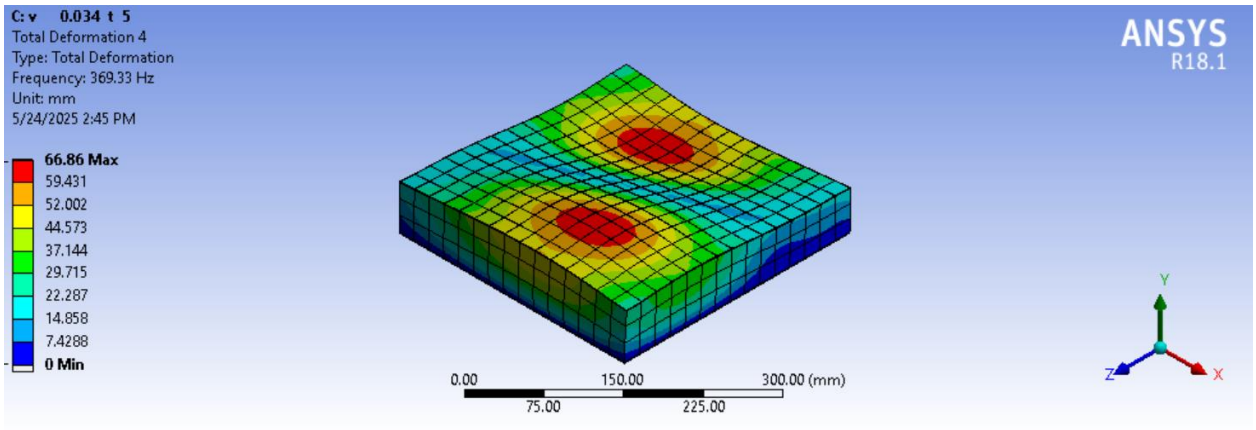

Figure 5.24: Mode Shape (1,2) of B1

4. Type (B2).

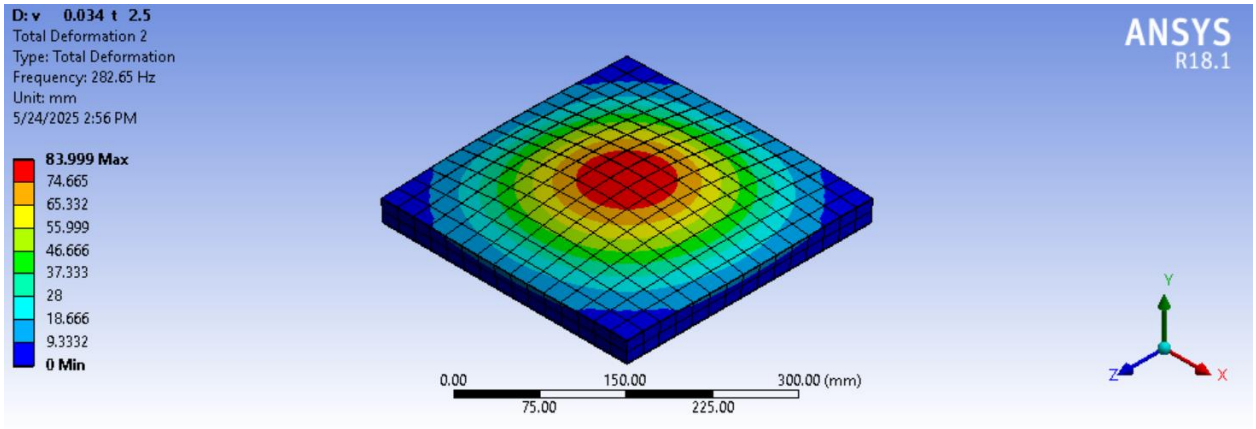

Figure 5.25: Mode Shape (1,1) of B2

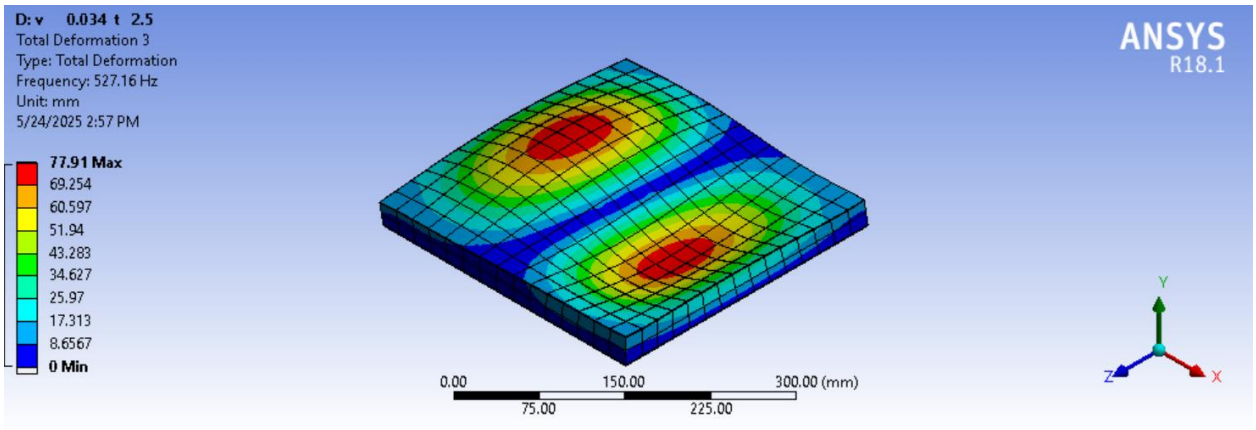

Figure 5.26: Mode Shape (1,2) of B2

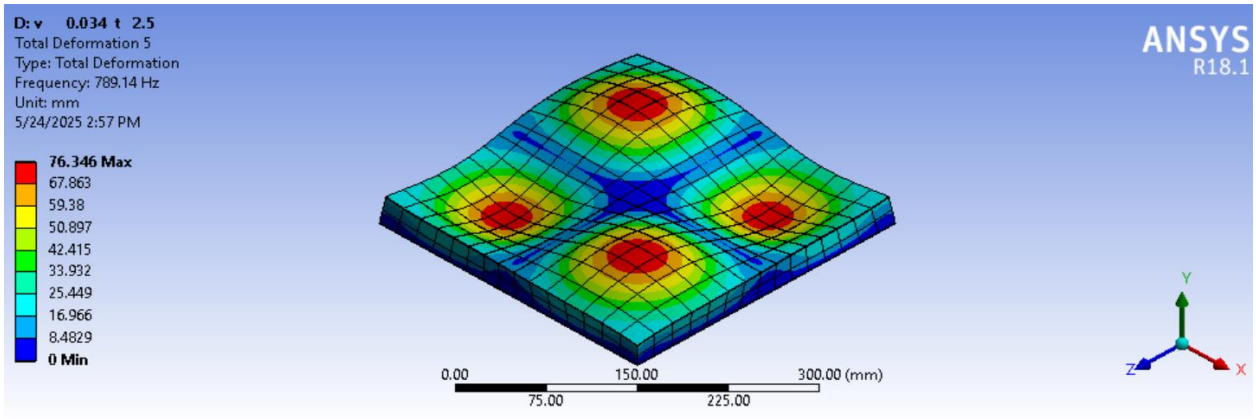

Figure 5.27: Mode Shape (2,2) of B2

5. Type (C1).

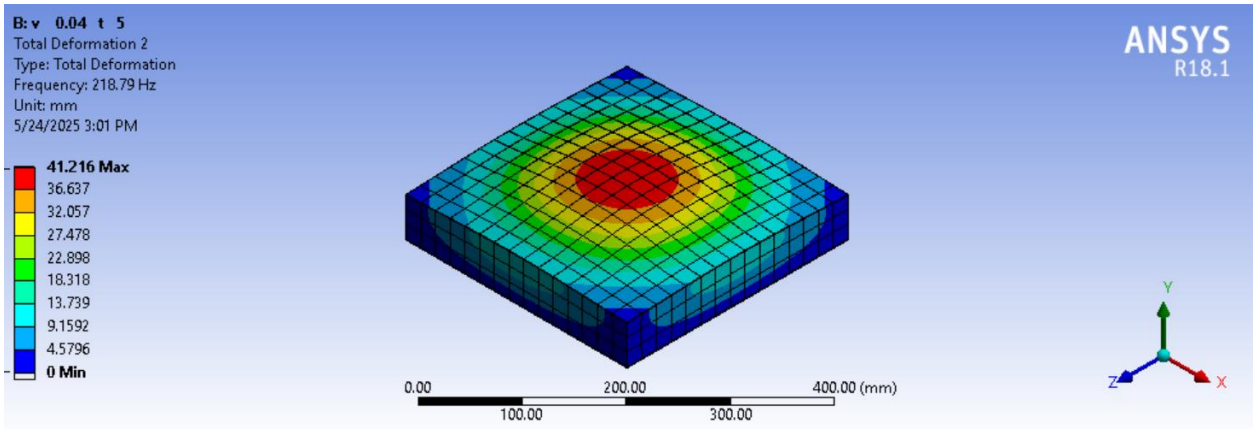

Figure 5.28: Mode Shape (1,1) of C1

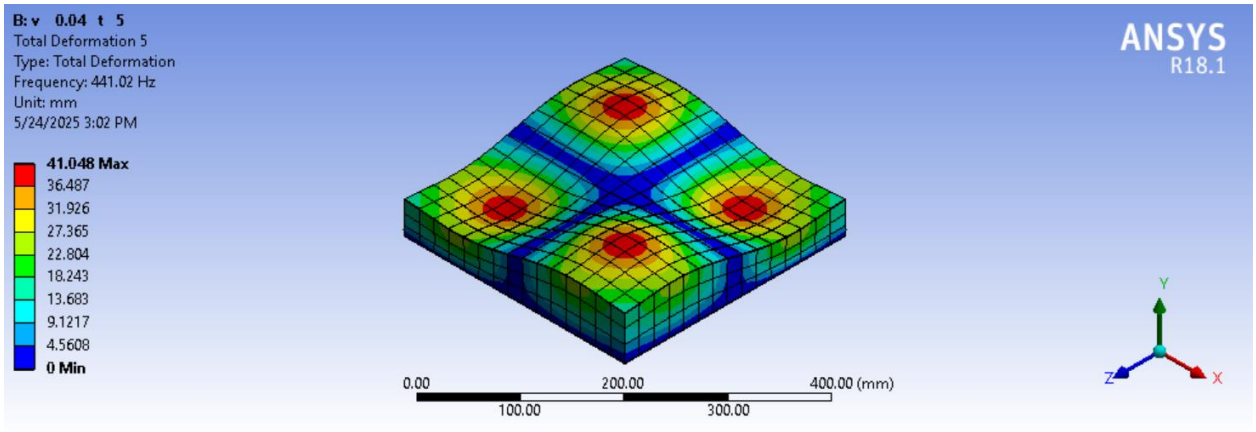

Figure 5.29: Mode Shape (2,2) of C1

6. Type (C2).

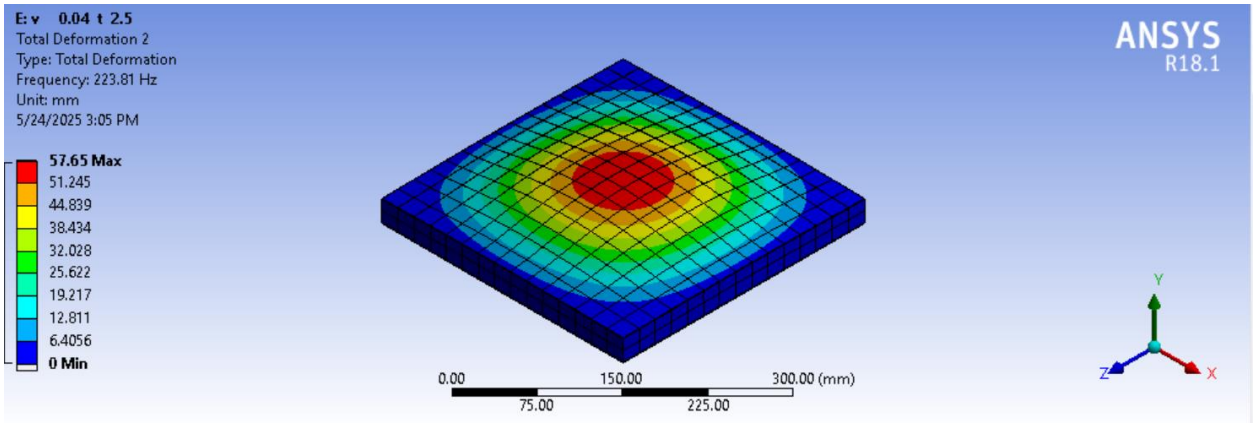

Figure 5.30: Mode Shape (1,1) of C2

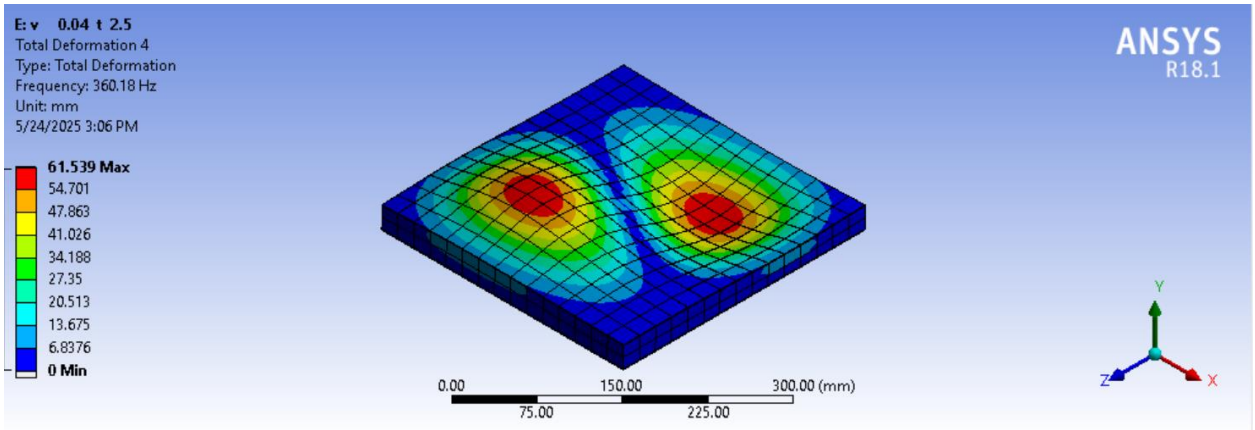

Figure 5.31: Mode Shape (1,2) of C2

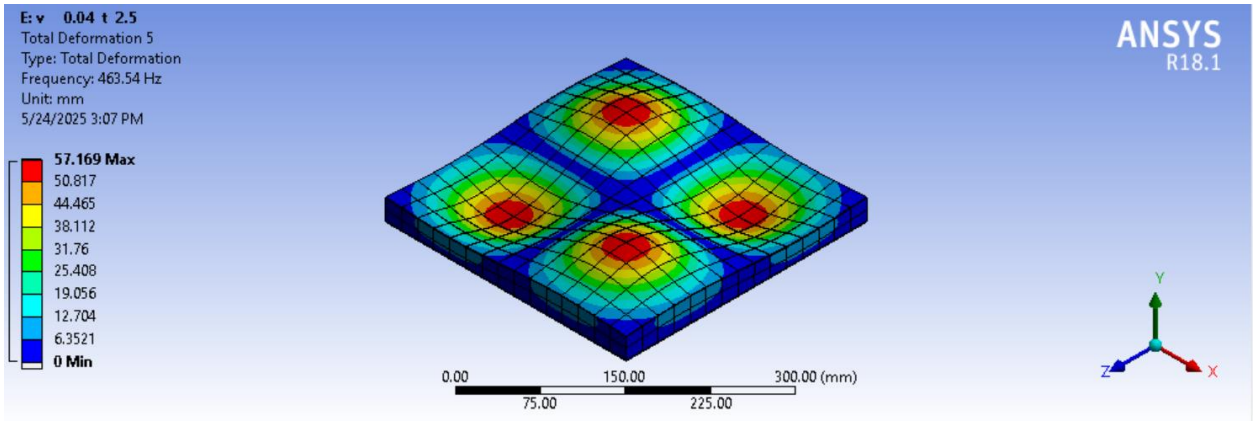

Figure 5.32: Mode Shape (2,2) of C2

5.6 Difference among Analytical, ANSYS, Experimental Program Results

In the fields of engineering and scientific research, the analysis of natural frequencies and vibrations is vital to assess the response of dynamic structures and systems. Frequency analysis methods vary depending on the tools and programs used, as some programs rely on Analytical modeling and simulation, while others rely on analyzing signals derived from practical experiments.

In this context, ANSYS is widely used for finite element analysis and determining the natural frequencies of structures based on detailed mathematical and physical models. ANSYS enables researchers and engineers to study the response of systems in a simulation environment that closely mimics realistic conditions, providing an accurate understanding of the behavior of the system under the influence of different loads.

On the other hand, SIGVIEW is used to analyze the signals, where the actual frequencies are extracted from experimental data taken from real measurements. SIGVIEW allows signal analysis through different techniques such as the Frequancy Response Function (FRF), providing a realistic view of how the system responds under actual environmental conditions and changing external factors. Tables (5.21), (5.23)and (5.23) show the difference for Foam of different thicknesses, and Figures (5.33), (5.34)and(5,35) depict the difference among the Analytical, Numerical and Experimental natural frequency.

Table 5.21: Comparison of natural frequency of (A) density (26 kg/ m^3)

Foam thickness	Natural frequency (Hz)				
	Analytical	**ANSYS**	**Experimental**	**Discrepancy %**	**Discrepancy%**
50	273.20	290.40	296.60	5.85	2.04
25	312.50	344.20	350.79	9.34	1.78

Table 5.21: When the foam thickness is reduced from 50 mm to 25 mm, the natural frequency increases, which leads to a higher stiffness relative to its weight, resulting . Among the different methods used, the ANSYS simulation results are much closer to the experimental values compared to the Analytical calculations. The Analytical method shows greater errors, especially at lower thicknesses, which suggests that the FEM (ANSYS) provides more accurate and reliable predictions in such cases**.**

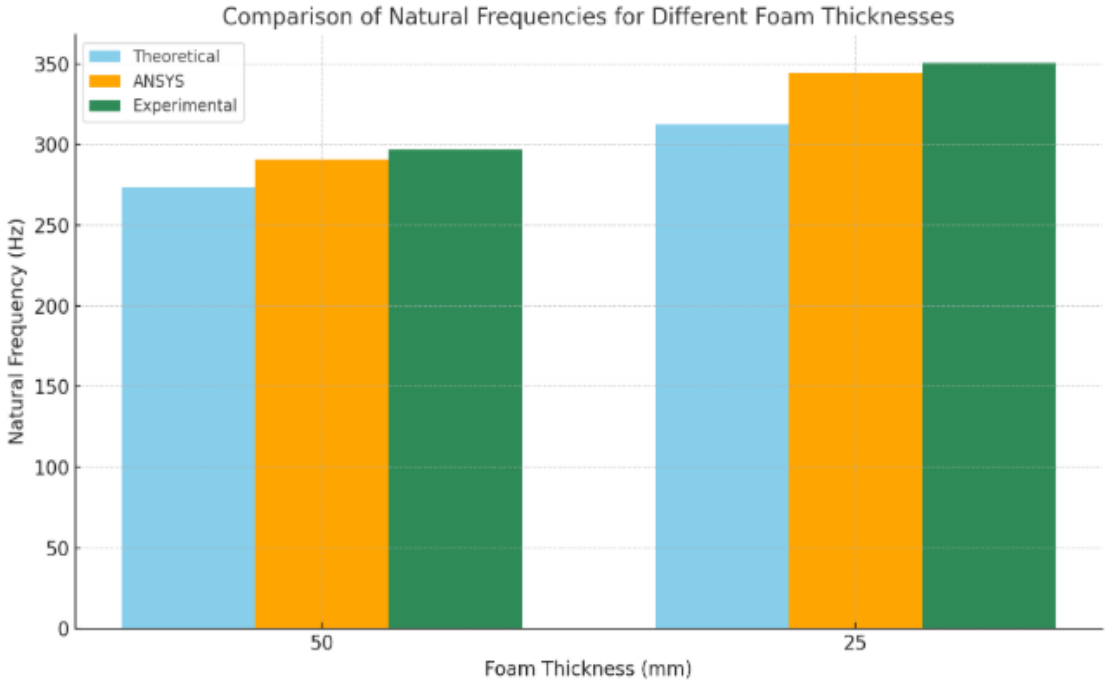

Figure 5.33: The difference among the analytical, numerical and experimental natural frequency

Table 5.22: Comparison of natural frequency of (B) density (34 kg/m3)

Foam thickness	Natural frequency (Hz)				
	Analytical	ANSYS	Experimenta	Discrepancy%	Discrepancy%
50	226.90	230.10	228.10	1.39	1.54
25	251.30	282.60	278.20	11.09	1.69

Table 5.22: As the foam thickness decreases from 50 mm to 25 mm, the natural frequency increases, which increases the system's stiffness-to-mass ratio, leading. The ANSYS simulation results show very small differences from the experimental data (around 1.5–1.7%), proving their accuracy. However, the Analytical results deviate more at smaller thicknesses (up to 11%), making them less reliable in such conditions. This highlights the importance of using FEM methods like ANSYS for more precise predictions, especially when the foam thickness is reduced.

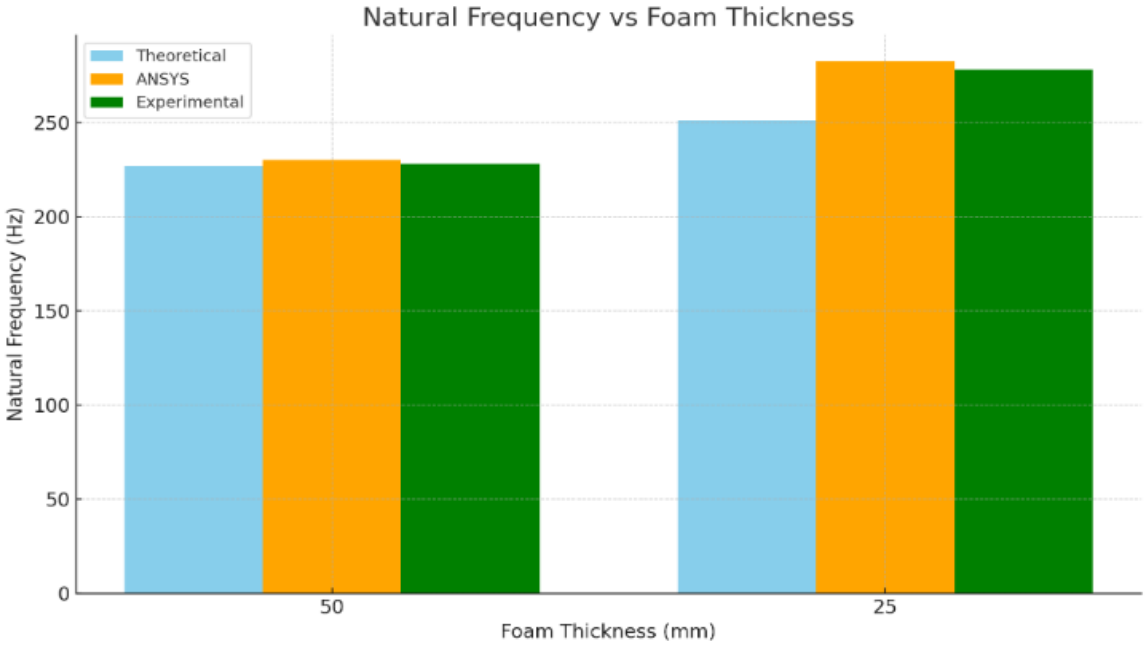

Figure 5.34: The difference among the analytical, numerical and experimental natural frequency

Table 5.23: Comparison of natural frequency of (C) density (40 kg/m3)

Foam thickness	Natural frequency (Hz)				
	Analytical	ANSYS	Experimental	Discrepancy%	Discrepancy%
50	221.90	218.70	220.30	1.18	3.04
25	244.30	223.80	266.50	8.39	16.02

Table 5.23: As the foam thickness decreases from 50 mm to 25 mm, the natural frequency increases. This is expected due to the reduction in mass, which increases the frequency. However, in this case, the accuracy of the prediction methods changes noticeably. At 50 mm thickness, both Analytical and ANSYS results are quite close to the experimental value, with discrepancies under 3%. But at 25 mm, the Analytical prediction deviates by over 8%, and the ANSYS result shows a significant 16% difference from the experimental value. This suggests that at low thickness and potentially higher densities, other factors, such as damping, boundary effects, or non-linear material behavior may impact the results and are not fully captured by the models, especially the FEM simulation.

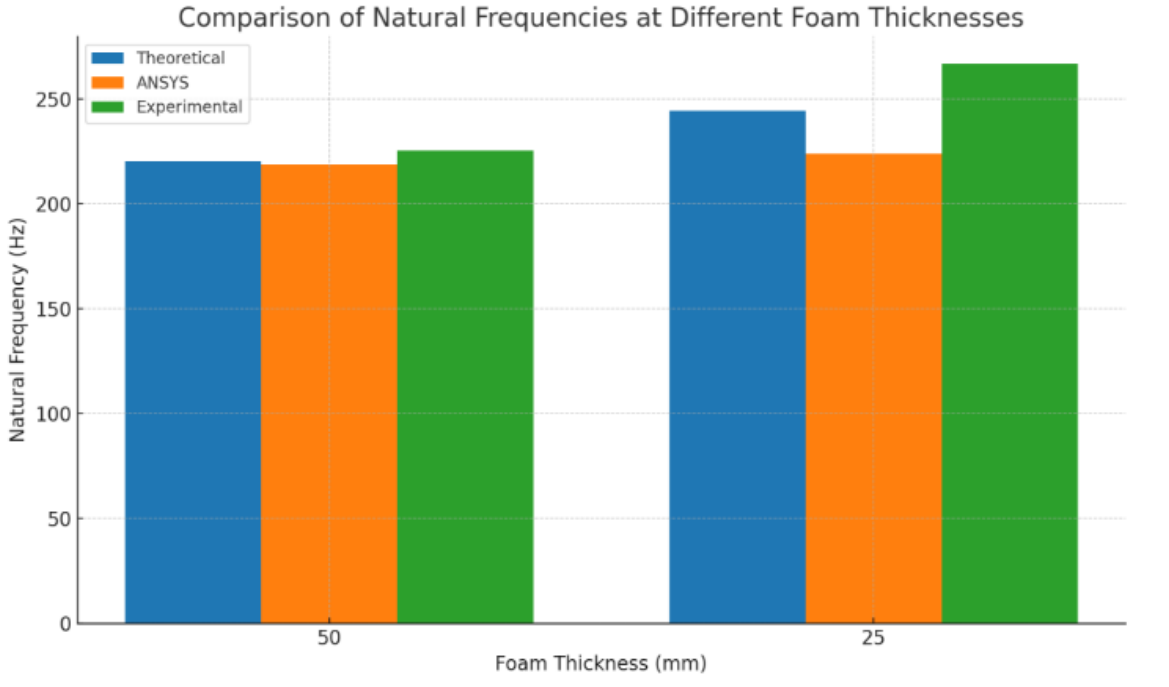

Figure 5.35: The difference among the analytical, numerical and experimental natural frequency.

5.7 Damping coefficient at difference analytical and experimental

Damping is the ability of a material or structure to absorb vibrational energy and dissipate it over time, reducing oscillation amplitudes. It is a key factor in controlling vibrations, noise, and the dynamic stability of foam and composite structures, Tables **(5.24–5.26**) present the comparison of damping coefficients between analytical and experimental results for foam with three different densities (**26, 34, and 40 kg/m³**) at thicknesses of (**50 mm** and **25 mm)**. The results show a very close agreement between the analytical and experimental values, which confirms the accuracy of the analytical model used toredict the damping coefficient. Figures (**5.36–5.38)** graphically illustrate the small differences between the analytical and experimental values for each foam density

Table 5.24: Comparison of Damping coefficient of (A) density (26 kg/m3)

Foam thickness	Damping		
	Analytical	Experimental	Discrepancy%
50	0.09861	0.08769	1.027
25	0.16463	0.15396	0.542

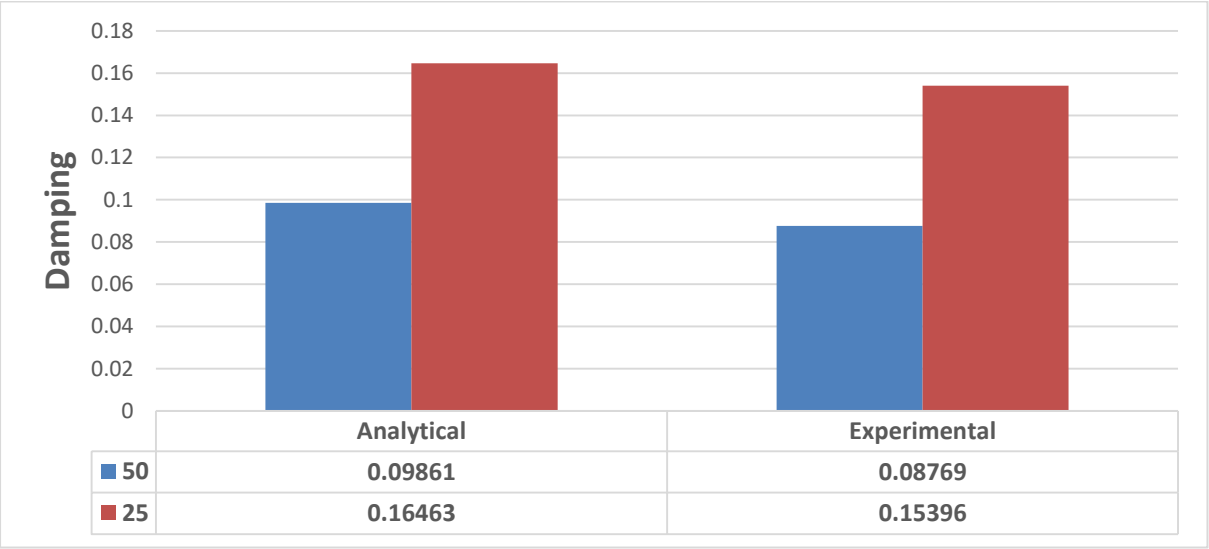

Figure 5.36: The difference among the analytical and experimental Damping.

Table 5.25: Comparison of Damping coefficient of (B) density (34 kg/m3)

Foam thickness	Damping		
	Analytical	Experimental	Discrepancy%
50	0.09613	0.08594	0.327
25	0.15451	0.14387	0.549

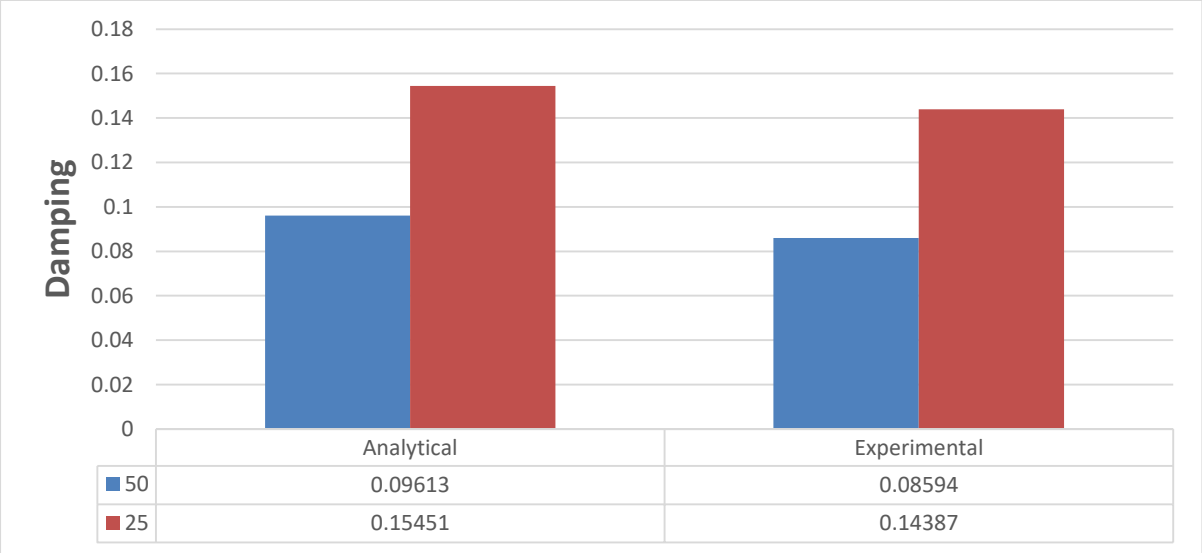

Figure 5.37: The difference among the analytical and experimental Damping

Table 5.26: Comparison of Damping coefficient of (C) density (40 kg/m3)

Foam thickness	Damping		
	Analytical	Experimental	Discrepancy%
50	0.09439	0.08317	1.344
25	0.14942	0.13734	0.329

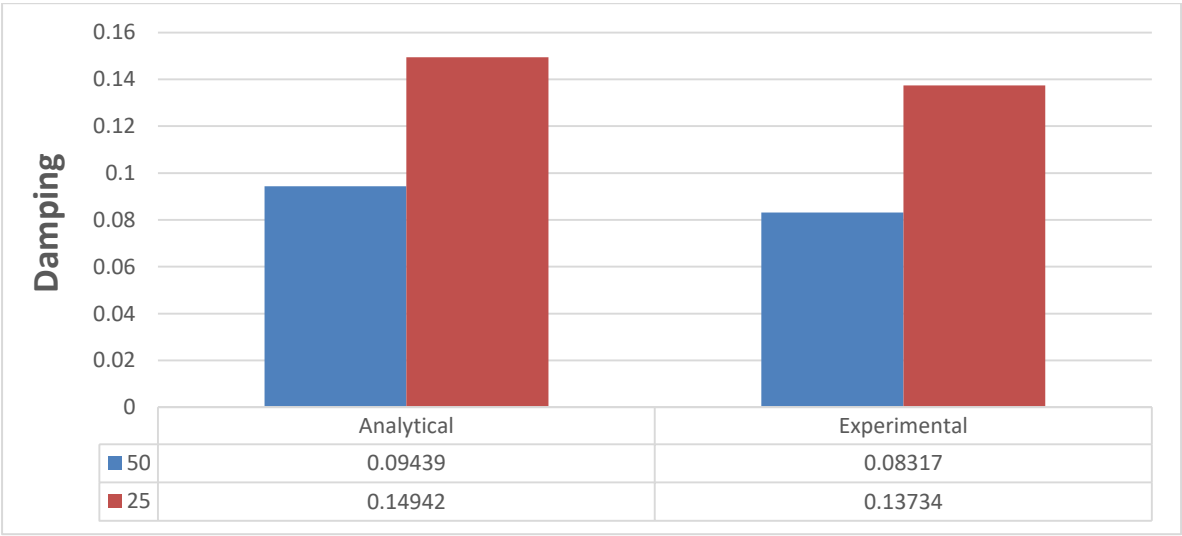

Figure 5.38: The difference among the analytical and experimental Damping

5.8 Parametric Study Effect of Foam Density on Natural Frequency

This study investigated the effect of varying foam density on the natural frequency of sandwich panels, with the thickness fixed at 80 mm. Both Analytical analysis and ANSYS simulations were employed. The results illustrated in Figure (5.39) and detailed in Table (5.27) show that increasing the foam density leads to a decrease in natural frequency. This is primarily due to the added mass, which reduces the system's vibration speed. Analytical models are based on simplified assumptions and are generally less accurate. In contrast, the ANSYS simulations offer more realistic results by accounting for the detailed material behavior. At higher densities, the ANSYS values tend to be slightly lower than Analytical predictions, indicating better accuracy. Overall, the findings confirm that the foam density has a significant influence on the natural frequency, and using both Analytical and numerical methods provides a clearer and more reliable understanding.

Table (5.27): Comparison of Natural Frequencies for Different Foam Densities (15–55 kg/m³)

Foam Density (kg/m³)	Naturalfrequency(Hz)		
	Analytical	ANSYS	Discrepancy%
55	172.5	178.3	4.81
45	185.2	194.3	5.03
30	210.4	220.8	5.14
20	235.7	248.6	5.78
15	248.2	263.9	6.25

Table (5.27): As the foam density decreases, the natural frequency increases, This is because the lighter foams have a less mass, which raises the frequency. The difference between Analytical and ANSYS results remains small, around (5-6%), showing a good agreement between the methods.

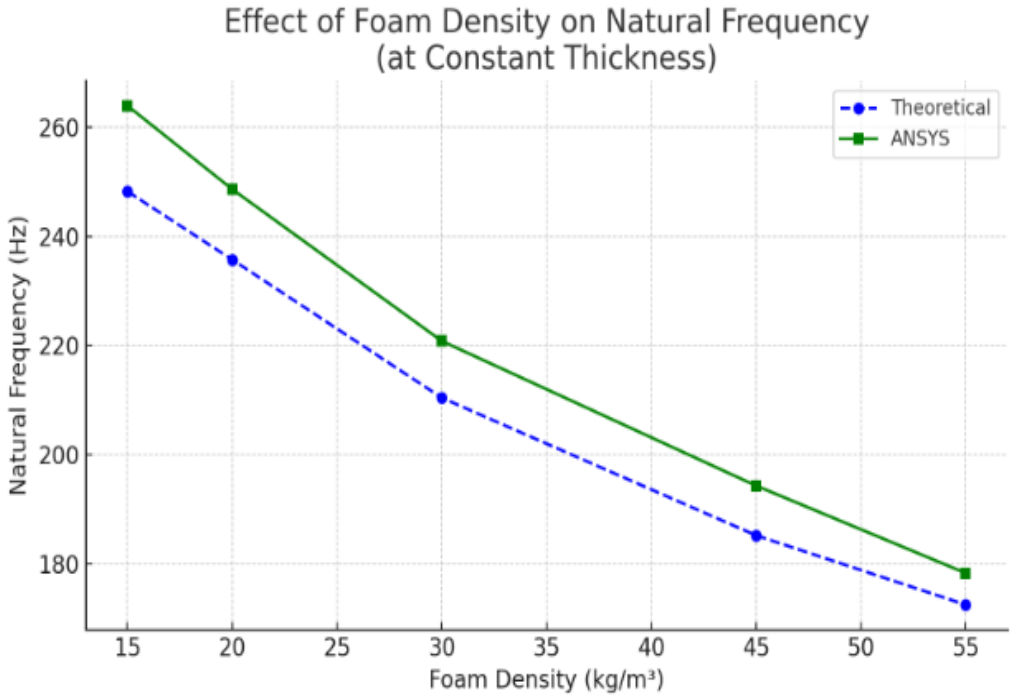

Figure (5.39): **The difference between the Numerical and the Analytical natural frequency.**

CHAPTER Six

Conclusions and Recommendations

6.1 Conclusions

This work aims to study the effect of foam density and thickness on the dynamic properties of the structure (natural frequencies, mode shape, and damping ratio). In this study, the effect of density, thickness, geometric shape, and their purposeful distribution on improving the vibration characteristics of the structure was investigated using analytical and finite element methods. Supported elastic boundary conditions were determined. The results obtained from the analytical solution and the results applied using ANSYS 2018 R1 are presented and summarized as follows:

1.Effect of Thickness on Natural Frequency and Damping coefficient:

- For all densities, natural frequency increases as foam thickness decreases from 50 mm to 25 mm.
- For all densities, damping coefficient increases as the foam thickness decreases from 50 mm to 25 mm, in both analytical and experimental results.

2. Effect of Density on Natural Frequency and Damping coefficient:

- At a given thickness, lower-density foam (26 Kg/m^3) has higher natural frequencies and Damping coefficient compared to higher densities (34 and 40 Kg/m^3).

3. ANSYS simulations demonstrated high reliability for dynamic analysis of sandwich structures, showing closer agreement with experiments than theory, with deviations from experimental results typically below 3%.

6.2 Recommendations for Future Research

To expand upon the findings of this study and explore further dimensions of the topic, the following directions for future research are proposed:

1. Utilization of Alternative Material Systems: Future investigations are encouraged to employ a wider variety of Cellular Material in order to develop improved damping models.
2. Examine how variations in temperature, humidity, or other environmental conditions affect the stiffness, damping, and vibration characteristics of foam cores.
3. Future work should focus on developing AI-driven numerical frameworks to improve the accuracy of frequency and damping estimations, and on validating the proposed methodology for aerospace structures, particularly aircraft wings.

References

REFERENCE

[1] P. A. Mouritz, *Introduction to Aerospace Materials*. Woodhead Publishing Limited, 2012.

[2] J. P. Nunes and J. F. Silva, "Sandwiched composites in aerospace engineering," in *Advanced Composite Materials for Aerospace Engineering*, Elsevier, 2016.

[3] T. Bitzer, *Cellular Core Technology*. Springer Netherlands, 1997. doi: 10.1007/978-94-011-5856-5.

[4] Z. Chen and N. Yan, "Investigation of elastic moduli of Kraft paper core sandwich panels," *Composites Part B: Engineering*, vol. 43, no. 5, pp. 2107–2114, Jul. 2012. doi: 10.1016/j.compositesb.2012.03.008.

[5] Hexcel, "HexWeb® Cellular Selector Guide. HexWeb® Foam provides exceptional stiffness and strength with little added weight for aerospace and industrial applications."

[6] E. Kharrazi, "Structural FEM analysis of innovative sandwich configuration for automotive application," Polytechnic of Turin, Torino, 2020.

[7] J. M. Davies, *Lightweight Sandwich Construction*. Manchester: International Council for Building Research, 2001.

[8] Y. Du, N. Yan, and M. T. Kortschot, "Light-weight cellular core sandwich panels containing biofiber-reinforced thermoset polymer composite skins: Fabrication and evaluation," *Composites Part B: Engineering*, vol. 43, no. 7, pp. 2875–2882, Oct. 2012. doi: 10.1016/j.compositesb.2012.

[9] J. Pflug and I. Verpoest, “Sandwich materials selection charts,” *Journal of Sandwich Structures & Materials*, vol. 8, no. 5, pp. 407–421, 2006.

[10] R. A. Staal, G. Mallinson, D. Horrigan, and J. Krishnan, “Failure of sandwich cellular core panels in bending,” 2006.

[11] E. Oterkus, C. Diyaroglu, D. De Meo, and G. Allegri, “Fracture modes, damage tolerance and failure mitigation in marine composites,” in *Marine Applications of Advanced Fibre-Reinforced Composites*, Elsevier, 2016,.

[12] D. Zenkert, *The Handbook of Sandwich Construction*. Engineering Materials Advisory Services, 1997.

[13] M. M. William, “Design of composite sandwich panels for lightweight applications in air cargo containers,” M.Sc. thesis, West Virginia Univ., 2016.

[14] J. Vinson, *The Behavior of Sandwich Structures of Isotropic and Composite Materials*. Routledge, 2018.

[15] Sudharsan, “Structural design and analysis of a lightweight composite sandwich space radiator panel,” 2003.

[16] Hexcel, “HexWeb® Cellular Core Attributes and Properties,” 2016. [Online]. Available: http://www.hexcel.com/contact/salesoffice

[17] F. A. Fazzolari, “Sandwich structures,” in *Stability and Vibrations of Thin-Walled Composite Structures*, Elsevier, 2017, pp. 49–90. doi: 10.1016/B978-0-08-100410-4.00002-8.

[18] N. Amsc and A. A. CMPS, *Composite Materials Handbook: Polymer Matrix Composites – Materials Usage, Design, and Analysis*. 2002.

[19] M. Tauhiduzzaman, “Design optimization of sandwich core,” Univ. of Texas, El Paso, 2016.

[20] L. Yuan, H. Wu, C. Bai, et al., “Nonlinear vibration analysis of the functionally graded sandwich plate under blast loading,” *Journal of the Brazilian Society of Mechanical Sciences and Engineering*, vol. 46, p, 2024.

[21] D. Li, D. Kong, and T. Chen, “Vibration and stability of functionally graded porous (FGP) sandwich plates under moving mass,” *Acta Mechanica*, 2024.

[22] V. N. V. Hoang, P. Shi, L. Toledo, et al., “Free vibration characteristics of FG-GRC sandwich shallow shells with porous core in thermal environments,” *Journal of Vibration Engineering & Technologies*, vol. 12, p. 2024.

[23] F. Li, W. Yuan, and C. Zhang, “Free vibration and sound insulation of functionally graded honeycomb sandwich plates,” *Journal of Intelligent Material Systems and Structures*, vol. 33, no. 10, pp. 1234–1245, 2022.

[24] A. Garg, H. D. Chalak, L. Li, et al., “Vibration and buckling analyses of sandwich plates containing functionally graded metal foam core,” *Acta Mechanica Solida Sinica*, vol. 35, pp. 1–16, 2022.

[25] S. J. Singh and S. P. Harsha, “Analysis of porosity effect on free vibration and buckling responses for sandwich sigmoid function based functionally graded material plate resting on Pasternak foundation using Galerkin–Vlasov’s method,” *Journal of Intelligent Material Systems and Structures*, vol. 32, no. 5, pp. 567–580, 2021.

[26] M. W. Zaitoun, A. Chikh, A. Tounsi, et al., “An efficient computational model for vibration behavior of a functionally graded sandwich plate in a

hygrothermal environment with viscoelastic foundation effects," *Engineering with Computers*, vol. 39, pp. 1127–1141, 2021.

[27] E. K. Njim, S. H. Bakhy, and M. Al-Waily, "Analytical and numerical investigation of free vibration behavior for sandwich plate with functionally graded porous metal core," *Pertanika Journal of Science and Technology*, vol. 29, no. 3, 2021.

[28] Z. Huang, Z. Qin, and F. Chu, "Vibration and damping characteristics of sandwich plates with viscoelastic core," *Journal of Vibration and Control*, vol. 22, no. 7, pp. 1783–1796, 2016.

[29] M. Afshin, M. Sadighi, and M. Shakeri, "Vibration and damping analysis of cylindrical sandwich panels containing a viscoelastic flexible core," *Journal of Intelligent Material Systems and Structures*, vol. 22, no. 7, pp.2011.

[30] R. A. Staal, G. Mallinson, D. Horrigan, and J. Krishnan, "Failure of sandwich honeycomb panels in bending," 2006.

[31] B. A. K. Jha, "Free vibration analysis of sandwich panel," 2007.

[32] U. K. S. Sendvi and N. I. H. P. Z. Napako, "A fatigue characterization of honeycomb sandwich panels with a defect," *Materiali in Tehnologije*, vol. 41, no. 4, pp. 157–161, 2007.

[33] M. Ma, W. Yao, W. Jiang, W. Jin, Y. Chen, and P. Li, "Fatigue behavior of composite sandwich panels under three point bending load," *Polymer Testing*, vol. 91, Nov. 2020.

[34] J. Qi, C. Li, Y. Tie, Y. Zheng, and Y. Duan, "Energy absorption characteristics of origami-inspired honeycomb sandwich structures under low-velocity impact loading," *Materials & Design*, vol. 207, Sep. 2021.

[35] N. Shafiei, M. Kazemi, and M. Hadizadeh, "Vibration analysis of rectangular plates using different boundary conditions," *Mechanics Research Communications*, vol. 108, p. 67, 2020.

[36] A. A. Shabana, *Theory of Vibration: An Introduction*. Springer, 2018.

[37] S. A. Salawu, M. G. Sobamowo, and O. M. Sadiq, "Dynamic analysis of non-homogenous varying thickness rectangular plates resting on Pasternak and Winkler foundations," *Engineering and Applied Science Letters*, vol. 3, no. 1, pp. 1–20, 2020.

[38] J. L. Meriam, L. G. Kraige, and J. N. Bolton, *Engineering Mechanics: Dynamics*. John Wiley & Sons, 2020.

[39] T. R. Tauchert, "Large plate deflections, von Kármán theory, statical problems," in *Encyclopedia of Thermal Stresses*, R. B. Hetnarski, Ed. Dordrecht: Springer, 2014, pp. 2697–2704.

[40] M. Troncossi et al., "Experimental characterization of a high-damping viscoelastic material enclosed in reinforced polymer components," *Applied Sciences*, vol. 10, no. 18, 2020.

[41] S. Tang, Z. Li, W. Sun, Y. Liu, J. Wang, X. Wang, and J. Lin, "Natural foam–butadiene foam blend composites potentially applied in damping bearings," *Polymers*, vol. 16, no. 13, p. 1945, 2024.

[42] S. Timoshenko, *Theory of Plates and Shells*. McGraw-Hill, 1959.

[43] C. M. A. Vasques, R. A. S. Moreira, and J. D. Rodrigues, "Viscoelastic damping technologies – Part I: Modeling and finite element implementation," *Journal of Advanced Research in Mechanical Engineering*, vol. 1, no. 2, 2022.

[44] J. Wang, H. Li, G. Sun, and L. Han, “Free vibration analysis of rectangular thin plates with corner and inner cutouts using C1 Chebyshev spectral element method,” *Thin-Walled Structures*, vol. 181, p. 110031, 2022.

[45] Q. Wang, Z. Sun, and H. Liu, “Axially moving plates in fluid: Dynamic response and stability,” *Journal of Applied Mechanics*, vol. 143, no. 5, pp. 106–144, 2022.

[46] Y. Wang, J. Fan, X. Shen, X. Liu, J. Zhang, and N. Ren, “Free vibration analysis of stiffened rectangular plate with cutouts using Nitsche-based IGA method,” *Thin-Walled Structures*, vol. 181, p. 2023.

[47] Z. Wu, A. Li, Y. Wu, Z. Yin, and S. Ullah, “New natural frequency studies of orthotropic plates by adopting a two-dimensional modified Fourier series method,” *Buildings*, vol. 14, no. 3, p., 2024.

[48] D. Xu, Z. Ni, Y. Li, Z. Hu, Y. Tian, B. Wang, and R. Li, “On the symplectic superposition method for free vibration of rectangular thin plates with mixed boundary constraints on an edge,” *Theoretical and Applied Mechanics Letters*, vol. 11, no. 5, p. 100293, 2024.

[49] H. Zhang, A. Li, Y. Su, S. Liu, and T. Liu, “Modification technologies and constitutive models of viscoelastic damping materials: Progress and future trends,” *Construction and Building Materials*, vol. 441, p. 137406, 2024.

[50] S. Raeisi and A. Tovar, “The effect of the cell shape on compressive mechanical behavior of 3D printed extruded cross-sections,” in *SAE Technical Papers*, SAE Int., 2018..

[51] L. Azzouz et al., “Mechanical properties of 3-D printed truss-like lattice biopolymer non-stochastic structures for sandwich panels with natural fibre composite skins,” *Composite Structures*, 2019.

[52] A. S. Hamzah, “Numerical and experimental study of the parameters affected on the honeycomb structures properties,” M.Sc. thesis, Univ. of Babylon, 2020.

[53] P. Dhananandh, V. R. Mamilla, and K. S. R. Murthy, “Design and analysis of hexagonal and octagonal honeycomb structures with various materials and FEM analysis,” *International Journal of Innovative Technology and Exploring Engineering*, vol. 9, no. 7, pp. 669–677, May 2020.

[54] H. Abedzade Atar, M. Zarrebini, H. Hasani, and J. Rezaeepazhand, “The effect of core geometry on flexural stiffness and transverse shear rigidity of weight-wise identical corrugated core sandwich panels reinforced with 3D flat spacer knitted fabric,” *Polymer Composites*

[55] S. E. Sadiq, M. J. Jweeg, and S. H. Bakhy, “Strength analysis of an aircraft sandwich structure with a honeycomb core: Theoretical and experimental approaches,” *Engineering and Technology Journal*, vol. 39, no. 1A, pp. 153–166, Jan. 2021.

[56] D. Sridhar and D. Shashikala, “Effect of foam and epoxy on aluminium honeycomb structure for automobile applications,” 2021.

[57] D. Pereira et al., “Cellular lattice cores of sandwich panels fabricated by additive manufacturing: Effect of dimensions and relative density on mechanical.

الخلاصـة

تُستخدم الألواح الساندويتش على نطاق واسع في التطبيقات البحرية والجوية، وكذلك في القطاعات الهندسية مثل السيارات والمدني، وذلك بفضل خفّة وزنها ومرونة تصميمها، حيث توفر تقليل الوزن مع الحفاظ على القوة الميكانيكية. تهدف هذه الدراسة إلى دراسة تأثير كثافة وسمك نواة الفوم على الأداء الديناميكي للألواح الساندويتش، مع التركيز بشكل خاص على الترددات الطبيعية وسلوك الاهتزاز .تم فحص ثلاث كثافات للفوم (26، 34، و40 كجم/م^3) إلى جانب سمكين للنواة (25 مم و50 مم) لدراسة تأثيرها على خصائص الاهتزاز للألواح.

تم اتباع منهجية تجمع بين الحسابات النظرية، والقياسات التجريبية، والمحاكاة العددية .استخدمت النماذج النظرية لتقدير الترددات الطبيعية للألواح الساندويتش بناءً على خصائص المواد والهندسة. تجريبيًا، تم تصنيع الألواح باستخدام نوى الفوم المختارة واختبارها عبر اختبارات الانحناء الثلاثي النقاط وفقًا لمواصفاتASTM ، بالإضافة إلى اختبارات الصدمات لمحاكاة الظروف الواقعية. أما المحاكاة العددية فتمت باستخدام برنامج ANSYS لحساب الترددات الطبيعية والتحقق من صحة البيانات التجريبية.

أظهرت النتائج أن زيادة كثافة الفوم تؤدي بشكل عام إلى انخفاض التردد الطبيعي الأساسي للألواح الساندويتش، وقد لوحظ هذا الاتجاه لكلا السمكين، مع انخفاض أكثر وضوحًا في النوى الأكثر سمكًا. يُعزى انخفاض التردد مع زيادة الكثافة إلى زيادة الكتلة للفوم الكثيف، مما يؤثر على خصائص الاهتزاز للوحة. وعلى النقيض، فإن الفوم منخفض الكثافة ينتج ترددات طبيعية أعلى بنسبة تقريبية 19%، وهو أمر مفيد في التطبيقات التي تتطلب التحكم في الاهـتزاز .بالإضافة إلى ذلك، تم حساب معاملات التخميد التجريبية للسمكيــن (25 مم و50) مم لثــلاث كــثافات للفــوم، حيث تراوحت القيـــم بين (0.15396 -0.08253) .

جمهورية العراق

وزارة التعليم العالي و البحث العلمي

جامعة كربلاء

كلية الهندسة

قسم الهندسة الميكانيكية

سلوك التخميد للمواد المسامية المستخدمة في هياكل الصفائح الطبائقيه

رسالة مقدمة الى مجلس كلية الهندسة / جامعة كربلاء وهي جزء من متطلبات نيل درجة الماجستير في علوم الهندسة الميكانيكية

المؤلف:

عباس صلاح هاشم

باشراف :

الأستاذ الدكتور محسن جبر جويج

الاستاذ المساعد الدكتور احمد قاسم حسن

1447هـ **2025م**